Topology optimization for ship structures with manufacturing constraints

Dennis Bos

Master Thesis Project

TU Delft

C-JOB
DEDICATED NAVAL ARCHITECTS

Thesis for the degree of MSc in Marine Technology

Topology optimization for ship structures with manufacturing constraints

By

Dennis Bos

Performed at

C-Job Naval Architects

23 August 2021

Company supervisors

Responsible supervisor:	Pieter de Boer

Thesis exam committee

Chair/Responsible Professor:	Carey Walters
Staff Member:	Fred van Keulen
Staff Member:	Jeroen Pruyn
Company Member:	Pieter de Boer

Author Details

Study number:	4980301

PREFACE

This report was written as part of the final phase of the master's degree in Marine Technology at the Delft University of Technology (TU Delft). This concerns the execution of a final assignment during the last year of the academic program.

The graduation assignment aims to put the knowledge and skills acquired during the master's program into practice by an independent technical research project at a company in the maritime industry.

The research is desk research commissioned by C-Job Naval Architects in Heerenveen.

Dennis Bos
Heerenveen, July 2021

ABSTRACT

Currently, most ships are designed on the basis of rules and reference ships for which often only the critical structural parts are calculated and designed in detail. This process can result in an over-dimensioned ship with the standard structural outcome of longitudinal stiffeners, transverse stiffeners, and bulkheads with a fixed distance due to ease of manufacturing. With the use of finite element analysis (FEA), the complete structure of a ship is analyzed against prescribed loads, which facilitates the determination of the detailed dimensions of all stiffeners and plates within a reasonable lead time and could result in better engineering in the form of a lighter ship. In addition, the most common structural forms could be optimized by replacing them with unique and optimal shapes.

Topology optimization (TO) uses FEA, and it facilitates unique structural shapes. TO generates an optimized material distribution for a set of loads and constraints within a given design domain. The result can be used to inform the design of an improved part. Although the results provide helpful insight, they often cannot be used literally, as they are organic and cannot be manufactured with typical steel shipbuilding methods. The objective of this study is to research the possibility to design the structure of a steel midship with TO where the resulting structural form is manufacturable using steel-cut plates and cost-effective from a shipbuilding perspective. However, constraints that result in a manufacturable structure that can be made cost-effectively from steel-cut plates have not been developed and implemented in TO.

To meet the objective, this project was initiated in cooperation with C-Job and the University TU Delft. The methodology was established based on a software comparison followed by an extensive trial and error-testing process. The study was executed in a case study for which the domain concerned the midsection of a 203m offshore vessel named Orion, as TO could result in substantial computational time such that analyzing a hull section is more efficient. The optimization was performed in multiple iterations with different design objectives using the method of Solid Isotropic Material with Penalization (SIMP). After a baseline comparison, the manufacturing constraints were implemented and developed.

Despite the availability of manufacturability constraints, it is currently not possible with the software used in this study to design the complete structure of a steel midship. However, it can be very useful to employ TO as a suggestion early in the design process, as this can result in manufacturable structures (see Figure 77). The TO software used in this study can help designers with structural suggestions in the basic design phase when there are fewer design limitations.

This case study resulted in unusual 45-degree, X-shape components that are highly efficient for sustaining shear loads and which resulted in a weight reduction of the mid-section of 2.4%. In addition, the result shows that unique structural shapes under various angles can result in an optimal strength-weight design rather than in orthogonal structural parts with a fixed span.

CONTENT

ABBREVIATIONS

FEA	Finite Element Analysis
FEM	Finite Element Method
TO	Topology Optimization
SIMP	Solid Isotropic Material with Penalization
BV	Bureau Veritas
LR	Lloyds Register
DNV	Det Norske Veritas
CAPEX	Capital expenditure
OPEX	Operating Expense

1 INTRODUCTION

When a ship's structure is engineered, it must meet the requirements set out in the rules by classification societies such as Bureau Veritas (BV), Lloyds Register (LR), or Det Norske Veritas (DNV). These requirements are incorporated into calculation programs, supplied via private companies or classification societies, whereby the structural parts are analyzed against prescribed loads to size a ship strong enough to sustain all limit states. The structural dimensions are not calculated for each structural component; for example, when multiple secondary structural components are on the same supporting primary structural component, then not every secondary structural component is calculated individually but is instead checked at expected critical points. For example, the first, middle, and last secondary structural components and are selected based on the experience of the analyst. This is because companies work with a lead time and budget arranged with the customer, and analyzing each structural detail requires too much time. With the use of finite element analysis (FEA), the complete structure is analyzed against prescribed loads, which enables the determination of detailed dimensions of all stiffeners and plates within a reasonable lead time (Goodwin & Dodkins, 2013). Using FEA for the design of the structure could result in better engineering in the form of a lighter ship (Bos, 2019).

The currently most common structural forms could be optimized by replacing them with a unique, natural shape. Structural design is well-established in shipbuilding, and for many years, has consisted of longitudinal stiffeners, transverse stiffeners, and bulkheads with often a fixed distance due to being easy to manufacture and driven by the production methods over time (Iqbal & Shifan, 2018). When considering nature, however, which has been evolving over billions of years, we do not often observe the standard structural form. Today, structural problems find solutions in nature and use more unique structural forms, such as the unique bone-like structure in Figure 1 of the Light Rider e-motorcycle, which is 30% lighter than conventionally manufactured e-motorcycles.

Figure 1—The Light Rider e-motorcycle (Altair & APWorks, 2016)

Topology optimization (TO) uses FEA, and it enables the unique structural forms discussed above. This mathematical approach generates an optimized material distribution for a set of loads and constraints within a given design domain, which can be an area or volume. The result can be used to inform the design of an improved part. Although the results provide helpful insight they often cannot be used literally as they are more organic in nature and cannot be manufactured with typical shipbuilding manufacturing methods other than additive manufacturing.

This project aims to research the possibility to design the structure of a ship based on TO, whereby the material of the ship is situated where it is needed. TO regards many variants; however, when "Topology Optimization" or "TO" is mentioned, structural topology optimization is assumed. The goal is that the new method results in a lighter structure with the help of unique structural forms. Applying TO to a ship's structure is fairly new and has only be performed as a concept design suggestion where the outcome of the optimization is often a complex structural form that cannot be made with standard shipyard tools from cut steel plates (Leidenfrost, 2015), (see Figure 2).

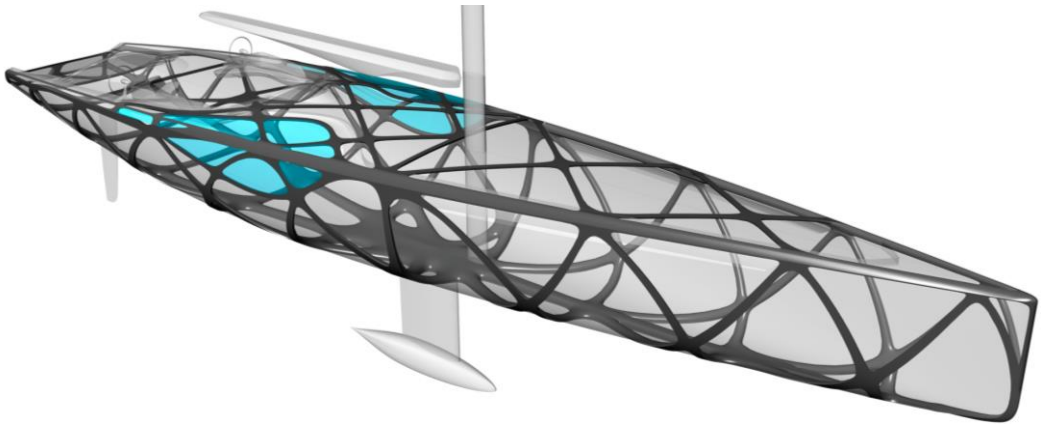

Figure 2 – TO structure of 46m concept sailing yacht (Leidenfrost, 2015)

Vuijk (2020) recently contributed a TO of the steel midsection structure of a trailing suction Hopper Dredger. This resulted in a weight reduction of the total midsection of 23%, but this number is likely to be lower in practice due to practical production considerations. This study did not consider compartmentation and productivity, and the used TO method was a crude analysis according to the author. The TO outcome was constrained to cut steel plates with a constant thickness to increase manufacturability. The result was optimal from a weight reduction perspective; however, it resulted in a complex structure that is neither cost-effective nor practical from a shipbuilding manufacturing perspective, (see Figure 3).

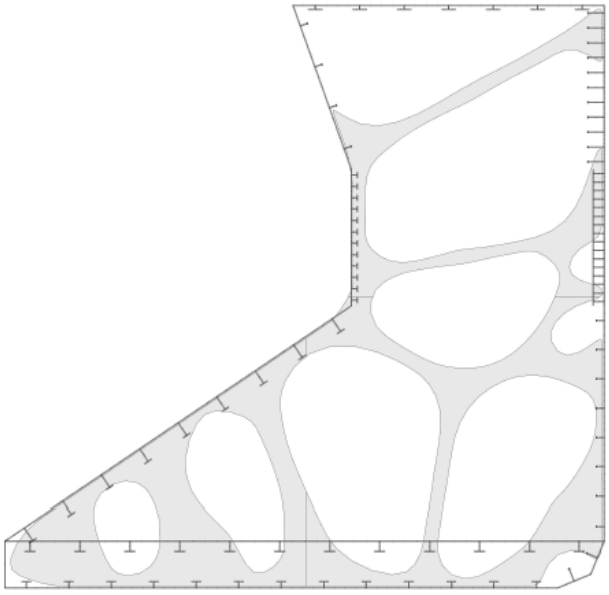

Figure 3 - Abstraction of web frame and longitudinal stiffener arrangement of the optimized ship midsection (Vuijk, 2020)

This study extends by translating the topological structures discussed above into practical shapes that are easier and cheaper to build and more favorable for inspection and maintenance.

The ship structure is currently calculated based on rules that have translated static and dynamic loads into easy formulas. TO does not use the formulas from the rules but instead utilizes them for the load cases and constraints from the client, defined by the designer, which requires research to be conducted into various loads on the ship's hull and translated for multiple load cases. This paper also concerns the research of available software programs and the current design process of C-Job to to advise how TO can be integrated into the company.

When it is possible to design a manufacturable structure with TO that can be made with standard shipyard tools – without additive manufacturing – from cut steel which is cost-effective and practical from a shipbuilding manufacturing perspective, this is new and will be used by C-Job.

1.1 Objective

The objective is to research the possibility whereby C-Job can design a lighter structure of a ship – while complying with the strength requirements – based on TO using unique structural forms that deviate from traditional longitudinal stiffeners, transverse stiffeners, and bulkheads but is manufactural using steel-cut plates.

The main research question is:
How can topology optimization be applied to design the structure of a steel midship where the resulting structural form is manufacturable using steel-cut plates and cost-effective from a shipbuilding manufacturing perspective?

1.2 Result

This research aims to deliver a clear conclusion and guideline of the possibilities to design the structure of steel ship with TO – using proposed software programs – that provides weight reduction while remaining within the limits of manufacturability.

2 LITERATURE REVIEW

This chapter provides knowledge to research the possibility to design the structure of a steel midship with TO in which C-Job can design a lighter structure while complying with strength requirements.

2.1 Current design method for scantling

How TO can be applied to design the structure of a steel midship requires an understanding of the current process and design stages; for example, there are different optimization performed during the basic and detailed phases. The design process is reviewed based on interviews with employees (Boer et al., 2020) and published works (Rigo & Caprace, 2011), (Okumoto et al., 2009), (Eyres & Bruce, 2012), (Shenoi & Guedes Soares, 2015), (Hughes & Paik, 2010).

The design phases within C-Job include:

- Concept design
- Basic design (Preliminary)
- Detail design (Contract)

Each phase undergoes an iterative 'trial and error' process whose result must meet pre-specified requirements. One begins with assumptions and determines whether the design meets the requirements, which is often not the case during the first iteration. Therefore, in the next iteration, some assumptions are adjusted, and the process is repeated several times which can be situated in a spiral, see Figure 4.

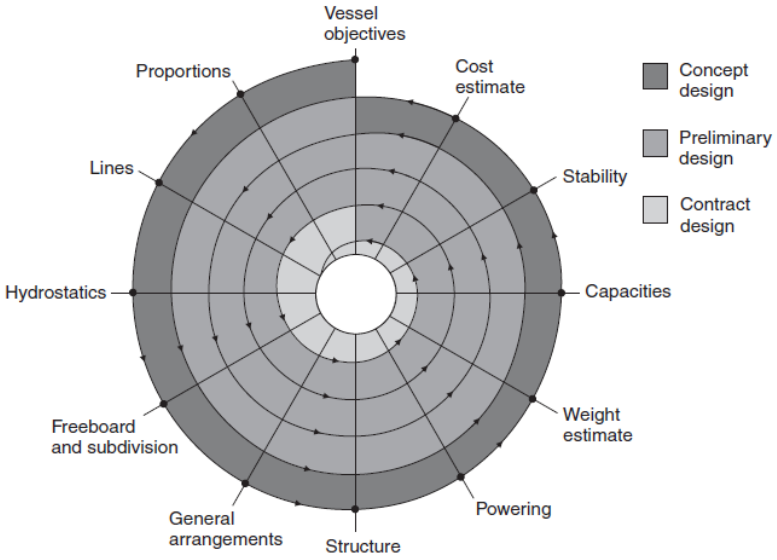

Figure 4 – Design spiral example (Eyres & Bruce, 2012)

The conceptual design phase begins with the required specifications proposed by the customer. The primary hull data are determined based on experience or reference ships, which enables calculating proportions such as displacement, L/B, installed power, speed, righting arm, and meta-centric height, and a preliminary design can be created using statistics from reference ships. In the first iteration, an entire round of the design spiral is fulfilled, and one can begin with the basic design after adjusting the main parameters during the second iteration.

The hull, tank, and deck can be arranged during the basic design phase, beginning with a (general) arrangement of the interior and exterior design using a 3D model required to estimate the initial weight and stability. The weight and stability are likely not correct, which results in multiple iterations. After determining the initial arrangement and 3D model, the scantling calculation can determine the structural dimensions. The structural dimensions are often calculated roughly; for example, when multiple secondary structural components are on the same supporting primary structural component, then not every secondary structural component is calculated individually but are instead checked at expected critical points. For example, the

first, middle, and last secondary structural components and are selected based on the experience of the employee.
After setting the structural dimensions during the basic design phase, the detailed design phase begins with an exact weight calculation and then a stability calculation, which enables the design of the final hull using the known displacement and hydrostatic characteristics. In a later iteration, this design step is the hull optimization, to optimize, for example, hull resistance, seakeeping, and stability.

The loads must be known before determining the strength requirements of a ship. During operation, a ship is subjected to the following different load patterns that result in material stress:

- Static loads, which do not vary with time beyond negligible effects. This includes the hydrostatic pressure, weight of the ship components, cargo, and ballast loads. The longitudinal load related to the overall strength of the hull, such as bending moment, shear force, and torsion moment, are also considered static loads.
- Dynamic loads have substantial variance over time, which requires dynamic analysis. The hydrodynamic pressure due to waves, impact loads, wind loads, and other operational loads are considered dynamic loads.

These loads are exerted on the ship's structure that generally consists of stiffeners that reinforce the plate to prevent distortion and local buckling, see Figure 16. Due to the complex interactions between the loads and strength requirements of the structure, programs are used for the structural design of the ship. Such programs are based on the rules of classification societies such as Bureau Veritas (BV, 2021), Lloyd's Register (LR, 2016), or Det Norske Veritas (DNV, 2020) whereby the structural parts are analyzed against prescribed loads to size a boat strong enough when used as intended.

The structure could be calculated in more detail by analyzing the entire structure concerning the requirements (Goodwin & Dodkins, 2013). Using FEA, the entire structure is tested against the prescribed loads which makes it possible to determine in more detail the dimensions of all stiffeners and plates. In addition, FEA is becoming more integrated into the ship classification society rules for design and analysis according to, for example, literature from DNV-GL (Rörup et al., 2016) and scholars at Harbin Engineering University in China (Iqbal & Shifan, 2018).

2.2 Finite element method

Finite element analysis is the application of the finite element method (FEM) to obtain approximated solutions of boundary value problems in engineering or so-called field problems that often involve a physical structure. In the FEM, a structure is divided into a mesh representing a finite number of elements interconnected by nodes. The mesh approximates the structure and becomes more precise when the mesh size decreases (see Figure 5) which results in a longer calculation time. The mesh size must fit in the smallest dimensions of a stiffener, s x s. Due to the development of analysis methods and progress of computing power, FEA is widely used in industries such as naval engineering, automotive, and aviation.

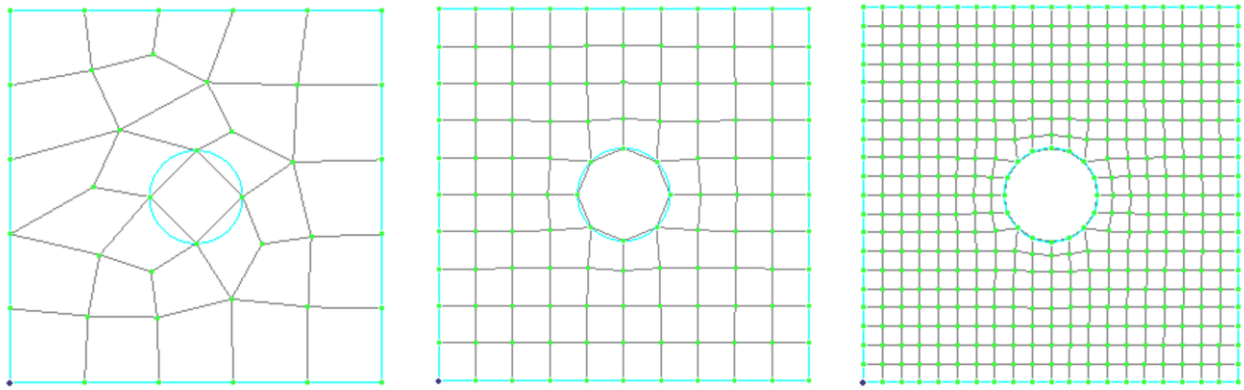

Figure 5 – Mesh refinement of a square structure with hole; blue lines represent structural shape, black lines represent elements, green interconnections represent nodes.

Using FEA for scantling could improve engineering in the form of a lighter ship (Goodwin & Dodkins, 2013). For example, in a study by Bos (Bos, 2019), FEA was used to reduce the structural weight on an existing mid-section of a 47m motor yacht. Prior to designing the structure with FEA, an intermediate optimization step was performed with the aim of reducing the structural weight by spending more hours with the existing method based on the rules. The intermediate step was performed with a fixed and varying frame spacing, which resulted in a total structural weight reduction of 3.74% and 6.65%, respectively.
The optimization using FEA was done iteratively, and the model was recalculated after each structural modification. This resulted in a structural weight reduction on the total midsection of 7.90%.

In a study from 2016 (Elhewy et al., 2016), the structure of an offshore supply vessel was optimized through a detailed FE model using MAESTRO software by reducing structural element thickness within safe limits. Blind search optimization was applied in four loops which reduced 42.4% of the total steel weight within safe limits. This figure's significance calls into question whether the initial design was constructed to be too heavy. In addition, this study lacks further information concerning the construction and building year.

Numerical methods such as FEA have traditionally been used to validate and refine existing designs, but this represents a poor use of powerful technology (Goodwin & Dodkins, 2013). Finite element analysis is most efficient when it can be performed during the concept design phase. The downsides of FEA are that it requires a 3D model, which is often not available at the beginning of the conceptual design phase, and it is generally expensive to create global FEA models for ships with standard pre-processors.

Studies from (Dumez, 2008), (Doig et al., 2009), and (Holmberg & Hunter, 2011) showed that the implementation of FEA into ship design using a global FE model during the concept design phase reduces costs. The simulation-driven design allows FEA to be used at the beginning of the design process, which enables a detailed assessment of the structural concept.

Global strength and cargo hold analyses are currently conducted using different FE models since the requirements for a model generation—in particular mesh size—are significantly different. Recent literature (Rörup et al., 2016) published by authors from DNV-GL showed a new Advanced Whole Ship Analysis procedure based on analyzing a global FE model using a mesh-based on stiffener spacing, which can be conducted efficiently using a basic 3D model. This new design process increased the quality of the results and reduced the analysis and 3D modeling time.

When the conceptual design is effectively predictable using FEA, the results can be used during the detailed design process. The current tendency in ship engineering is to develop methods for a merged design process, where the 3D ship model is in one software program and used for multiple steps during the design process (Iqbal & Shifan, 2018).

2.3 Topology optimization

In combination with FEM, TO can be used to optimize material distribution for a set of loads and constraints within a given design space, which can regard an area or volume and provide an optimum solution for predefined design objectives such as minimizing mass, stress, or maximizing stiffness.

2.3.1 BASICS

Structural optimization can be categorized into 3 techniques (displayed in Figure 6) (Bensoe & Sigmund, 2003):

- Size optimization, which aims to find the optimal dimensional distribution of a predefined plate or truss structural design.
- Shape optimization is the extension of size optimization and optimizes the shape of a predefined layout with the help of additional degrees of freedom within a given design domain, but the topology stays unchanged.

- Topology optimization extends size and shape optimization and allows the determination of features such as the number, location, shape of holes, and connectivity of the design domain.

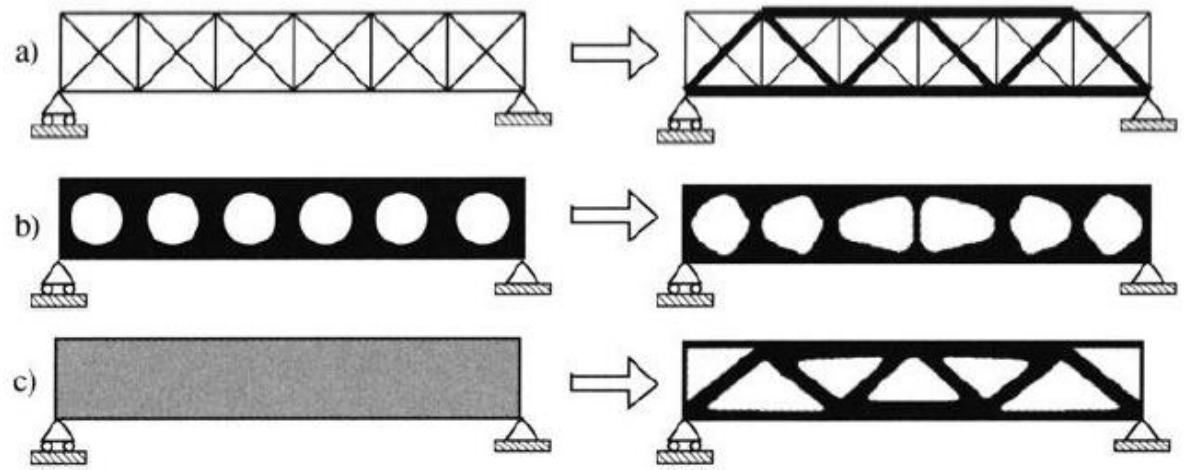

Figure 6 - a) sizing optimization, b) shape optimization, c) topology optimization (Bensoe & Sigmund, 2003)

Topology optimization has been successfully applied in the aerospace and automotive industries, primarily to reduce product mass and improve product efficiency. Airbus represents a high-profile adopter of TO in the aerospace industry and used it in 2002, (Krog et al., 2011), to design the wing ribs for the A380, which resulted in 500kg weight savings in the structure of the wing. Stress and buckling were included in this simulation-driven design.
Jaguar Land Rover was an early adopter of TO within the automotive industry for the design of vehicle components (Zeguer & Bates, 2012) and used the technology to improve robustness and optimally design their components.
SAICS Motor has recognized the benefits of TO and produced 4.5 million vehicles in 2014. The company used TO to optimize the rapid development of new passenger vehicles (Husson & Burke, 2011).
In 2018, static analysis TO was performed to optimize the structure of an aluminum motorcycle frame (Bala Manikandan et al., 2018), which resulted in a weight reduction of 28% without compensating for the performance of the frame and proves the technique's efficacy.

2.3.2 SCIENTIFIC DEVELOPMENTS

Topology optimization can be divided into gradient-based and non-gradient-based. The latter is based on repeated function evaluations using a stochastic or population-based algorithm, and the design variables are discrete values. In stochastic optimization, the variables are random while the population-based algorithm maintains an entire set of candidate's solutions. The iterative outcome of this method is the distribution of solid and void elements of the structure, which are performed, for example, using the Evolutionary Structural Optimization (ESO) or Level-Set Methods (LSMs).

In the ESO method, a criterion function—for example, stress or energy density—is calculated for each element. During each iteration of this method, some elements with the lowest criterion function value are eliminated. In the bi-directional ESO (BESO) method, new elements are added next to elements with a high criterion function value. Due to the contribution of (Ling & Steven, 2002) and (Edwards et al., 2007), a recent version of ESO regards a two-stage procedure to improve the result, which begins with solving large numbers of equations using the standard ESO method and calculation the performance index for each solution. The global optimum of the performance index is then determined via a numerical comparison. This method, however, lacks evidence that the element elimination or admissions provide the optimal solution, and it is not efficient to select the best solution through numerical comparison (Tanskanen, 2002). In addition, there is no control over the final volume fraction, and the method cannot be easily extended to multiple constraints and load problems (Rozvany, 2009).

The LSM approach defines the boundary of the design with a zero-level contour of the level-set function, while the structure is defined with the domain where the level-set function takes positive values. The level-set-based TO regards different approaches, for example, discretizing the level set function, mapping the level-set field onto the mechanical model, and updating the level-set field during the optimization process (Dijk et al., 2013). The shortcomings of this method include its reliance on regulation techniques and that it can result in inconsistencies during the optimization process, where the convergence behavior due to oscillation also poses a challenge (Dijk et al., 2013).

The gradient-based optimization uses modeling of the densities with continuous variables, whereby the density can attain values between zero and one but must be modeled in a continuous setting achieved through interpolation. The SIMP method developed by Bendsoe and Sigmund (2013) is currently most often used.

The SIMP approach provides the relation between the density design variable and material property through a power law that uses penalization to make intermediate densities or thicknesses unattractive: $E_i = \rho_i^p * E_0$ where p is the penalization parameter and E is Young's modulus of the solid material. The goal is to minimize the strain energy density by varying the stiffness of the element with the Young's modulus. The penalization will suppress intermediate values with checkerboard instabilities and encourages the development of either void (ρ=0) or solid (ρ=1) elements. This will result in a nonconvex problem and therefore the optimum cannot be guaranteed, which is true for all gradient-based methods (Sigmund & Maute, 2013). The p-value can be changed within limits, where too low or too high p results in too much greyscale, and the most efficient p-value for a favorable convergence is 3 (Bendsoe & Sigmund, 1999). This method requires few iterations compared to others and can process a combination of multiple constraints, multiple load conditions, multi-physics problems, and large systems (Rozvany, 2009). In addition, the SIMP method is based on anisotropic material.

2.3.3 APPLICATIONS

Topology optimization is recently applicable to the shipbuilding industry. In 2020, Vuijk (2020) optimized the steel midsection structure of a trailing suction hopper dredger in 2 steps with the objective to minimize mass. The first step was a shape optimization for the longitudinal stiffener arrangement. The second step was a TO for the transverse web frame. This optimization order follows the hierarchy in which stress is introduced into the structure; from hull plates toward the stiffeners and eventually the web frames. The total optimization was performed for 7 different web frame spacings ranging from 25% to 175% of the original web frame spacing.
A Simulated Annealing algorithm was used for the shape optimization with a simplified model of the ship to parametrize the geometry into only 11 panels with T-stiffeners. Each panel has a set of variables that describe its geometry; the number of stiffeners, plate thickness, web height, flange width, web and flange thicknesses. This resulted in feasible optimization outcomes, however, no clear parallel was found between the plates of different web frame spacings. The TO was performed for each of the 7 web frame spacings with the BESO method. The outcome showed that structural components not in an orthogonal way and along ship hull but under various angels could reduce the mass of the web frame.

Vuijk used this method because it concerned a large model, and it is easily adapted. This resulted in a weight reduction of the total midsection of 23%, which is likely to be lower in practice due to practical production considerations. According to the author, the used TO method was a crude analysis and the study did not consider compartmentation and productivity. The structural development of the TO was constrainted to cut steel plates with a constant thickness to increase manufacturability. The result was optimal from a weight reduction perspective, however, it resulted in a complex structure that is neither cost-effective nor practical from a shipbuilding manufacturing perspective, (see Figure 3).

Leidenfrost (2015) developed the composite hull structure of a 46m sailing yacht (see Figure 2) using TO software Altair Hyperworks/Optistruct and determined a conceptual load-dependent structural layout. This was realized using a design suite that includes all necessary functions and data. To represent the actual forces

acting on the hull within a time domain, the multi-load cases are quasi-static based on first principles and applied to the global FE model according to a worst-case sailing condition, which is validated using a simple pontoon structure.
The multiple load cases consisted of two load groups: wave-induced, and rig-induced global loads. The objective of this study was to develop the primary structure of the hull with respect to global loads, and therefore, local and dynamic loads are neglected. The wave-induced loads from the hydrostatic pressure—that is in balance with the weight—are applied by dividing the hull into 20 equal sections and for the corresponding cross-sections, weight and buoyancy loads are separately calculated and distributed the way they act on the hull in sailing condition. Weight forces are applied to the whole area of each section since the whole yacht is exposed to the same gravity and buoyancy forces are only applied to areas representing the wetted hull. Each cross-sectional load is distributed to the global FE Model corresponding to its hull section. RBE3 beam elements are utilized, which transfer loads without inducing additional stiffness. This method resulted in favorable results with little change to the overall structural behavior of the yacht. The rig loads were calculated based on standard methods and were applied to the FE model at their designated hull attachment points, such as chain plates and mast base.
The design space begins with a Rhinoceros 3D model and is simplified to a closed surface model in CatiaV5 according to the interior layout, where a minimum distance of 500mm between the outer and inner skin is maintained for structural evolution. Using the FE software, the design space is auto-meshed with 280mm solid elements (tetrahedral) and constrained only at 1 random node to enable computations as the forces and gravity are in balance and reflect a steady-state sailing condition.
The final hull structure is developed in 4 SIMP-based TO iterations within the design space according to maximize stiffness with varying, volume fraction, draw direction, and the following parameters:

- Design objective to maximize stiffness and minimize displacement, which is equal to minimizing compliance (strain energy).
- Design constraint with a volume fraction upper boundary of 0.3, meaning that the optimized volume is a maximum of 30% of the design space volume.
- Geometric constraint which is a symmetry constraint over the midship plane, and a draw direction constraint in the z-axis, which defines the direction in which material with high density should be accumulated.

To further refine the results, a surface model is used from the 3rd TO iteration since the material is only distributed along the hull skin, main deck, and the two bulkheads. In addition, the design space remains defined by surface elements with a mesh size of 100mm, while the minimum distance of 500mm between outer and inner skin is maintained.
The final results concern surface load paths exported as surfaces using CatiaV5 and traced with spline curves that refine the exported topology results. Along with these spline curves, half-cylinders are extruded that represent the truss members of the hull structure.
This study showed that it is possible to formulate the design space of TO according to the interior layout from the customer, which can result in design spaces that consider additional parameters that could lead to increased control of manufacturability when the hull structure of a steel ship is designed using TO. In addition, applying balanced loads represents effectively a steady-state sailing condition.

In a study by (Altena, 2019), the structural weight of a composite planing yacht of 13m is reduced by applying concepts from bionic engineering. The structure was designed using the TO software Altair Inspire, which is less advanced and more user-friendly than Altair Optistruct. The SIMP method based on minimizing mass is used in three iterations to optimize the structure of the hull and is validated via FEA. The loads were applied separately for each corresponding structural section according to standard regulation with a safety margin of 20% and categorized into, bottom planing pressure, side pressure, and deck pressure.
The model has different constraints for each loading condition to prevent unrealistic stress concentrations. During the first iteration, the generated structural forms could not be used since the design space was too unbounded (see Figure 7). This was improved by applying a draw direction constraint in the z-axis to define the direction in which material should be accumulated. Another problem in this stage was that the structure

was distributed at the constraints which are not present during a real situation, which was slightly addressed by applying the constraints for each loading condition at the largest distance of the load.
The composite structural weight was reduced by 15% while complying with the strength requirements. This research provided a method for designing the structure of a ship using TO. To improve the manufacturability of the hull structure, the design domain was bounded with constraints at the bulkheads to accumulate material distribution at those locations. The shortcomings of this method include the application of three different load case models and the constraints, and the latter provides an unrealistic model.

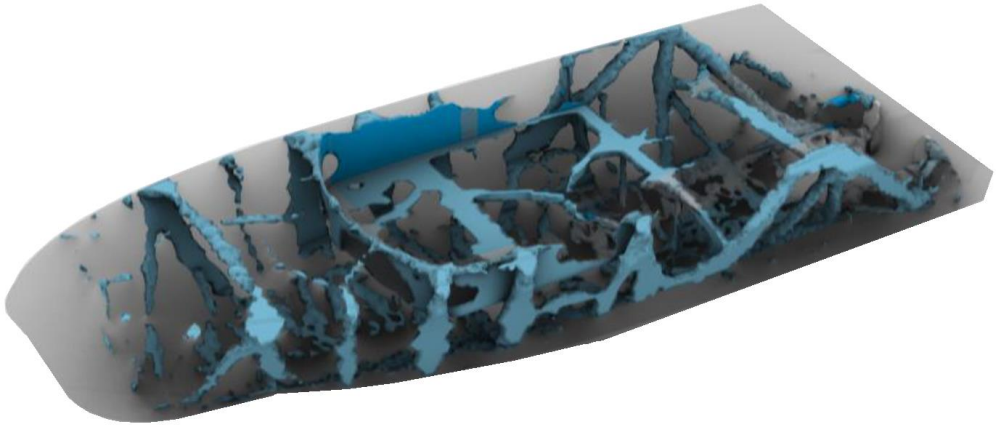

Figure 7 - Merge To output from load cases, bottom planing pressure, side pressure, and deck pressure (Altena, 2019)

Bakker (2020) proposed a SIMP TO method that allows for simultaneous optimization of the topology of modular stiffeners and layout on the base shell or plate. This was realized by introducing a fixed number of module stiffeners, which are subjected to a density-based TO, and a mapping of these modules to a ground structure of stiffeners. The method can be utilized as a design tool in the conceptual design phase of structures with stiffeners. It was applied successfully to several examples of stiffened plates and resulted in clear topologies for any number of modules and a distinct layout on the base.
This study results in a more efficient method for the current TO process that optimizes the topology and the layout on the base individually in an iterative process. The numerical examples in this study were converted into physical structures using additive manufacturing (3D printing) and were optimal from a weight reduction perspective. However, it resulted in a complex structure that is neither cost-effective nor practical from a shipbuilding manufacturing perspective, see Figure 8.

Figure 8 – 3D print result of the simply stiffened plate for the case of 4 templates per type *(Bakker, 2020)*

2.4 Manufacturability

Many different processes with different characteristics are used in the manufacturing of parts and machines, the most common being (Kalpakjian & Schmid, 2009):

- Forging
- Casting
- Milling
- Turning
- Extrusion
- 2D plate cutting
- Rolling
- Welding

Only the last three are relevant for the construction of the structure of a steel ship (Boer et al., 2020).

Cutting 2D steel plates is commonly executed via laser, plasma, or waterjet Computer Numerical Control (CNC) machines. A laser cutting machine uses an electromagnetic radiation source that emits light focused to a fraction of a millimeter, which enables cutting through 30mm-thick steel, often supported by a cutting gas. Plasma cutting is a high speed, low cost, less precise than a laser, and it functions using electrically conductive materials. It can cut up to 38mm-thick steel using hand-held torches and 150mm-thick steel using CNC machines. A waterjet machine uses a high-pressure water pump that results in 4000bar through a diamond spray head with a speed of 900km/h, which can cut through any material with a maximum thickness of 200mm. (Kalpakjian & Schmid, 2009)

Rolling is the manufacturing process of compression loads applied through a set of rolls for plate steel to reduce its thickness, form a radius, or create a profile. With a roll radius, a smooth curvature radius is produced with a constant transverse cross-section. The rolling can be performed with high temperatures (hot-rolling) or ambient temperatures (cold-rolling), which can result in the same geometries but with different material properties, such as strength and hardness.

Welding locations must be accessible for the operator to weld and perform an inspection. From a drawing, it is relatively simple to indicate a weld, but the accessibility requires careful planning, especially when the outcome of the TO regards a complex structure. Most welding processes are limited by the torch size and angle of the electrode. To provide adequate clearance for the electrode in a horizontal fillet welding, the clear distance from the welded element should be half of the height of the obstructed part, and there should be clear space around the joint of 45 cm (AISC, 2015). This is further specified by C-Job with a maximum welding angle of 25 degrees (Boer et al., 2020).

Topology optimization is effective for generating an optimal solution, which often includes complex geometries that are neither cost-effective nor practical from a manufacturing perspective, for example, see Figure 2. Post-processing the result using interpolation functions and curve smoothening usually results in a modified model that loses its optimized characteristics (Bensoe & Sigmund, 2003). The manufacturability of the TO design has also been assured using density or sensitivity-based filtering techniques. The disadvantage of these methods concerns the gray transition regions between void and solid; however, this has been alleviated via various projection methods (Wang et al., 2011).

In an engineering software study by (Vatanabe et al., 2016), design variable domains were projected onto intermediate(pseudo)-density domains to exclude undesirable solutions of the optimized problem. This method uses different advanced design domain constraints that consider the independent manufacturing process discussed above and was used by (Guest et al., 2004) and (Guest, 2009) to minimize length scale on structural members generated by TO and to reduce checkerboard problems.

To implement the previously described manufacturing constraints for the 2D cutting, rolling and welding of steel plates into a TO framework, the design geometric constraints could be (Vatanabe et al., 2016):

- member size
- hole size
- draw direction
- extrusion
- pattern repetition
- symmetry

With the member size constraint, the minimum and maximum dimensions of structural members can be controlled, which was implemented by (Guest et al., 2004) and (Zhou et al., 2001). This minimizes the checkerboard effect and provides a more discrete design, and this constraint is highly effective at improving welding since the accessibility of the welded spot can be controlled.

Minimum hole size controls the distance between members and the dimension of holes by generating a minimum required space, which could improve the accessibility of welding. This method was successfully implemented in a study (Guest et al., 2004). Because this method sets the minimum size of holes for the optimal solution, it could lead to an unstable solution when applying it combined with the member size constraint due to the conflict of constraints (Almeida et al., 2009).

Draw direction constraints are most effective for the casting process, where cavities that are not open and aligned with the sliding direction of the die cannot be constructed. This constraint fixes the outcome of the TO in the sliding direction of the die so that it is manufacturable via a casting process that can be arranged in a single or split die. This constraint could be used to reduce the complexity and improve the manufacturability of the TO outcome as the direction of the structural development is limited in one assigned direction (Strömberg, 2010) and was successfully implemented on a high-performance sports car dashboard (Mantovani et al., 2017).

The extrusion constraint is similar to a single draw direction constraint, but it results in a design characteristic with a constant cross-section along a given path suitable for parts manufactured through an extrusion process. The constant cross-section of structural members can be attained regardless of the boundary conditions and loads and can improve the manufacturability of non-extrusion products since constant cross-sections are faster and cheaper to build (Patel et al., 2009). This constraint could be used to further reduce the complexity and improve the manufacturability of the TO outcome as the structural development is limited to a constant cross-section, like for example T, L, and H beams (Ishii & Aomura, 2004).

Pattern repetition allows linking different structural components to produce similar topological layouts, including when the regions are subjected to different load cases. A master pattern is defined followed by several sub-patterns that mimic the main pattern. This constraint was successfully used in TO for a more practical design for the constructability of high-rise buildings (Stromberg et al., 2011). This constraint could further reduce the complexity of the TO outcome of the structure of a steel ship and, for example, improve construction time and cost.

Symmetry constraint allows the TO result to be symmetrical independently of the boundary conditions and loads. Some manufacturing parts are symmetrical and benefit from symmetrical TO for their further design and manufacture. This is possible by adding a symmetry constraint into the optimization formulation. This constraint results in a set plane symmetry that can be independently arranged for multiple planes and reduces geometry complexity, which can result in a manufacturable steel structure when, for example, 2D plate cutting and rolling are considered as construction methods. This constraint was successfully used in non-maritime TO studies by (Almeida et al., 2010) and (Zuo et al., 2006).
When applying these manufacturing constraints, it is recommended that a baseline comparison without the additional constraints is performed (Zhou et al., 2002) to assess the relative efficiency loss due to the constraints. Applying TO and including manufacturing constraints generally results in a trade-off between cost and structural performance in the decision process.

The selection of these geometric constraints depends on the used software and its available functions. In addition, the functions of the geometric constraints need to be tested, see Section 3.3. The use and implementation of the manufacturing constraints—for the final method to design the structure of a steel ship with TO—will be selected in an iteration case study, see Chapter 6.

3 METHODOLOGY

In this chapter, the methodology used to answer the research question is discussed.

3.1 Knowledge gap

Section 2.1 describes the current design method, and sections 2.2 and 2.3 show that applying TO with FEA is most effective during the concept-design phase. However, TO requires a 3D model of the structure of a steel ship, which is not available at the beginning of the project. Because no overview of the required data and parameters for a successful TO design process for the structure of a steel ship currently exists, research is needed to apply TO in the most efficient manner given the trade-off between the availability of the 3D model and conducting TO early in the process.
In Section 2.4, the manufacturability was defined, and the primary issue concerning TO is addressed, which is that the outcome of the design often regards a complex geometry that is neither cost-effective nor manufacturable from a shipbuilding perspective. This section describes research that alleviates this problem by applying projection techniques that consider manufacturing constraints for each construction process. Currently, however, these solutions have only been implemented during standard static engineering problems and not during the TO design of the structure of a steel ship. In addition, due to dynamic multi-load cases and constraints, applying these manufacturing constraints to the design of the structure of a steel ship by using TO is more complex than a normal static engineering problem.

In light of the extensive literature review given in the previous chapter, the following research gap:
Constraints which result in a ship structure that is manufacturable and cost-effective (from a shipbuilding perspective) using cut-steel plates have not been developed and implemented in topology optimization.

3.2 Software

The main general-purpose structural-optimization systems which have capabilities for size, shape, and topology optimization are Genesis, MSC Nastran, and Optistruct. In this chapter, the main software systems are compared based on research and literature (Choi et al., 2016), as summarized in Table 1.

There are no major differences in the optimum results for small-to-medium scale optimizations. The Genesis system offers efficient computational time while Optistruct offers a better optimal solution for size, shape, and topology optimizations. MSC Nastran provides good solutions for size and shape; however, this system needs more computer power resulting in a larger calculation time than Genesis and Optistruct.

For large-scale optimizations, the three systems also give similar results. However, the Optistruct system had the best computational time. The elapsed time of MSC Nastran was significantly higher than that of the other software systems.

Software system	Company	Conclusion
Genesis	Ansys	Efficient calculation time and results similar to those of the other software systems.
MSC Nastran	MSC Software	Results similar to those of the other software systems but with a significantly longer computational time.
Optistruct	Altair Engineering	Best structural TO outcome for small-to-medium scale and excellent computational time for small-to-medium and large-scale optimizations.

Table 1 – TO software system comparison.

Based on the literature review and investigation of the available software, Altair Inspire/Hyperworks was used as the topology-optimization software which operates with the SIMP and Optistruct as the solver

system. Optistruct was used because the optimization domain concerns the large-scale mid-section of a steel ship and Opistruct has the most efficient computational time (see Chapter 4).

In addition, Altair Inspire/Hyperworks includes the manufacturing constraints discussed in Subchapter 2.4 and is compatible with other software programs used within the company, which makes it highly suitable for this project. It is a complete software package for optimization problems in engineering and is shell-element based.

Ansys was used to process and edit the 3D model of the ship's steel structural mid-section because the final section of the structure within the company is in Ansys Spaceclaim, which is compatible with the TO software.

3.3 Verification of SIMP and design objective

To verify the software and SIMP, the TO model was checked to see if the results are logical and resemble existing results from the literature. This literature comprises the common bridge example in TO (Bensoe & Sigmund, 2003). See Figure 6c. This can be performed with a visual check, and the results do not have to match completely, as the structural dimensions of the bridge example and loads are not known. However, a good comparison can be made because, in both situations, it was optimized by maximizing stiffness, which does not depend on the load value but on the load location. In addition, different design objectives and constraints were tested. The latter are explained in Section 2.4.

The TO generates an optimized material distribution by removing unneeded material from the design spaces, thereby creating the lightest structure capable of withstanding the applied forces and moments. Depending on the boundary conditions, the type of applied loads, the design space, and the geometric constraints, there are several TO design objectives: i.e., maximize stiffness, minimize mass, or maximize frequency. The latter is not considered in this study.

Maximizing stiffness of a design space results in a shape that generates the least amount of displacement in the model. This can be realized with a mass target or a set percentage of each design volume. This design objective reflects the concept of lightweight designs in which a maximum stiffness with a minimum amount of material are used. Making the optimized model as stiff as possible is equal to minimizing compliance. In other words, it involves keeping the total strain energy to a minimum. However, the yield limits of the material were not considered, and a post-analysis with FEA is required, which was performed in an iterative process to obtain an optimal solution. Whether maximizing stiffness is desirable or to what degree it is so is defined by the designer, as the stresses also need to be considered.

The verification model is loaded and constrained the same as the literature reference in Figure 6c, which is a uniform deck load in the negative z-direction on the bottom bridge deck plate load indicated in red and is pinned at A and B and can roll at B in the x-direction, see Figure 10. The bridge example has a length of 10 meters, a width of 1 meter, and a height of 2 meters. After each TO an FEA analysis is performed with the legend colors displayed in Figure 9.

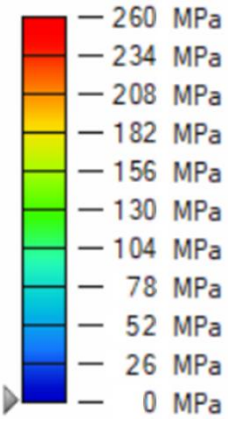

Figure 9 - Von Mises stress legend colors for coarse mesh

For the first iteration, the design objective was to maximize stiffness with a design volume set at 0.3, which resulted in an optimized volume with a maximum of 30% of the original design space (see box lines in Figure 10). No geometric constraints were implemented in this iteration. As can be seen in Figure 10, the outcome

is not symmetrical over the y-z plane, and the outcome is not manufacturable from cut steel plates with standard shipyard tools.

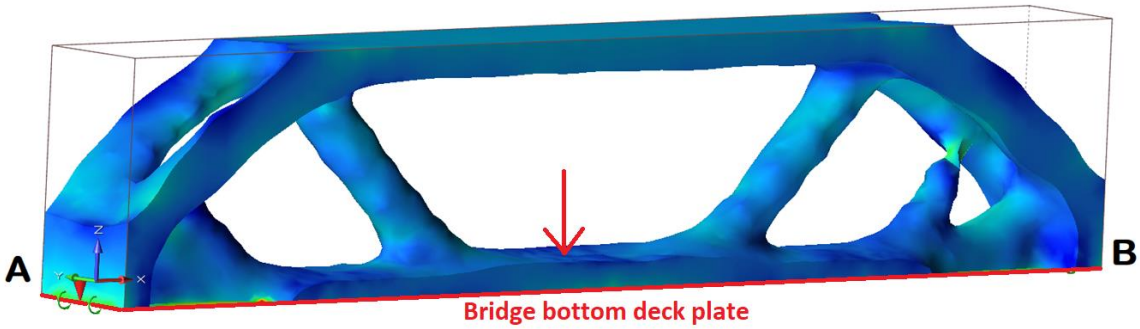

Figure 10 – First verification/test iteration.

The second test iteration uses maximizing stiffness with a design volume set at 0.3 and a draw direction constraint in the y direction. In addition, a symmetry constraint was implemented over the y-z plane which resulted in the FEA TO outcome, which the software developed in two minutes as displayed in Figure 11.

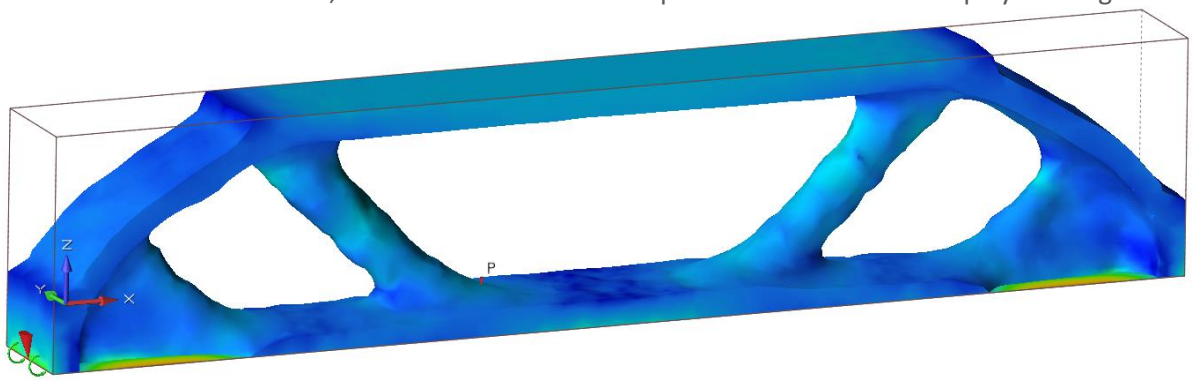

Figure 11 - Second verification/test iteration.

In addition to the second iteration, the third iteration has a member-size constraint of at least 0.5 m and a maximum of 1 m, which increases the TO calculation time significantly to five minutes (see Figure 12).

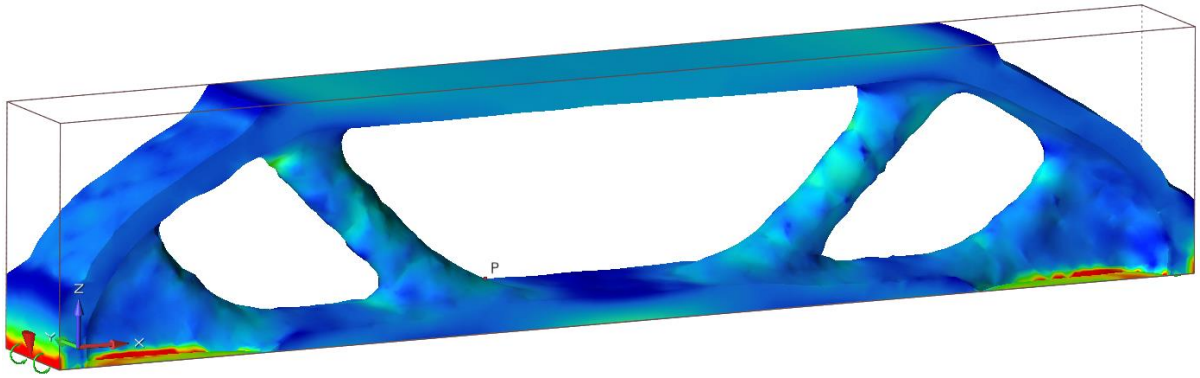

Figure 12 – Third verification/test iteration.

In the fourth iteration, the geometric constraint draw direction was replaced with an extrusion constraint. As can be seen in Figure 13, the structural layout is similar to that of the common bridge example in TO in Figure 6c, which verifies the SIMP. The TO optimization was performed in six minutes.

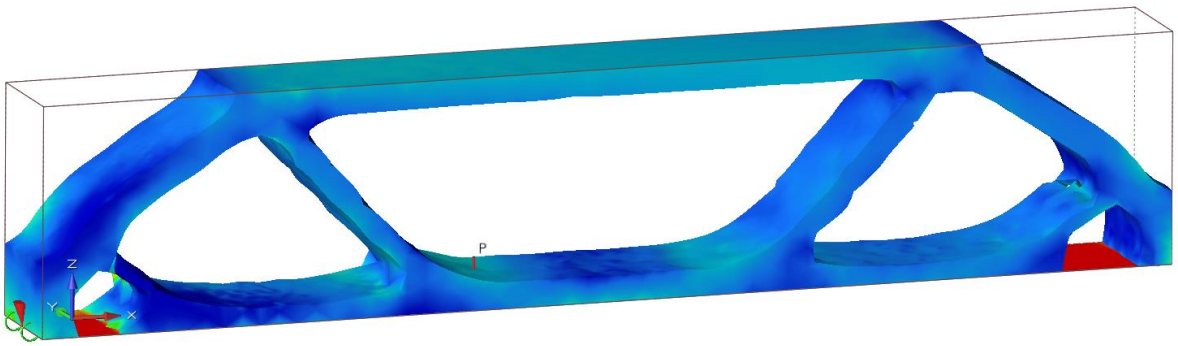

Figure 13 – Fourth verification/test iteration (48 tons)

Minimizing mass of a design space will result in a shape that has the lightest weight possible which can still support the applied loads. This can be realized with a safety factor for each design volume. The higher the safety factor, the more material will be added to the optimized shape to limit the overall stress in the model. With this global stress constraint, a post-analysis with FEA is not needed, as the stresses are already considered within the set maximum stress limit.

In the fifth iteration, a 15 minute TO was performed with a minimizing mass and a safety factor of 1.36. This resulted in a maximum allowable von Mises stress of 260 MPa (see Figure 14).

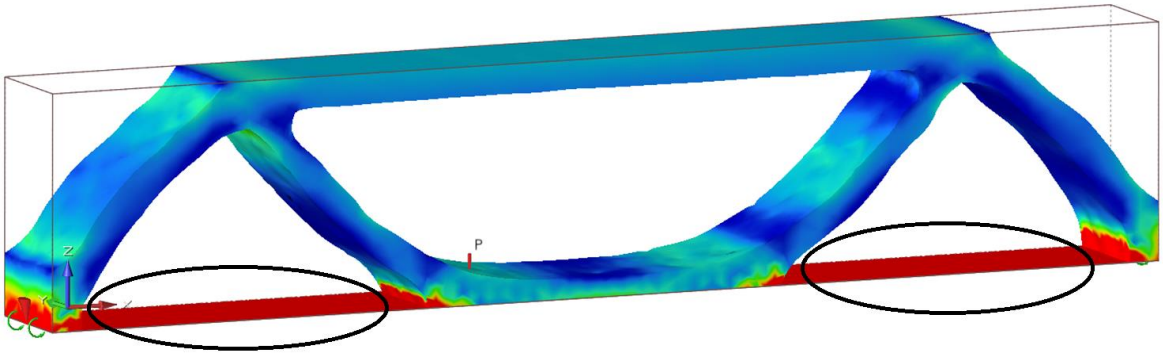

Figure 14 – Fifth verification/test iteration (40 tons)

Minimizing mass design objective targets the highest stress in the design volume to developed structural components. In Figure 15, the von Mises stress is displayed for the total design volume. A scaled display color is used to highlight the higher stress areas. The high stresses in this figure resembles the structural development in Figure 14. However, the stresses in the design space near the deck plate are mostly below the safety factor of 1.36, thereby resulting in a lighter structure that, in this situation, does not support the deck plate sufficiently and so results in distortion, as indicated in Figure 14.

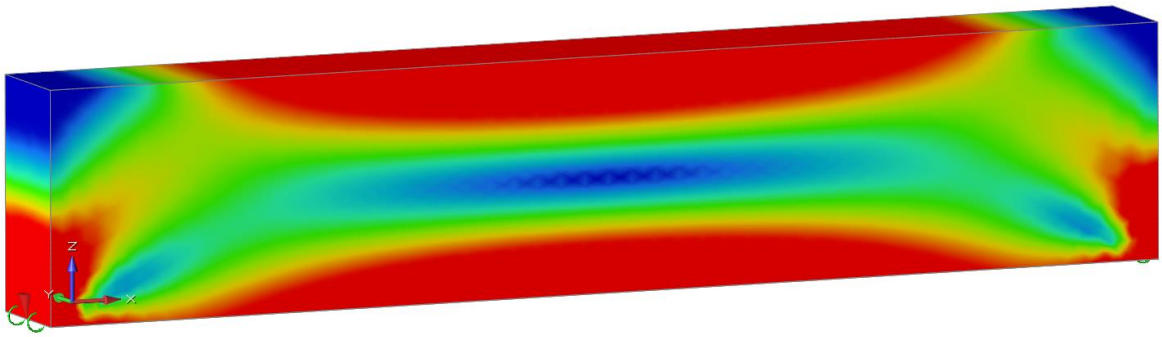

Figure 15 – Von mises stress in the total design volume with a scaled legend color

Upon increasing the safety factor from 1.36 to 2.5, the structural development became comparable with the TO outcome based on maximizing mass in Figure 13 (see Figure 16). As indicated in Figure 16, the unsupported deck-plate problem is minimized but continues to result in distortion, as this deck plate is over its maximum stress limit.

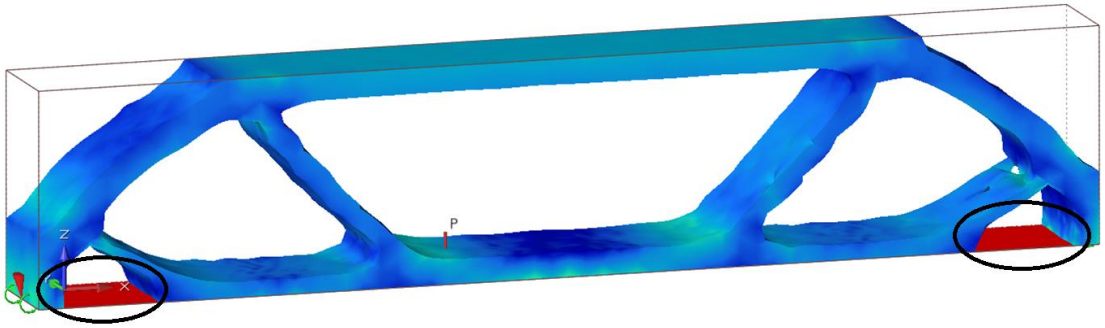

Figure 16 – Minimizing mass with safety factor 2.5 and extrusion constraint in the y-direction (47 tons)

The overall design objective used in other studies is to maximize stiffness (i.e., to minimize compliance) (Altena, 2019) (Bakker, 2020) (Leidenfrost, 2015) (Vuijk, 2020). With maximizing stiffness, a mass target is set that can be performed in an iterative process to reduce structural weight and maintain the minimal required stiffness to sustain the prescribed loads. However, due to developments in software, studies and the example above show that minimizing mass based on a safety factor can be used successfully. They also show a TO output similar to that obtained by maximizing stiffness (Bruggi & Duysinx, 2012) (Shimels et al., 2017). In addition, minimizing mass does not require a post-analysis with FEA. Still, the calculation time of minimizing mass in comparison with maximizing stiffness is substantially higher.

3.4 Approach

This section describes how the study—with the literature review as a starting point—was conducted. The research began by defining the hull section of the structure of a steel ship, which was converted to a file type usable for the TO software. A hull section was used because FEA and TO software can result in substantial computational time, and analyzing a hull section is more efficient.

After defining the hull section, the load cases and adjacent constraints were established and applied. The TO was performed in multiple iterations using the SIMP method and started with the design objective of maximizing stiffness, as this gives a similar TO result with a shorter computational time. For a baseline comparison, the TO began without extra constraints for manufacturability. The next step is to implement and develop the manufacturing constraints that consider the construction process of steel-cut plates which are 2D cutting, rolling, and welding.

The TO with extra constraints was executed for multiple iterations, and the results were then compared with those of the baseline data. Finally, the research question was answered by defining how TO can be applied to design the structure of a steel midship, where the resulting structural form is manufacturable using steel-cut plates and cost-effective from a shipbuilding manufacturing perspective. This TO iteration approach was performed as a case study, as documented in Chapter 6 (with a subsequent guideline situated in Chapter 7).

The above can be summarized as follows:

1. Define a 3D model of a structural section of the hull.
2. Refine and improve the hull section.
3. Convert the hull section to a usable file type.
4. Define load cases and constraints.
5. Run SIMP TO with multiple iterations for the baseline data.
6. Develop and implement manufacturability constraints.
7. Run SIMP TO in multiple iterations with added manufacturability constraints.
8. Compare the results with the baseline data.
9. Answer the research question.

Due to the large calculation time of TO, the software was installed and used on the company mainframe computer, which is equipped with a 16-core processor (3.70 GHz) and 64 GB of memory.

4 DOMAIN

In this chapter, the domain is set for the case study which concerns the midsection of the offshore vessel Orion – see the front cover and Figure 17 – which has the following main data:

Type	Offshore Heavy Lift DP3 Installation Vessel
Classification	Det Norske Veritas & Germanischer Lloyd
Length between P/P	203.0 m
Breadth moulded	49.0 m
Depth main deck	16.8 m
Depth freeboard	14.7 m
Draught scantling	11.0 m
Draught design	8.5 m
Displacement at 10.5m (installation)	93177 tons
Displacement at 8.5m (sailing)	74648 tons
Light ship weight	39355 tons

Table 2 – Main data Orion offshore vessel

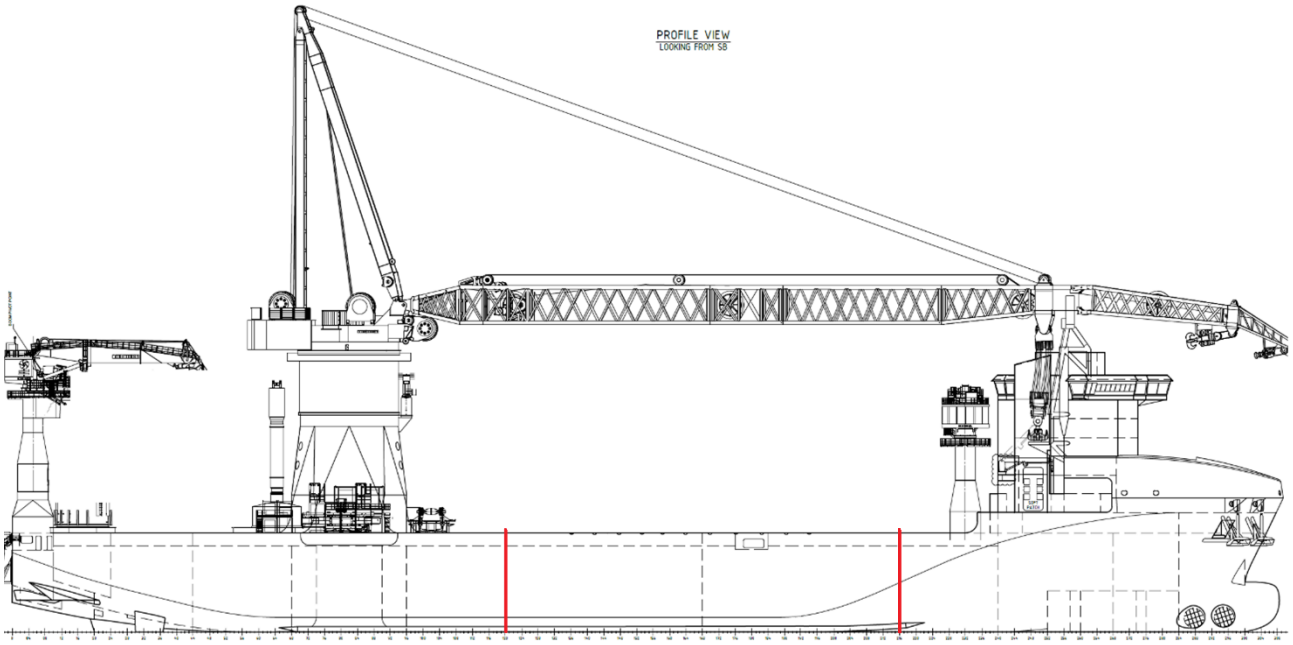

Figure 17 – Profile view Orion Vessel (Boer et al., 2020)

Because the structural midship area of the Orion has symmetrical properties, and to reduce the TO calculation time, a section was used from frame 144 to 192, which is the most critical compartment. The two adjacent compartments, forwards and aft, were modeled to correctly introduce loads into the model, as is recommended by the DNV-GL code (DNV, 2020). The model, therefore, extends from frames 120 to 216 (see Figure 17). The coordinate-system origin of the model starts at frame 120 at baseline on the centerline. A right-hand-coordinate system was used, with the x-axis pointing forward, the y-axis pointing portside, and the z-axis pointing up.

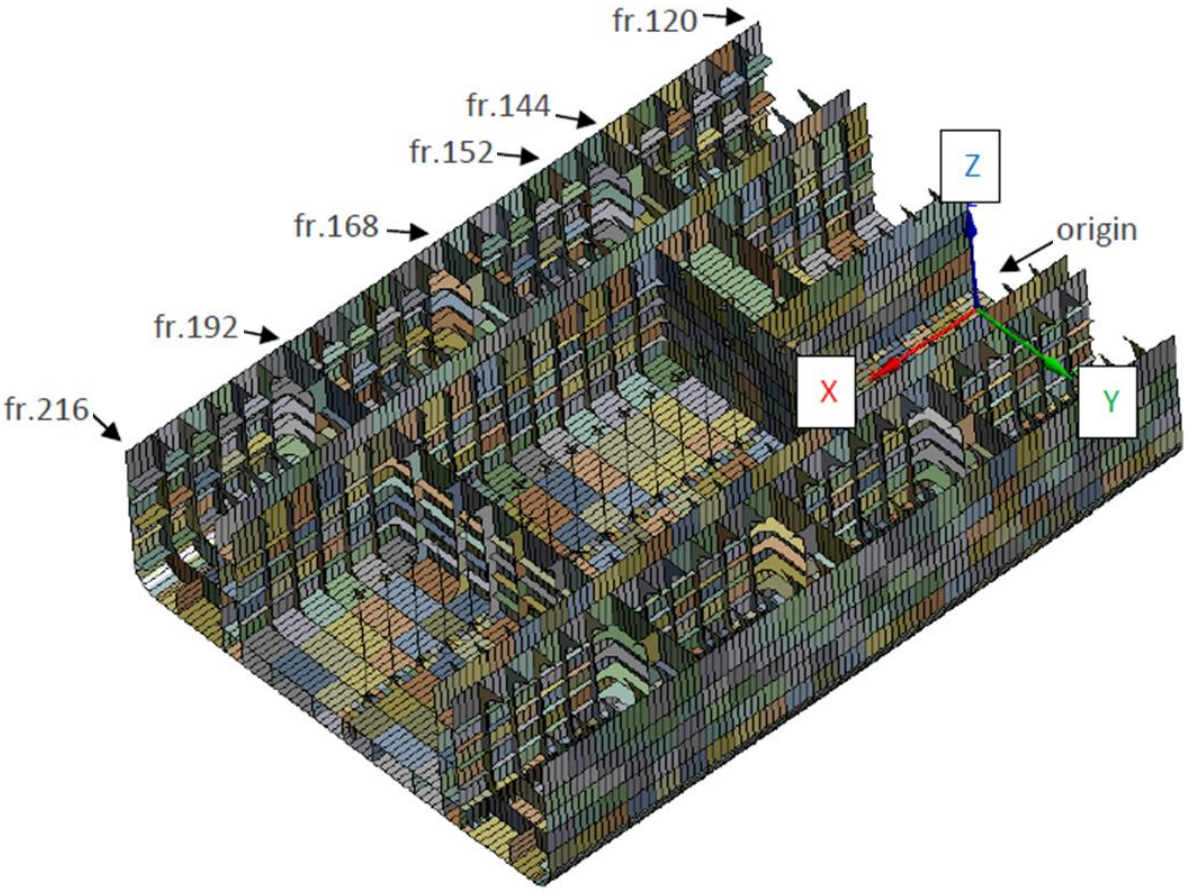

Figure 18 – Midsection model (10830 tons)

The main dimensions of the midsection—including the deck structure—displayed in Figure 18 are as follows:

Length	67.2 m
Breadth	49.0 m
Height	16.8 m
Weight	10830 tons

The TO can result in large calculation time. Thus, in consultation with C-Job, the complexity of the optimization model was reduced. The reduced complexity model has a total weight of 1980 tons (see Figure 19). In general, the model has no transverse bulkheads and consist of the double-deck structure plates, double bottom structure plates, 2 fixed longitudinal bulkheads instead of 4, with the following thicknesses:

- 20mm main deck plate
- 14mm second lower deck pate
- 14mm side hull plate and longitudinal bulkhead plate
- 14mm bottom plate
- 12mm tank top plate

The structural components and stiffeners were removed, as the objective was to design the structure of a steel ship with a new method based on the TO and yield strength of the material such that the resulting structural form is manufacturable using steel-cut plates and is cost-effective from a shipbuilding perspective.

The reduced complexity, the TO model is a trade-off between unconstrained TO and manufacturability implementations from C-Job's clients. Maintaining the double plates and bulkheads limits the unconstrained TO and presumably results in a less-than-optimal structure. However, a totally unconstrained TO is neither cost-effective nor practical from a cut-steel shipbuilding perspective (see Figure 2, Figure 3). In addition, double decks and bulkheads are required for damage-stability criteria.

5 NUMERICAL MODEL

Topology optimization requires a numerical model which creates a domain that includes all necessary functions and data. In this chapter, the boundary condition, loads, and design space are defined. The latter is a bound design space with fixed boundaries in which the structural layout can develop. The results are highly dependent on the predefined constraints and loads.

5.1 Definition of load case

A ship is constantly exposed to a huge variety of loads which depend on sea state, wind condition, heading, cargo, and weight distribution. These loads are exerted on the ship's structure, which generally consists of stiffeners that reinforce the plate to prevent distortion and local buckling. Due to complex interactions between the loads and strength requirements of the structure, it is very difficult to determine a ship's scantling by direct calculation. These loads are most often determined with the technical minimal standard for construction and operations of ships defined by classification societies such as BV, LR, or DNV. In these rules, formulas define these loads to analyze the structural parts and size a boat strong enough when used as intended.

One state-of-the-art method used to define the loads exerted on the ships is computation fluid dynamics (CFD). Computation fluid dynamics is an engineering tool used to simulate the action of thermo-fluids in a system and to calculate the hydrodynamic and static wave pressure in a sailing condition. However, such a simulation would be too extensive and specific for this study, as this thesis is focused on the design method of TO and not on accurate load prediction. For this reason, a worst-case loading condition was defined, and the corresponding loads were calculated based on DNV-GL rules for classification (DNV, 2020).

5.2 Boundary conditions

As stated above, the results are highly dependent on the predefined constraints and loads. Therefore, boundary conditions were applied using commands forming a rigid region on the cut-edges of the model, thereby to reduce the reaction forces to a minimum. All DOF`s were transferred to a dummy node at the neutral line of the cross-section. This resulted in a realistic, statically determinant bridge-boundary condition situation. The resulting model exhibits hogging and sagging movement as well as torsion movement (see Figure 19).

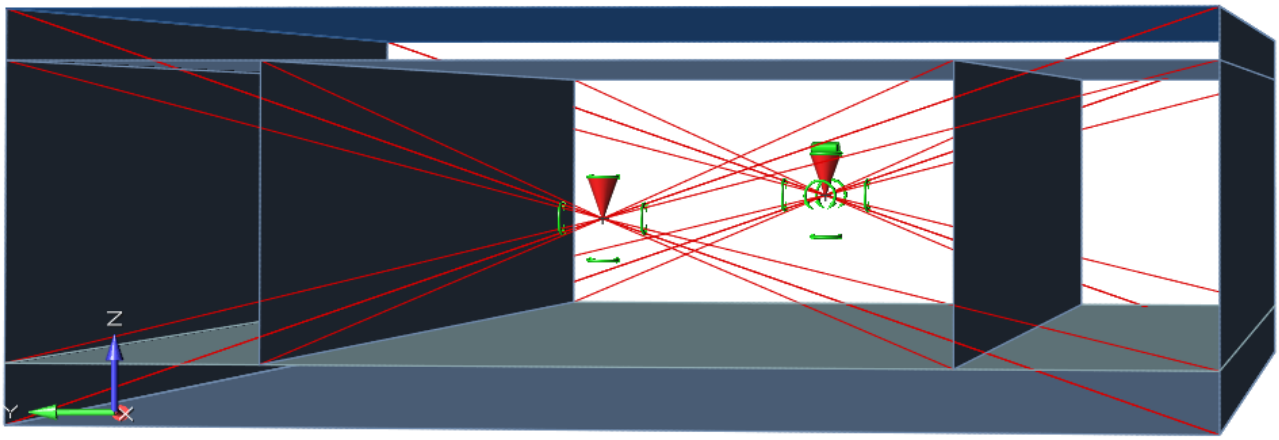

Figure 19 - reduced complexity TO model of the Orion vessel with boundary conditions

The following boundary conditions were applied at the dummy master nodes. Note that the boundary conditions are in the global coordinate system, as shown in the plot above.

	Ux	Uy	Uz	Rx	Ry	Rz
AFT master node	Fix	Fix	Fix	Fix	Free	Free
FWD master node	Free	Fix	Fix	Free	Free	Free

Table 3 – Boundary conditions

5.3 Loads

In this section, the loads which were used within the TO are defined.

5.3.1 Deck load

Because this ship carries loads distributed on the deck (for example, deck cargo or other equipment), static and dynamic pressures due to this load must be considered (DNV, 2020). The static distributed load (Pdl-s), including self-weight, was defined by the client as being less than 2.5 kN/m^2. The pressure for the static-plus-dynamic design-load scenario was derived for each dynamic load case as follows: $P_{dl} = P_{dl\text{-}s} + P_{dl\text{-}d}$

where:

$P_{dl\text{-}s}$ = static pressure, in kN/m^2, due to the distributed load

$P_{dl\text{-}d}$ = dynamic pressure, in kN/m^2, due to the distributed load

= $P_{dl\text{-}s} \cdot a_z/g$

a_z = vertical envelope acceleration, in m/s^2.

This resulted in a distributed deck load of 4.84 kN/m^2 (see Appendix A). However, the offshore heavy lift installation vessel needed to carry heavy monopiles, jackets, and windmill pillars. For this reason, the complete main deck must be able to carry a uniform load of 10t/m^2, which is equal to 98.1 kPa.

5.3.2 Hydrostatic pressure

The hydrostatic pressure was calculated for the midsection with the selected software. A plot is displayed in Figure 20. Pressures in the plot above are in Pa. Pressure increases linearly from 0 at 11 m AB to 110 kPa.

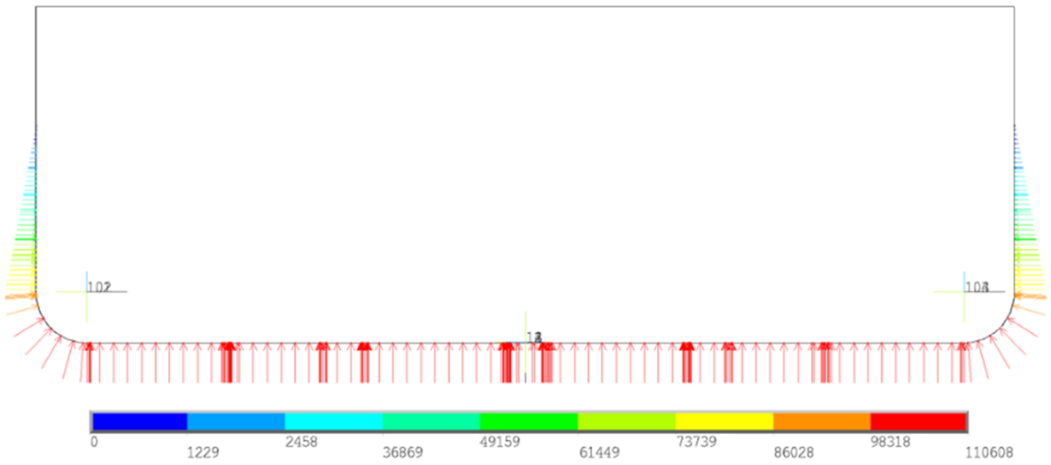

Figure 20 – Hydrostatic pressure midsection [Pa]

5.3.3 Corrective loads

After implementing the general loads like, for example, deck load, and hydrostatic pressure the shear force and bending moment must be correct according to the target value. This is calculated with the following procedure (DNV-GL, 2015):

- Solve case with deck load, hydrostatic pressure, and without corrective loads
- Obtain uncorrected target values for shear force and bending moment at relevant locations
- Calculate correction for shear force
- Calculate the influence of shear force corrective moment on the bending moment line
- Calculate correction for bending moment line
- Apply corrective moments

Shear-force target locations are the AFT and FWD bulkheads of the center compartments. In model coordinates, these are x = 11.2 m (Frame 144) and x = 56 m (Frame 192), respectively. The bending moment target 'location' is the highest value found between the AFT and FWD bulkheads of the center compartments. Shear forces in the z-direction were corrected using parallel bending moments at the model supports. Bending moment around the y axis was corrected by opposite bending moments at the model supports. Loads were only corrected if they were lower than the target values. If they were higher, no correction was made. The target values for this midsection are given in Table 4 and were calculated by rules (DNV, 2020).

Component	Load
Shear force z-direction	105 MN
Bending moment y-direction	5800 MNm

Table 4 – corrective loads for shear, bending, and torsion.

The bending moment and shear force diagram without corrective loads are as follows:

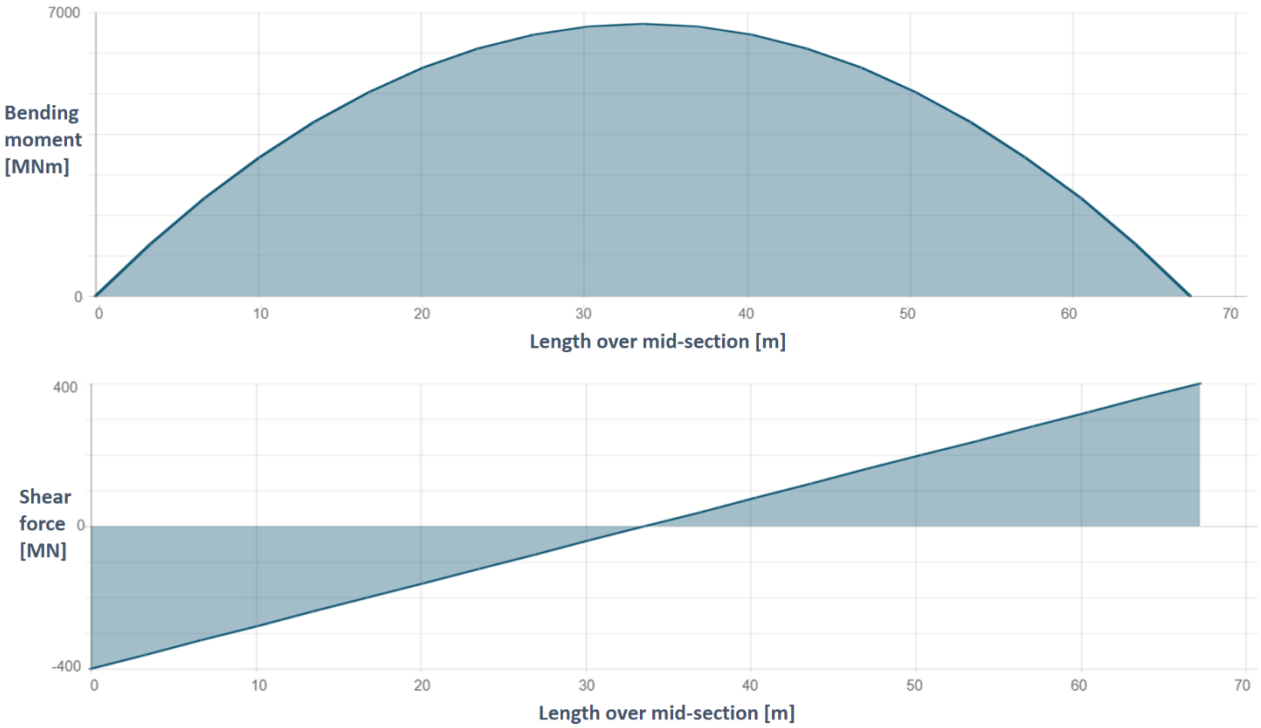

Figure 21 – Bending moment and shear force diagram over the length of the mid-section

The deck load and hydrostatic pressure do result in a sufficient bending moment but do not cause shear force. Therefore, the shear was corrected by implementing parallel moments at the AFT and FWD model supports:

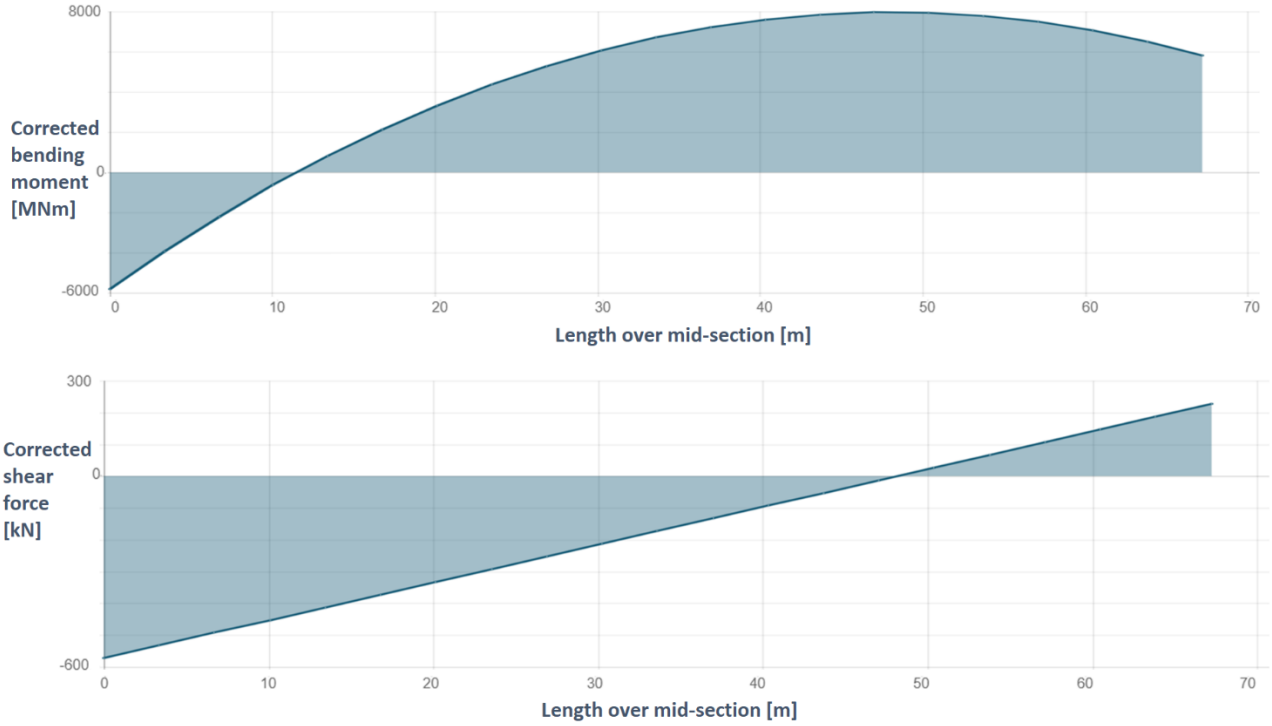

Figure 22 – Corrected bending moment and shear force diagram over the length of the mid-section.

5.4 Materials and stress limits

The structure was built with A36 steel with the following material properties:

Minimum yield stress (R_{Eh})	355 MPa
Minimum shear stress (T_{eH})	205 MPa
Young's Modulus (E)	20600 MPa
Poisson's ratio (v)	0.3
Density (ρ)	7850 kg/m^3

Table 5 – Material properties A36 Steel

The von Mises stress (σ_{vm}) is used as the stress limit for this study. It is calculated for all plates of the structural members based on the membrane normal and shear stresses of the shell element. The stresses were evaluated at the element centroid of the mid-plane, resulting in the following:

1) $$\sigma_{vm} = \sqrt{\frac{(\sigma_{xx} - \sigma_{yy})^2 + (\sigma_{yy} - \sigma_{zz})^2 + (\sigma_{zz} - \sigma_{xx})^2 + 6(\tau_{xy}{}^2 + \tau_{yz}{}^2 + \tau_{zx}{}^2)}{2}}$$

where:

σ_{xx}, σ_{yy}, σ_{zz} = element normal stresses, in N/mm^2
T_{xy}, T_{yz}, T_{zx} = element shear stress, in N/mm^2

When designing the scantling of a ship that uses combined stresses with the von Mises stress limit, high peak stresses could be encountered. If the minimum dimensions of the stiffeners described in the regulation are considered, however, this situation will not occur (DNV, 2020) (BV, 2021) (LR, 2016).

In this study, the loads and constraints were applied on a mesh-based TO mid-section model, whereby the structural parts were analyzed to size a boat strong enough when used as intended. This partial ship strength analysis was used to demonstrate that the stresses do not exceed the maximum permissible stresses. The static allowable stress limits were determined with the permissible utilization factor (λ_{perm}), which is based on element types and mesh size.

For a coarse mesh, this factor is equal to 0.8 for steel plating of all longitudinal hull-girder structural members, primary supporting structural members, and bulkheads with a thickness of 150 mm or lower (DNV-GL, CG-0127 Finite element analysis, 2015). Coarse mesh follows the stiffening system so far as is practicable and shall present the actual plate panels between the stiffener (for example, s by s, where *s* is the stiffener spacing). When the mesh could not adequately represent the geometry of the structure and the stress exceeds the allowable criteria, a finer mesh was used. When a smaller mesh size was being used, an average weighted von Mises stress calculated over an area equivalent to the original mesh size was accepted. The structural elements comply with the following criteria:

$$\lambda_y \leq \lambda_{perm}$$

where:

$$\lambda_y = yield\ utilization\ factor = \frac{\sigma_{vm}}{R_Y}$$

R_y = nominal yield stress,
taken equal to 235/k = 326 N/mm^2.

This results in a maximum Von Mises Stress (σ_{VM}) of 260 MPa for standard coarse mesh, see Figure 23.

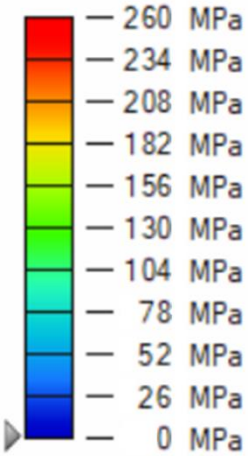

Figure 23 – Von Mises stress legend colors for the coarse mesh.

After defining the loads and stress limit a case study can be performed in the next chapter.

6 CASE STUDY

The goal of this study is to design the structure of the Orion vessel with TO while complying with strength requirements. The outcome of the TO should be manufacturable from cut steel plates and should be cost-effective from a manufacturing perspective. This can be validated when the TO outcome can be made with the standard shipyard tools from Section 2.4. In addition, the weight of the optimized mid-section is to be compared to see if it represents an overall improvement on the original. For example, an optimized structure that is manufacturable but has doubled in weight is not desired. The original total midsection (Figure 18) and the reduced-complexity TO model (Figure 19) weigh 10,830 tons and 1,990 tons, respectively, which has the result that the structural TO must be lower than 8,8850 tons to realize a favorable weight reduction.

6.1 Implementation of manufacturability / design space

With TO, a design space is created in which the structure optimization can develop. Implementing design spaces is a trade-off between the most unconstrained (optimal) design and manufacturability. Without design spaces, the most optimal structure is created based on stiffness or minimizing mass, which results in a complex geometry that cannot be made with standard shipyard tools (see Figures 2 and 7).

With only one large design space that does not consider compartmentation, the structural development is mostly unconstrained, thus resulting in a highly unmanufacturable result (see Figure 24). It should be noted that this can be further improved by geometric constraint, but it does not consider compartmentation.

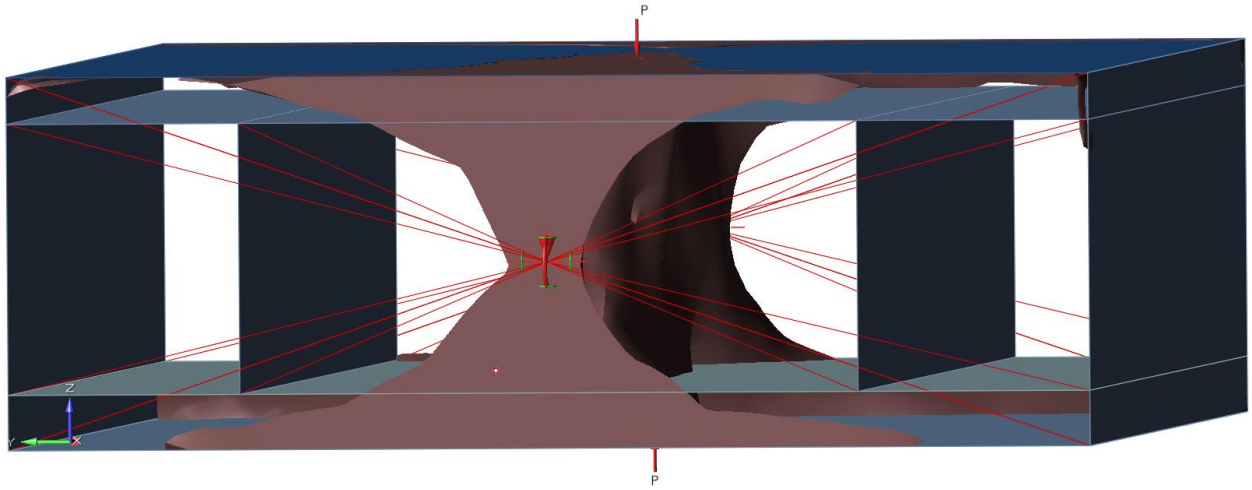

Figure 24 – TO model with 1 large unconstraint design space

Therefore, the TO model contains seven design spaces (see Figure 25). For each of the seven design spaces, a geometric constraint (addressed in Section 2.4) and a mass target can be set. The mass target can be realized with a set maximum weight or a volume fraction. The latter defines the volume ratio of the optimized structure with respect to the original design space. For example, an upper boundary of 0.3 results in an optimized volume with a maximum of 30% of the design-space volume.

One way to implement and control manufacturability at the first level is to create design volumes with the client specification concerning compartmentation. The four outward longitudinal-design volumes ensure a structural development that protects the side-hull and longitudinal-bulkhead plates from distortion and local buckling. The middle design-volume space presumably supports the double-bottom and double-deck plates, as there were originally pillars in this location.

The lower design volume provides structural development in a double-bottom situation, which is currently mandatory. With the double-bottom configuration, no modifications or special designs have to be considered for cables and pipes. A heavy-lift support vessel needs to withstand heavy deck loads; therefore, the double-deck situation is maintained, and a design space is situated to develop the structure that supports the deck plate.

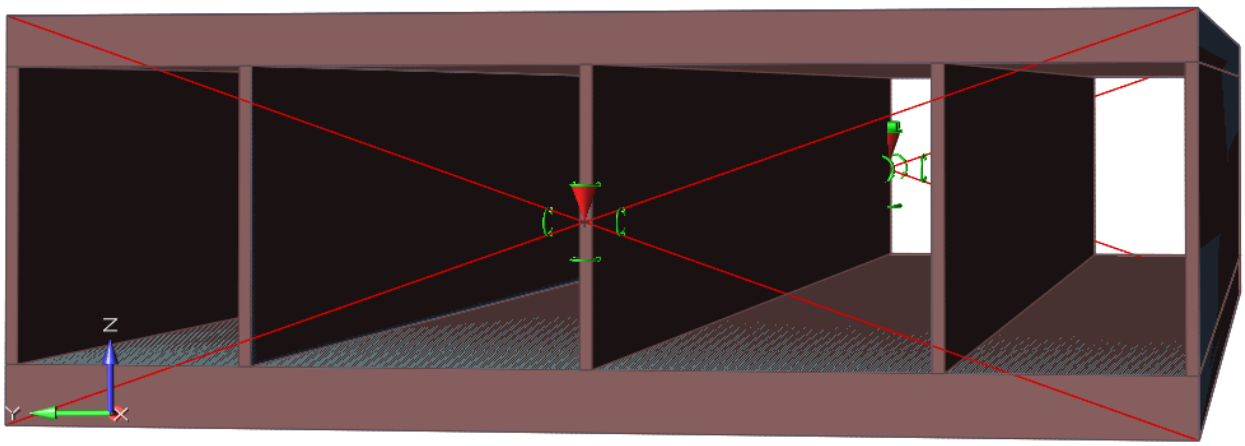

Figure 25 – TO model with 7 design spaces

6.2 First iteration

Due to its short computational time, the case study began by considering maximizing stiffness as the design objective. Because maximizing stiffness does not consider the stresses in the model, a post-analysis with FEA was performed to see if the structural TO outcome is within the set stress limit. The total design volume has a volume-fraction mass target of 0.3. In combination with a post FEA and the mass target defined by the designer, this results in an iterative process.

Within 25 hours, the software developed the overall structural components shown in Figure 26, with a total structural weight of 40,101 tons (excluding plates). The structural weight of the double bottom is 12,391 tons, the double-deck plate weighs 13,290 tons, the hull side plates weigh 3,073 tons, the longitudinal bulkheads weigh 2,753 tons, and the mid-support weighs 2,768 tons.

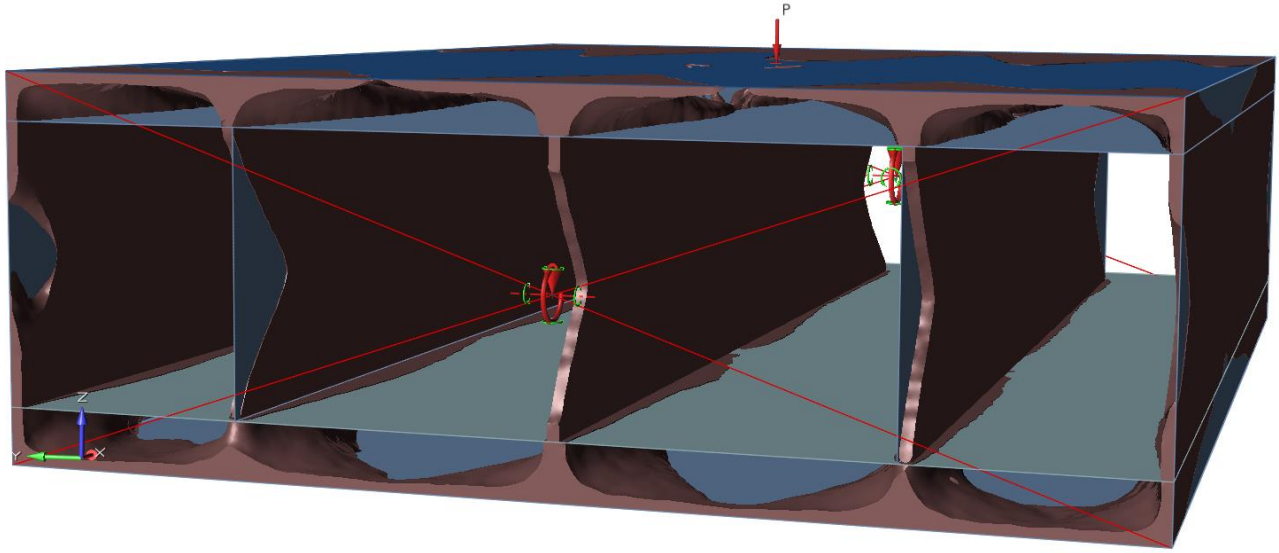

Figure 26 – TO outcome first iteration

The TO outcome including plates was analyzed with respect to the von Mises stress with FEM and is situated in Figure 27. For detailed figures, see Appendix A. The maximum allowable von Mises stress is 260 MPa (legend colors in Figure 23).

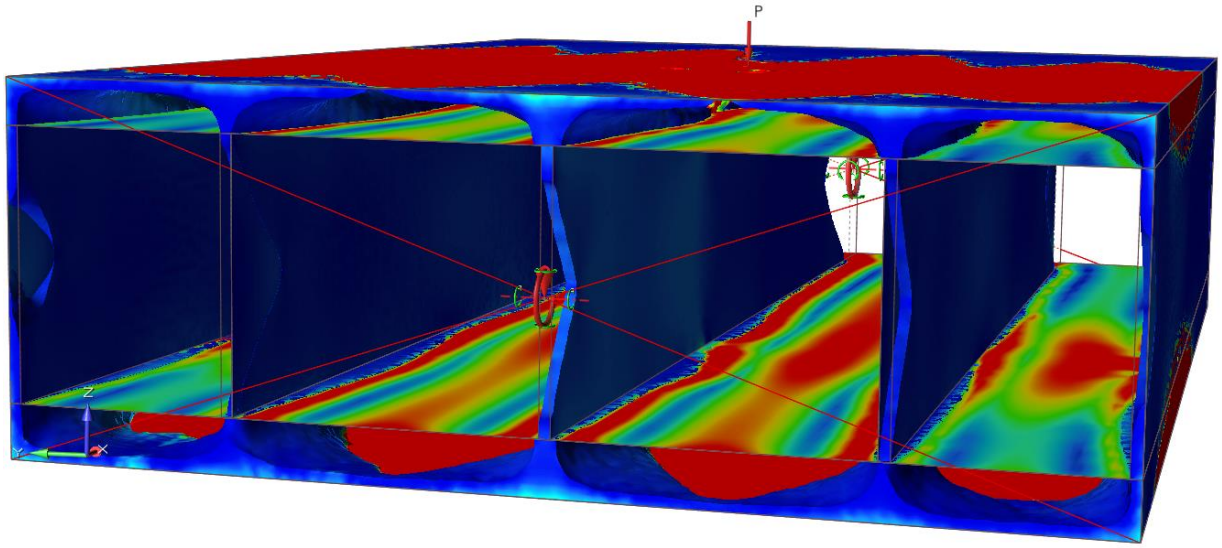

Figure 27 – FEA of the first iteration with Von Mises stress limit

The development is not manufacturable from cut-steel plates with standard shipyard tools like 2D cutting, rolling, and welding. Nor is it optimal, as the deck and bottom plate are not sufficiently supported, resulting in high stress and distortion. The longitudinal TO outcome is solid with a thickness of 500mm, which is highly inefficient from a shipbuilding perspective.

This TO outcome cannot be used or implemented. In the next iteration, the TO output is adjusted with the design constraints—discussed in Section 2.4—to achieve a more manufacturable result. The mass target of the total design volume is substantially lowered.

6.3 2nd Iteration

The design objective for the second iteration is to maximize stiffness with a volume-fraction mass target of 0.3 for each design space. The mass target for this iteration is set for each design volume to implement more TO output control and to improve the structural development of the double bottom and double deck in the last iteration. The geometric constraint for this optimization is draw direction, which is perpendicular to each design-volume plane and outwards directed of the supporting plate. For the longitudinal midsection support, the design space is constrained with a split draw direction. A member-size constraint was used in this iteration to improve manufacturability and was set at a minimum of 1 m and a maximum of 2 m.

Within 45 hours, the software developed the structural components depicted in Figure 28, with a total structural weight of 28,747 tons (excluding plates). The structural weight of the double bottom is 13,859 tons, the double-deck plate is 12,258 tons, the hull side plates yield 881 tons, the longitudinal bulkheads contribute 893 tons, and the mid-support weighs 856 tons.

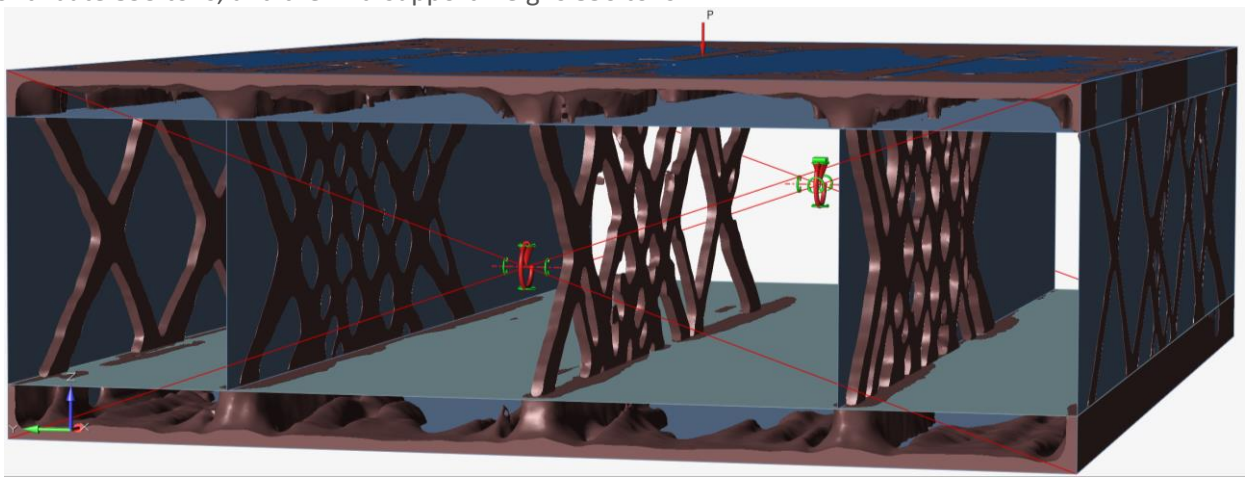

Figure 28 – TO outcome second iteration

The TO outcome including plates was analyzed with respect to the von Mises stress with FEM, as depicted in Figure 29 (for detailed figures, see Appendix B). The maximum allowable von Mises stress is 260 MPa (legend colors in Figure 23).

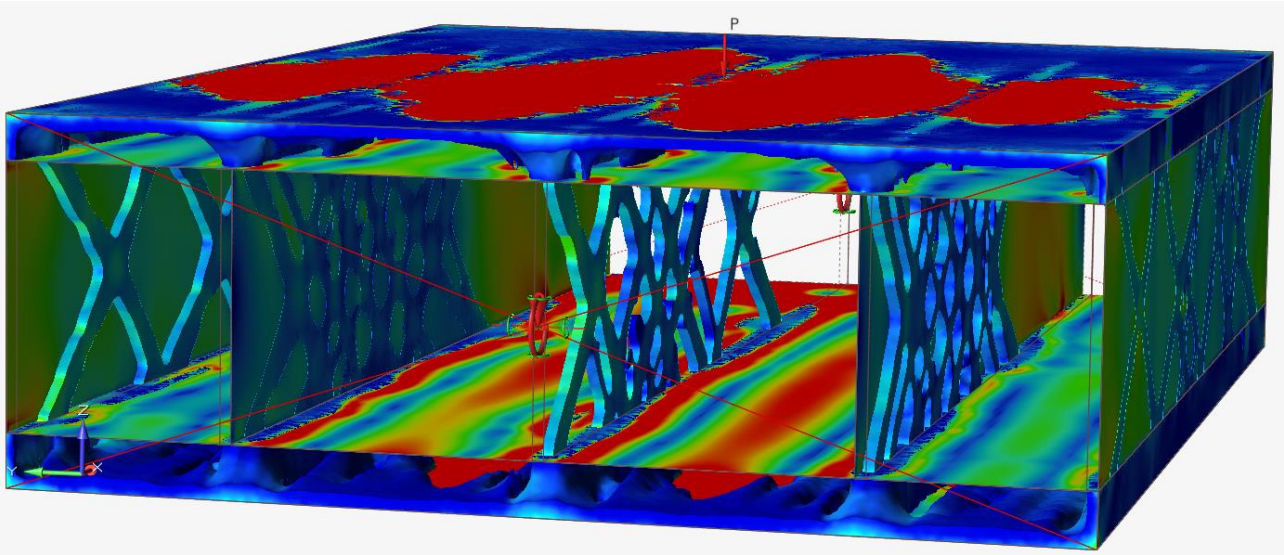

Figure 29 - FEA of the second iteration with Von Mises stress limit

The structural development in the bottom and deck-design areas is neither manufacturable from cut-steel plates nor optimal, as the deck and bottom plates are not sufficiently supported, thereby resulting in high stress and distortion.

The structural development in the longitudinal design spaces could be considered manufacturable when the output is used to indicate the locations and dimensions of structural components like square tubes, H beams, or L beams. Also, the structural components are better optimized, which can be observed by the color stress indicator. However, the structural distribution on the longitudinal bulkhead should be modified, as the bulkhead plate experiences high stress concentrations.

In the next iteration, the mass target for the bottom and deck-design volume is lowered substantially to reduce weight. Also, a symmetry constrain was applied for a better distribution of the structural development on the longitudinal bulkheads, which are currently unsymmetrical over the y-z plane. The problem of an unsupported deck plate cannot be solved by increasing the mass target, as this will only result in a more inefficient result. It must instead be solved with other geometric constraints or design objectives if possible.

6.4 3rd Iteration

The design objective for the third iteration is to maximizing stiffness with an adjusted volume-fraction mass target of 0.1 for the top and bottom structure and a mass target of 0.25 for the longitudinal design volumes. The geometric constraint for this optimization is draw direction, which is perpendicular to each design-volume plane and to the outwards direction of the supporting plate. For the longitudinal mid-section-support, the design space is constrained with a split draw direction. A member-size constraint is used in this iteration. It is set to a minimum of 1 m and a maximum of 2 m. This iteration included additional symmetry constraints, which could improve the structural-distribution problem with the longitudinal bulkhead in the last iteration. The symmetry constraints were applied to each design volume over the y-z plane.

Within 55 hours, the software developed the structural components with a total structural weight of 10,950 tons (excluding plates). See Figure 30. The structural weight of the double bottom is 4,811 tons, the double-deck plate is 4,062 tons, the hull side plates weigh 725 tons, the longitudinal bulkheads comprise 721 tons, and the mid-support weighs 632 tons.

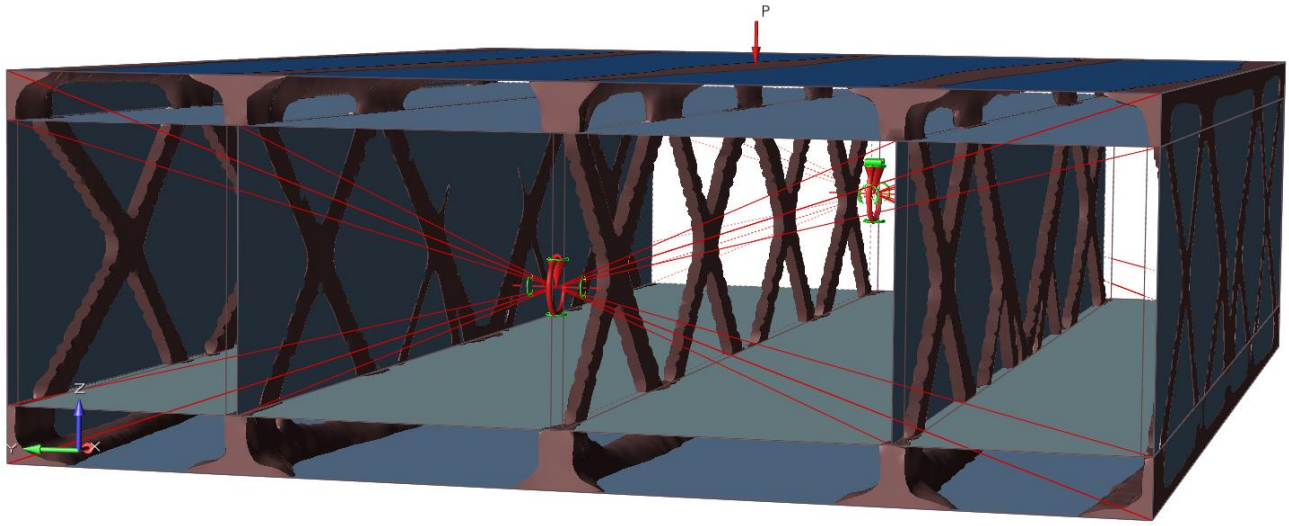

Figure 30 – TO outcome 3rd iteration

The TO outcome including plates was analyzed with respect to von Mises stress with FEM, as can be seen in Figure 31 (for detailed figures, see Appendix C). The maximum allowable von Mises stress is 260 MPa (legend colors in Figure 23).

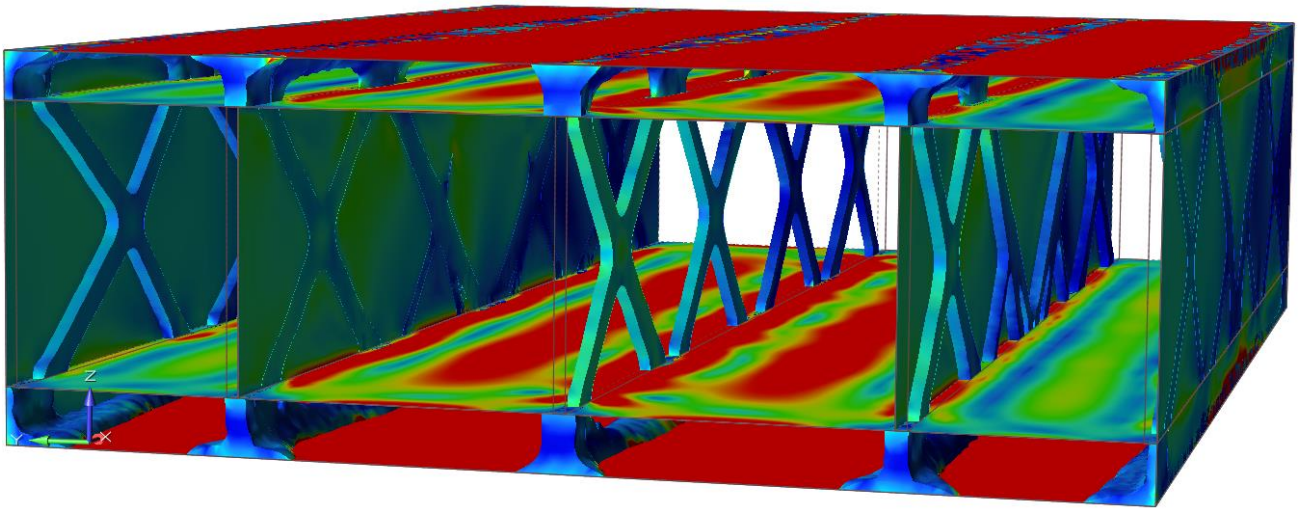

Figure 31 – FEA of the 3rd iteration with Von Mises stress limit

The structural development in the longitudinal design spaces is improved in comparison with the second iteration and shows a symmetrical structure over the y-z plane. This is considered manufacturable when the output is used to indicate the locations and dimensions of structural components. In addition, the symmetry constraint eliminated the high stress concentrations in the bulkhead plates, which were observed in the second iteration.

However, the structural development in the double-deck and bottom were improved but remain neither fully manufacturable from cut-steel plates nor optimal, as the deck and bottom plate are insufficiently supported, thus resulting in high stress and distortion.

The total structural weight of 10,950 tons is 24% higher than the structural optimization limit of 8,853 tons, which is most induced by the bottom and deck structural development. The structural output can be controlled with a mass-target percentage for each design volume, and an optimal design can be realized with an iterative process. See the past iterations.

6.5 4th Iteration

The design objective for the fourth iteration was to maximize stiffness with a set mass target for the total optimization of 8,853 tons, which resulted directly in the desired structural weight. The geometric constraints are the same as they were in the third iteration.

Within 60 hours, the software developed the structural components with a total structural weight of 8,853 tons (excluding plates). See Figure 32. The structural weight of the double bottom is 3,890 tons, the double-deck plate weighs 3,284 tons, the hull-side plates weigh 586 tons, the longitudinal bulkheads weigh 583 tons, and the mid-support contributes 711 tons.

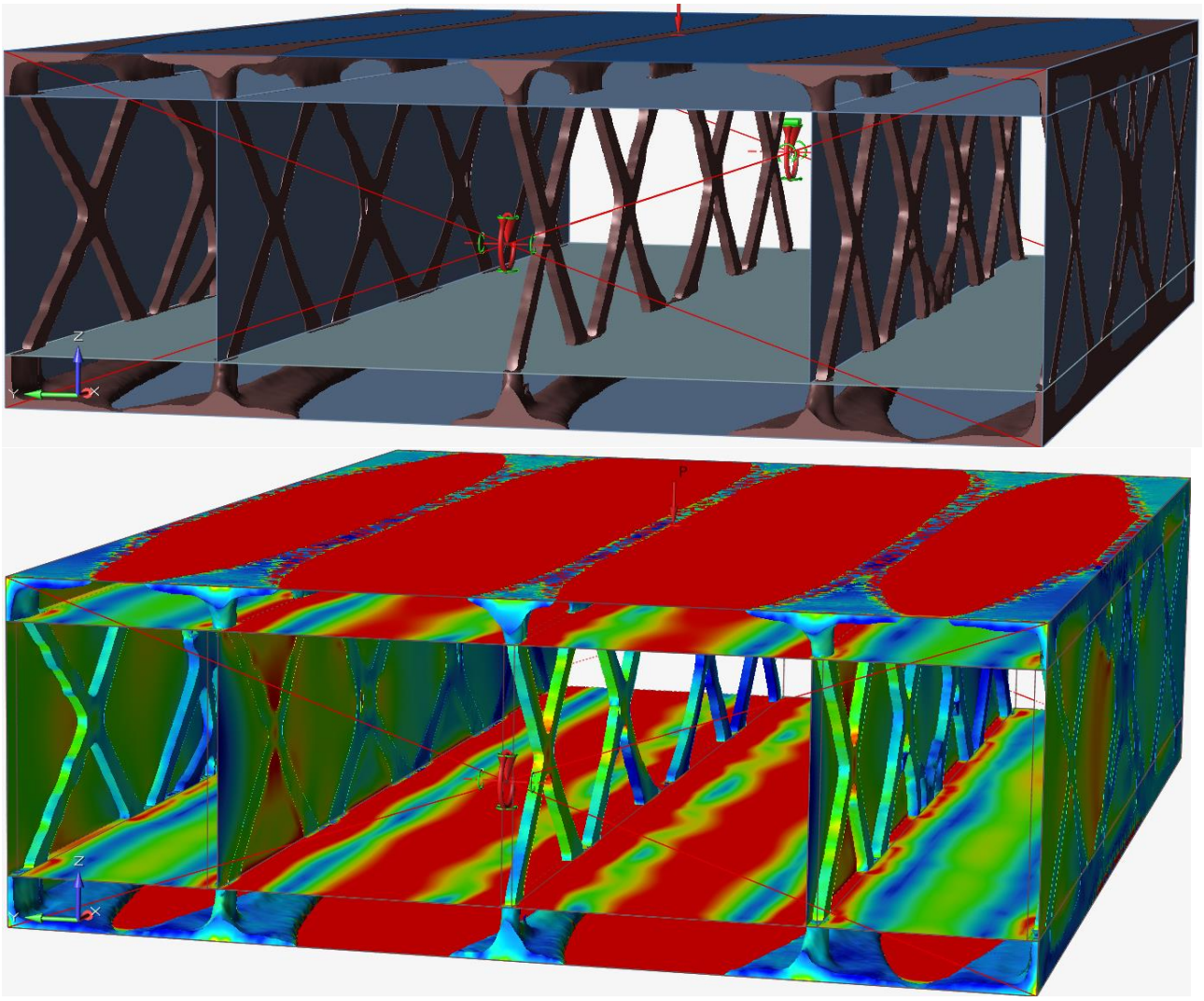

Figure 32 - TO outcome 4th iteration

The TO outcome in the bottom and deck design are not manufacturable, but the structural development in the longitudinal design spaces could be manufacturable if the output is used to indicate the locations and dimensions of structural components.

6.6 5th Iteration

In the fifth iteration, the design objective minimizing mass was used with a safety factor of 1.36, which is a maximum von Mises stress of 260 MPa. This iteration was conducted to validate the observations reported in Section 3.3, according to which minimizing mass yields results similar to maximining mass but with a larger computational time for this large-scale model. The geometric constraints are the same as they were for the third iteration.

Within 126 hours, the software had developed the structural components depicted in Figure 33, with a total structural weight of 9,734 tons (excluding plates). For detailed figures, see Appendix D. The structural weight of the double bottom is 4,277 tons, the double-deck plate weighs 3610 tons, the hull-side plates contribute 644 tons, the longitudinal bulkheads weigh 641 tons, and the mid-support weighs 562 tons.

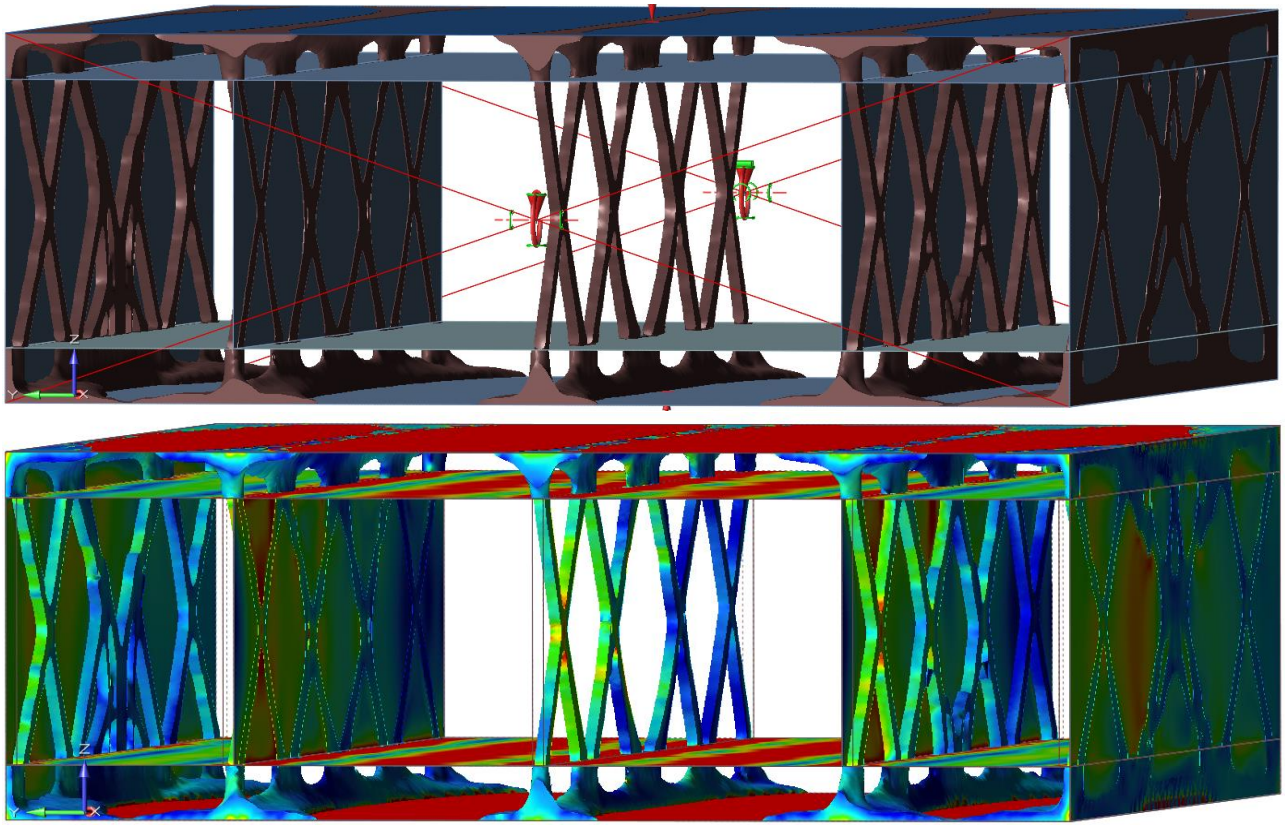

Figure 33 - TO outcome 5th iteration

The unsupported plate problem with maximizing stiffness and minimizing mass discussed in Section 3.3 was also observed in the past iteration of this case study. Given the TO software programs used in this study, the loads and constraints cannot be applied directly to the design area; they therefore had to be set on non-design areas to achieve results. Therefore, the stresses for the optimization were considered only in the assigned design area and not in the plates, thus resulting in unsupported deck plates with an insufficient structure. Within the set design spaces, the TO software realizes the stiffest or lightest structure possible with no correlation to the supporting plates.

6.7 6th Iteration

As can be seen in the past iteration, the TO outcome develops the most stiffened or lightest structural shape on a global level, which does not include the local buckling of large plate fields. Also, the structural development in the double-deck and bottom cannot be made with rolling from cut steel plates. In addition, the angular structures in the longitudinal bulkheads are solid, 0.5 m x 0.5 m x-shaped beams that can be made with cut-steel plates via cutting, rolling, and welding. However, they are highly cost-ineffective.

However, the TO outcome of the longitudinal structure at the side-hull plates, bulkheads, and mid-support can be used to indicate the location and dimensions of the global structural components (see Figure 34 and Appendix E).

The grid was multiplied, and secondary stiffeners were added to prevent local stresses and buckling. In addition, four longitudinal plates were added to reduce stress in the deck and bottom design space. The dimensions of the large grid and small grid are 5.6 x 6.1 m and 1.4 x 1.5 m, respectively.

By adjusting the thickness of the shell elements, the structure was optimized via an FEA-iterations process based on the maximum von Mises stress of 260 MPa. On a global level, the longitudinal bulkheads and hull plates are within the stress limits. However, the double-bottom and deck plate are not sufficiently supported, which results in high stress and distortion.

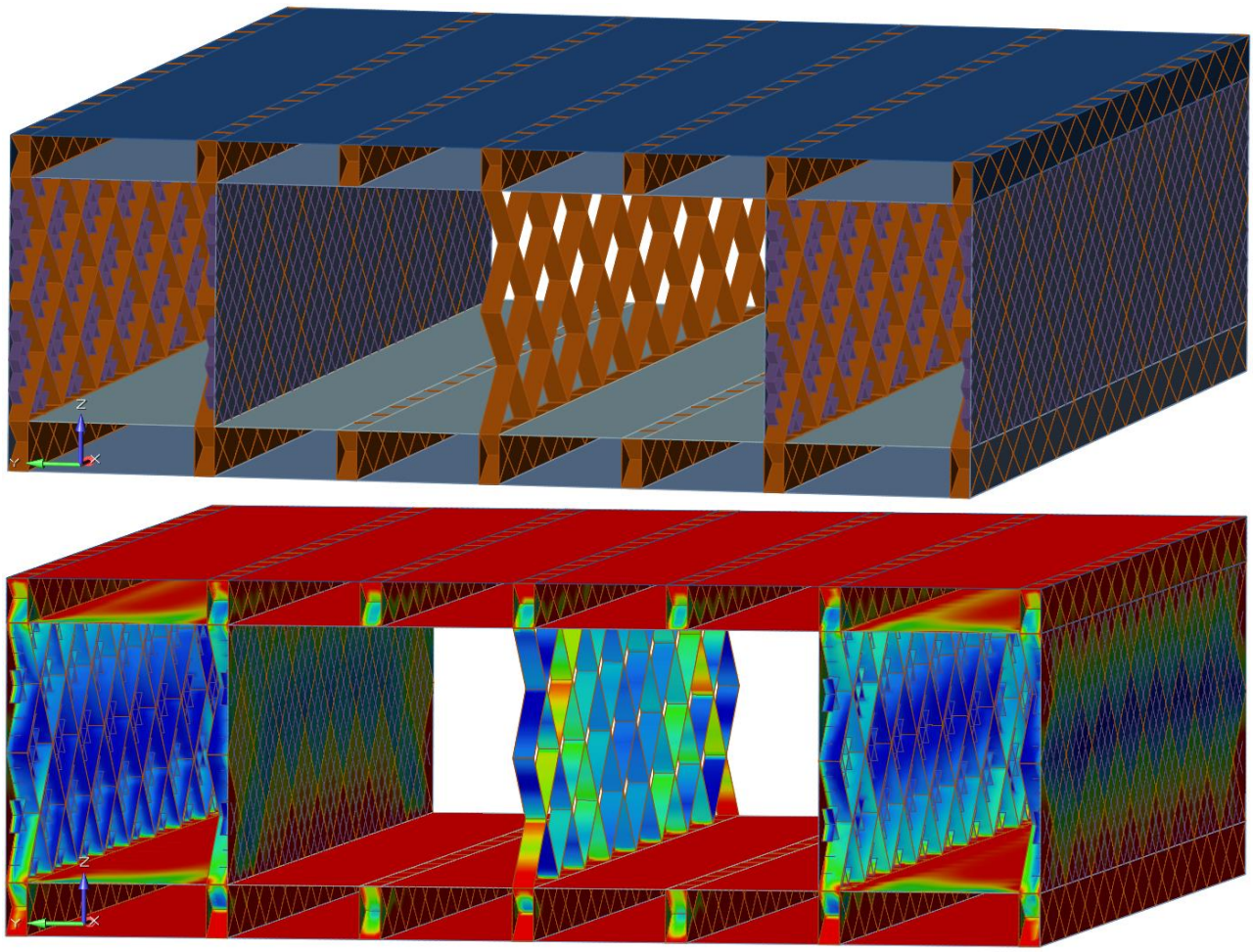

Figure 34 – Implementation TO outcome 3rd iteration

The global TO with minimizing mass does not result in sufficient structural development for the double bottom and deck, thus resulting in distortion of the bottom and deck plate on a local level. Therefore, the original structure is implemented as situated in Figure 35. For detailed figures, see Appendix F.

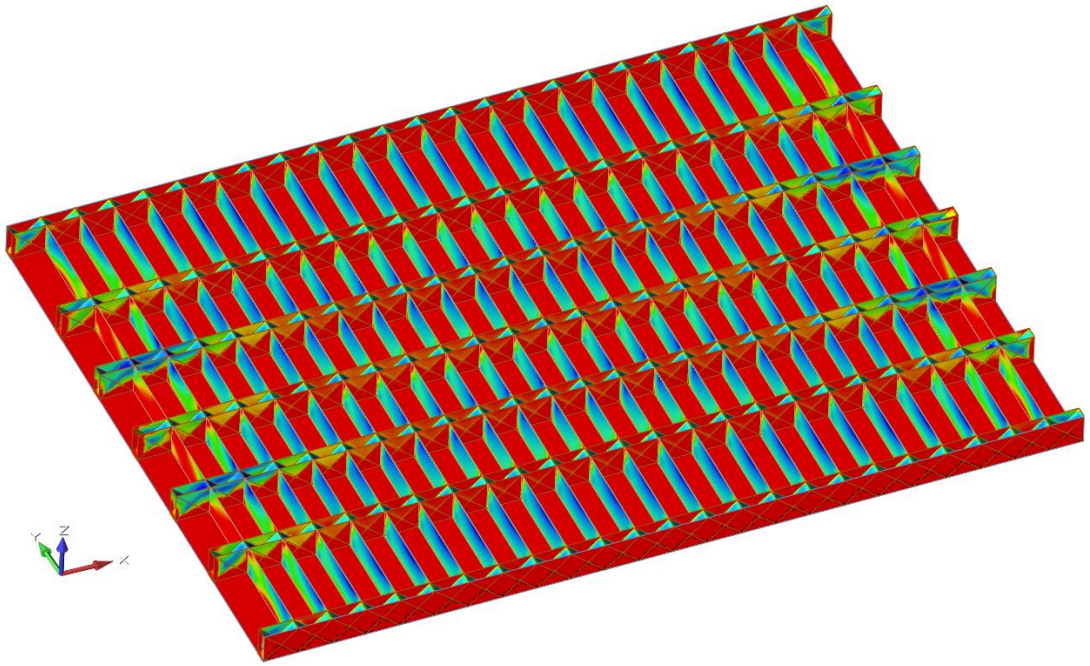

Figure 35 - Implementation TO outcome third iteration with original double deck and bottom structure

However, the bottom and deck plate still yield under the local stress—probably because the relatively thin plates have too large a span (of 2.8 m). Therefore, inspired by the suggested TO structure developments of the fourth and fifth iterations, structural stingers were used on the deck and bottom plate to sustain the local loads. The dimensions of the small grid are 1.2 m x 1.4 m. As can be seen in Figure 36, the structure is within the maximum stress limit of 260 MPa and can sustain the worst-case sailing condition (see Appendix G).

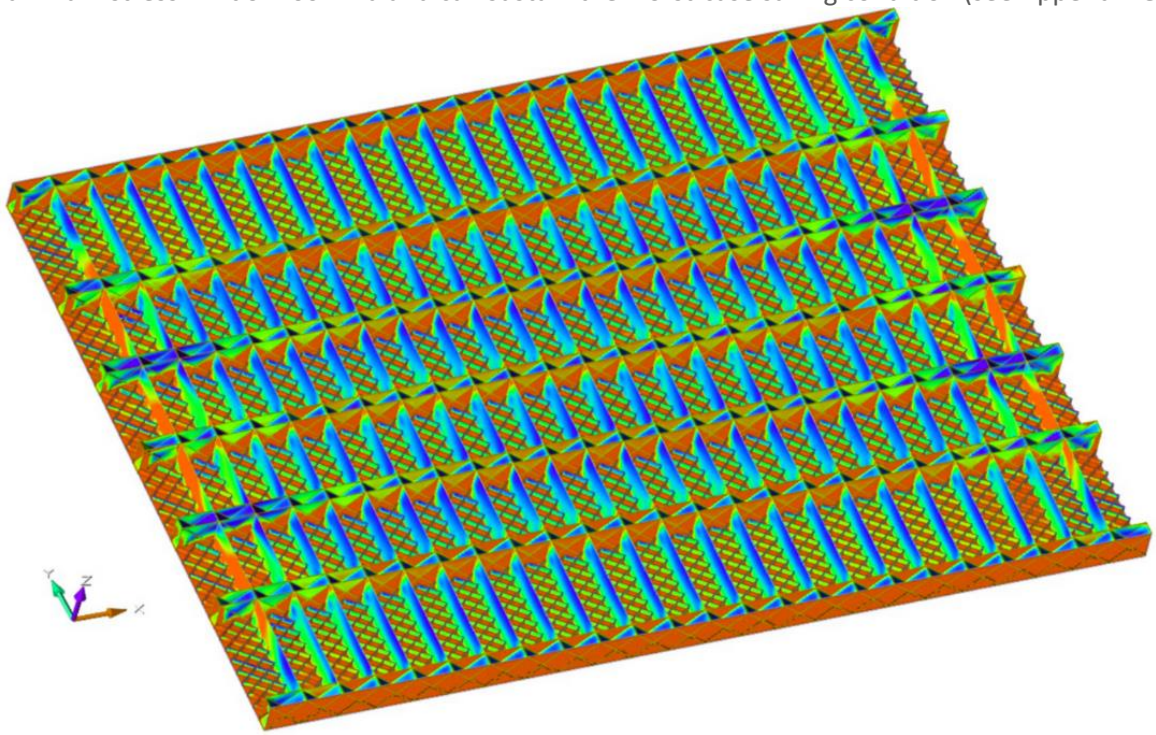

Figure 36 – Improved implementation TO outcome third iteration with original double deck and bottom structure

Because the outcome of this iteration is made from a suggestion of the TO, it can be made with standard shipyard tools. The total structural weight, excluding plates, is 8,594 tons which is a weight reduction of 2.4%. However, the original TO outcome is not manufacturable using steel-cut plates; nor is it cost-effective from a shipbuilding perspective.

7 GUIDELINE

Topology optimization is an advanced tool that is successfully used for small-scale mechanical-engineering problems in the industry. However, the use of large-scale TO for shipbuilding with standard shipyard tools is in its infancy and needs efficiency guidelines.

The TO requires considerable computational power, which increases drastically when the model size and the number of finite elements increase in particular for the design objective of minimizing mass (which in general increases the calculation by 200-300% compared to maximizing stiffness, depending on the complexity of the model). See Section 3.3 and Chapter 6. In addition, when adding geometric constraints, the calculation time increases further. The software is shell element-based. Therefore, the minimal and optimal element size is the smallest dimension within a design space. For example, in the case study, a mesh size of 0.5 m is equal to the width of the longitudinal bulkheads. This mesh size decreases the calculation time while maintaining the accuracy of the TO outcome.

Minimizing mass and maximizing stiffness will result in a similar TO outcome. The latter was used in an iterative process with FEA, as the stress limit is not considered in the design objective. With this FEA post-analysis, the von Mises stress was checked to see if the structural development could sustain the loads. Due to the reduced-complexity model within the case study, this required two or three iterations to obtain a final result. This iterative process was performed by setting mass targets for the total optimized model or for each design area and was realized with a weight target or volume fraction. The latter defines the volume ratio of the optimized structure to the original design space, which results in more iterations. With a set weight target that has, for example, a 5% weight reduction, the TO software developed a structural shape that was as strong as possible within a set safety factor. However, iterations increase when the complexity of a model becomes larger and more complex. When optimizing with larger and more complex models—when the required computational power is no issue—minimizing mass is preferred, as no iterative process with FEA is needed and as this will decrease the number of iterations.

In Chapter 6, the problem was observed that the plates supported by the TO structural development were not within the design spaces, thereby resulting in unfavorable results for the double-deck and bottom in particular. Given the TO software programs used in this study, the loads and constraints cannot be applied directly to the design area and therefore need to be set on non-design areas to achieve results. Therefore, the stresses for the optimization were considered only in the assigned design area and not in the plates, thus resulting in unsupported deck plates with insufficient structure. Within the set design spaces, the TO software realized the stiffest or lightest structure possible with no correlation to the supporting plates on a local level. Therefore, given the software used in this study, TO cannot be used as the final structural design and can currently be used only as a suggestion early in the design process of shipbuilding when compartmentation, loads, and constraints are roughly known, which can be further detailed by an iterative process.

When considering the design spiral and the different design phases discussed in Section 2.1, TO cannot be successfully performed in the conceptual design phase, as there is no 3D model of the hull; therefore, the loads and constraints based on the rules cannot be realized. In the conceptual-design phase, the required specifications of the client were translated to a 2D preliminary arrangement, tank, and deck layout determined on the experience of the designer and reference ship.

The hull, tank, and deck can be arranged during the basic design phase, beginning with a (general) arrangement of the interior and exterior design using a 3D model to estimate the initial weight and stability. After determining the initial arrangement and 3D model, a scantling calculation can be used to determine the structural dimensions. With the 3D model, the TO can be used as a suggestion to define the scantling. It can work simultaneously with defining the compartmentations.

The loads and constraints were determined by the rules and regulations for directed calculation based on the dimension of the ship. As the standard shipbuilding design method for scantling is an iterative process, this iterative method also applies to TO when used in the basic design phase. The optimization will start with the failure mode of maximum von Mises stress; however, if needed, buckling and fatigue can also be checked in later iterations with the TO software used in this study.

Use of TO in the basic design phase is very beneficial, as optimizing early in the design process results in fewer design limitations compared to optimizing in the detail-design phase, during which, for example, changing the hull dimensions is highly cost-inefficient. In addition, it is therefore not advised to use TO in the detail-design phase.

In addition, when TO is used as a suggestion for scantling, the geometric constraints must be used to realize suggestions that are manufacturable via standard shipyard tools, as discussed in Section 2.4. With no geometric constraints, a TO outcome is realized, which is often only manufacturable using additive manufacturing, which facilitates inefficient suggestions during the design phases.

8 CONCLUSION

Through the use of a case study, some of the potentials and limitations of using TO to design a steel midship have been identified. Within the case study, design areas and geometric constraints were specified that result in manufacturable structures. However, the geometric constraints do not separately consider the specification for 2D plate cutting, rolling, and welding. This resulted in a more complex TO outcome than desired for these manufacturing processes. In addition, given the commercial software used in this study, the problem with unsupported plates due to be excluded from the design area can result in unusable results.

Therefore, despite the availability of manufacturability constraints, it is currently not possible with the software used in this study to design the complete structure of a steel midship with TO where the resulting structural form is manufacturable using steel-cut plates and cost-effective from a shipbuilding manufacturing perspective. However, using TO as a suggestion early in the design process can be very useful. It can result in manufacturable structures. Given the TO software used in this study, it can help the designer with structural suggestions in the basic design phase, when there are fewer design limitations.

The case study resulted in unusual, 45-degree, X-shape components which are highly efficient for sustaining shear loads and which resulted in a weight reduction of 2.4% of the mid-section. See Figure 77. This could be beneficial for the capital expenditure (CAPEX) and operating Expense (OPEX), as lighter ships require less material and fuel. Because the reduced-complexity model was used due to limited computational power, it should be noted that the weight-reduction number could be different in practice or when used with other types of ships. In addition, the result showed that unique structural shapes under various angles could result in an optimal strength-weight design rather than in orthogonal structural parts with a fixed span.

9 FUTURE WORK

The first commercially available TO software was developed in 1994 by Altair Engineering (Schramm, 2020) and is currently successfully used in small-scall mechanical engineering (featuredcustomers, 2021). The use of TO for the scantling of shipbuilding, and in particular for shipbuilding that uses standard shipyard tools, is in its infancy, and the software used in this study can currently only be used as a suggestion. However, this limitation is informed by the software choice and may change in the future when, for example, the manufacturability constraints are improved in commercial software.

Using TO for complex large-scale models such as the scantling of a ship is only efficient when significant computational power is available. Within the case study that utilized a 16-core processor (3.70 GHz) with 64 GB of memory, the calculation time extended to 126 hours for this relatively simple mid-section TO model. Given a complex large-scale model, this would result in a calculation time of weeks. Therefore, reducing the complexity of a TO model as much as possible for future work is recommended.

The midsection of a ship, in general, is exposed to global bending moments, shear loads, and torsion. The latter was not considered to reduce the complexity of the loads, as this report is focused on the process and method used to design a steel ship with TO. Therefore, this study uses a relatively simple, worst-case sailing condition. The global loads were corrected only if they were lower than the target values. If they were higher, no correction was made (see Section 5.3.3). Bending moments and shear forces were correct by respectively, opposite, and parallel bending moments at the model support resulting in a complex multi-load problem. However, due to the deck and bottom pressure loads, a sufficient bending moment was realized that resulted solely in a correction for the shear load. Therefore, in this situation, research on the multi-load case problem was not performed. Such research could be highly interesting in the future, as TO and multi loads are in their infancy.

This study shows that TO can yield efficient suggestions in the basic design phase. The TO was performed based on the maximum allowable von Mises stress. For future work, it may be interesting to investigate the possibility of including the other failure modes: buckling, and fatigue.

With TO and given the software programs considered in Section 3.2, the loads and constraints cannot be applied directly to the design area and therefore must be set on non-design areas to achieve results with no errors. Within shipbuilding, the loads are applied on plates that are supported by structural components which were, in this case, developed by TO software. The deck and bottom plates were excluded from the design area. This resulted in a TO that considers the stresses only in the assigned design area and not in the excluded plates, which were observed in the case study. This is currently the major drawback of designing the structure of steel ships with TO and should be addressed in the future to use it successfully within shipbuilding.

REFERENCES

AISC. (2015). Steel Construction Manual, Chapter 8: Design Considerations for Welds. *https://www.aisc.org/Steel-Construction-Manual-14th-Ed-Fourth-Printing-Print*.

Almeida, S., Paulino, G., & Silva, E. (2009). A simple and effective inverse projection scheme for void distribution control in topology optimization. Struct Multidisc Optim 39, 359-371. *https://doi.org/10.1007/s00158-008-0332-6*.

Almeida, S., Paulino, G., & Silva, E. (2010). Layout and material gradation in topology optimization of functionally graded structures: a global–local approach. Structural and Multidisciplinary Optimization volume 42, 855-868. *https://doi.org/10.1007/s00158-010-0514-x*.

Altair, & APWorks. (2016). The Light Rider motorcycle. *https://www.airbus.com/newsroom/press-releases/en/2016/05/APWorks-Launch-Light-Rider.html*.

Altena, R. (2019). Bionische Constructie. Vripack Yachting International. *Available on request: d.m.bos-1@student.tudelft.nl*.

Bakker, C. (2020). Simultaneous optimization of the topology and the layout of modular stiffeners on shells and plates. Master Thesis TU Delft 3mE. *https://repository.tudelft.nl/islandora/object/uuid%3Adf4ede63-3135-42b7-92bd-e03142b6cc02*.

Bala Manikandan, C., Balamurugan, S., Balamurugan, P., & Lionel, B. (2018). Weight reduction of motorcycle frame by topology optimization. Journal of Achievements in Materials and Manufacturing Engineering 2, 67-77. *10.5604/01.3001.0012.9664*.

Bendsoe, M., & Sigmund, O. (1999). Material interpolation schemes in topology optimization. Archive of Applied Mechanics 69, 635–654. *https://doi.org/10.1007/s004190050248*.

Bensoe, M., & Sigmund, O. (2003). Topology optimization: Theory, methods, and applications. Berlin: Springer. *ISBN: 9783662050873*.

Boer, P. d., Ganzinga, D., Vlaar, T., & Muller, T. (2020). Interviews with employees from C-Job. (D. Bos, Interviewer)

Bos, D. M. (2019). Alternatieve ontwerpmethode scantling. Thesis NHL Stenden Marine Technology. *Available on request: d.m.bos-1@student.tudelft.nl*.

Bruggi, M., & Duysinx, P. (2012). Topology optimization for minimum weight with compliance and stress constraints. Struct Multidisc Optim (2012) 46:369-384. *https://link.springer.com/article/10.1007/s00158-012-0759-7*.

BV. (2021). Rules for the Classification of Steel Ships NR 467.

Choi, W.-h., Kim, J.-m., & Park, G.-J. (2016). Comparison study of some commercial structural optimization software systems. Struct Multidisc Optim (2016) 54:685–699. *https://link.springer.com/article/10.1007/s00158-016-1429-y*.

Dijk, N. v., Maute, K., Langelaar, M., & Keulen, F. v. (2013). Level-set methods for structural topology optimization: a review. Struct Multidisc Optim 48, 437–472. *https://doi.org/10.1007/s00158-013-0912-y*.

DNV. (2020). Rules for classification: Ships. *https://rules.dnvgl.com/ServiceDocuments/dnvgl/#!/industry/1/Maritime/1/DNV%20GL%20rules%20for%20classification:%20Ships%20(RU-SHIP)*.

DNV-GL. (2015). CG-0127 Finite element analysis. *https://www.google.com/url?sa=t&rct=j&q=&esrc=s&source=web&cd=&cad=rja&uact=8&ved=2ahUKEwiCzpX1jdPwAhWksaQKHU55D8kQFjAAegQICBAD&url=https%3A%2F%2Frules.dnvgl.com%2Fdocs%2Fpdf%2FDNVGL%2FCG%2F2015-10%2FDNVGL-CG-0127.pdf&usg=AOvVaw34AoHIhEVM89ywksPfmUja*.

Doig, R., Bohm, M., Stammer, J., Hernandez, P., Griesch, S., Kohn, D., . . . Bitterling, B. (2009). Integrating Structural Design and Assessment. Computer and IT Applications in the Maritime Industries Conference (COMPIT 2009), 374-389.

Dumez, F.-X. (2008). A Tool for Rapid Ship Hull Modelling and Mesh Generation. Computer and IT Applications in the Maritime Industries Conference (COMPIT 2008), 6-18.

Edwards, C., Kim, H., & Budd, C. (2007). An evaluative study on ESO and SIMP for optimising a cantilever tie-beam. Struct Multidisc Optim 34, 403-414. *https://doi.org/10.1007/s00158-007-0102-x*.

Elhewy, A., Hassan, A., & Ibrahim, M. (2016). Weight optimization of offshore supply vessel based on structural analysis using finite element meth. Alexandria Engineering Journal 55(2) 1005-1015. *https://doi.org/10.1016/j.aej.2016.02.032*.

Eyres, D., & Bruce, G. (2012). Ship Construction 7th Edition. Elsevier Science & Technology. *ISBN: 9780080972398*.

featuredcustomers. (2021). Altair Case Studies. *https://www.featuredcustomers.com/vendor/altair/case-studies/all*.

Goodwin, T., & Dodkins, A. (2013). Simulation Driven Structural Design in Ship Building. The 9tk UK Altair Technology Conference. *https://resources.altair.com/altairatc.com/country/United%20Kingdom/FINAL_SIMULATION_DRIVEN_STRUCTURAL_DESIGN_IN_SHIPBUILDING_UK_ATC_100913.pdf*.

Guest. (2009). Topology optimization with multiple phase projection. Computer Methods in Applied Mechanics and Engineering 199(1-4), 123-135. *https://doi.org/10.1016/j.cma.2009.09.023*.

Guest, J., Prévost, J., & Belytschko, T. (2004). Achieving minimum length scale in topology optimization using nodal design variables and projection functions. International Journal for Numerical Methods in Engineering 61(2), 238-254. *https://doi.org/10.1002/nme.1064*.

Holmberg, T., & Hunter, S. (2011). Increasing Efficiency in the Ship Structural Design Process. Computer and IT Applications in the Maritime Industries Conference (COMPIT 2011), 536-550.

Hughes, O., & Paik, J. (2010). Ship Structural Analysis and Design. *ISBN: 9780939773783*.

Husson, D., & Burke, A. (2011). *The Application of Process Automation and Optimisation in the Rapid Development of New Passenger Vehicles at SAIC Motor.* SAIC Motor & Altair ProductDesign.

Iqbal, J., & Shifan, Z. (2018). Modeling and Simulation of Ship Structures Using Finite Element Method. International Journal of Industrial and Manufacturing Engineering 12(7), . *https://doi.org/10.5281/zenodo.1317394*.

Ishii, K., & Aomura, S. (2004). Topology Optimization for the Extruded Three Dimensional Structure with Constant Cross Section. JSME International Journal 47(2), 198-206. *https://doi.org/10.1299/jsmea.47.198*.

Kalpakjian, S., & Schmid, S. (2009). Manufacturing, Engineering and Technology. *ISBN: 9789810681449*.

Kim, I. (2006). A development of data structure and mesh generation algorithm for whole ship analysis modeling system. Advances in Engineering Software 37(2), 85-96. *https://doi.org/10.1016/j.advengsoft.2005.04.007*.

Krog, L., Tucker, A., & Rollema, G. (2011). Application of Topology, Sizing and Shape Optimization Methods to Optimal Design of Aircraft Components. Airbus. *https://www.semanticscholar.org/paper/Application-of-Topology%2C-Sizing-and-Shape-Methods-Krog-Tucker/89177d8089987d109622766f577d0aa36d612446*.

Leidenfrost, D. (2015). Development of a Nature Inspired Hull Structure for a 46m Sailing Yacht , Master thesis, Hochschule Bremen, Dykstra Naval Architects, Alfred-Wegener-Institut. *https://hdl.handle.net/10013/epic.47738*.

Ling, Q., & Steven, G. (2002). A performance-based optimization method for topology design of continuum structures with mean compliance constraint. Computer Methods in Applied Mechanics and Engineering 191(13-14), 1471-1489. *https://doi.org/10.1016/S0045-7825(01)00333-4*.

LR. (2016). Rules and Regulations for the Classification of Ships.

Mantovani, S., Presti, I., Cavazzoni, L., & Baldini, A. (2017). Influence of Manufacturing Constraints on the Topology Optimization of an Automotive Dashboard. Procedia Manufacturing 11, 1700-1708. *https://doi.org/10.1016/j.promfg.2017.07.296*.

Okumoto, Y., Takeda, Y., Mano, M., & Okada, T. (2009). Design of Ship Hull Structures: A Practical Guide for Engineers. Springer-Verslag Berlin and Heidelberg. *ISBN: 978354088444-6*.

Patel, N., Penninger, C., & Renaud, J. (2009). Topology Synthesis of Extrusion-Based Nonlinear Transient Designs. Journal of Mechanical Design 131(6), 0610031-06100311. *https://doi.org/10.1115/1.3116255*.

Rigo, P., & Caprace, J.-D. (2011). Optimization of Ship Structures. 1st International Conference of Maritime Technology and Engineering. *http://hdl.handle.net/2268/126690*.

Rörup, J., Maciolowski, B., & Darie, I. (2016). FE-based strength analysis of ship structures for a more advanced class approval. DNV-GL.

Rozvany, G. (2009). A critical review of established methods of structural topology optimization. Struct Multidisc Optim 37, 217-237. *https://doi.org/10.1007/s00158-007-0217-0*.

Schramm, U. (2020). Topology Optimization and the Lessons of History. *https://www.altair.com/newsroom/executive-insights/topology-optimization-and-the-lessons-of-history/*.

Shenoi, R., & Guedes Soares, C. (2015). Analysis and Design of Marine Structures. 5th International Conference on Marine Structures. *https://doi.org/10.1080/17445302.2011.546686*.

Shimels, H., Engida, D., & Mohd, F. (2017). A comparative study on stress and compliance based structural topology optimization. Materials Science and Engineering 241. *https://iopscience.iop.org/article/10.1088/1757-899X/241/1/012003/meta*.

Sigmund, O., & Maute, K. (2013). Topology optimization approaches: A comparative review. Struct Multidisc Optim 48(6), 1031-1055. *https://doi.org/10.1007/s00158-013-0978-6*.

Stromberg, L., Beghini, A., Baker, W., & Paulino, G. (2011). Application of layout and topology optimization using pattern gradation for the conceptual design of buildings. Struct Multidisc Optim 43, 165–180. *https://doi.org/10.1007/s00158-010-0563-1*.

Strömberg, N. (2010). Topology optimization of structures with manufacturing and unilateral contact constraints by minimizing an adjustable compliance–volume product. Struct Multidisc Optim 42, 341–350. *https://doi.org/10.1007/s00158-010-0502-1*.

Tanskanen, P. (2002). The evolutionary structural optimization method: theoretical aspects. Computer Methods in Applied Mechanics and Engineering 191(47-48), 5485-5498. *https://doi.org/10.1016/S0045-7825(02)00464-4*.

Tasdemir, A., & Nohut, S. (2012). Practical Experience with Efficient Generation of Finite-Element Models of Ships using POSEIDON. 11th International Conference on Computer and IT Applications in the Maritime. *http://data.hiper-conf.info/compit2012_liege.pdf*.

Vatanabe, S., Lippi, T., de Lima, C., Paulino, G., & Silva, E. (2016). Topology optimization with manufacturing constraints: A unified projection-based approach. Advances in Engineering Software 100, 97-112. *https://doi.org/10.1016/j.advengsoft.2016.07.002*.

Vuijk, H. (2020). Shape and Topology Optimized TSHD Midsection. Master Thesis TU Delft 3mE. *http://resolver.tudelft.nl/uuid:dffac044-cefd-45c1-a2ba-1709c8e11ed4*.

Wang, F., Lazarov, B., & Sigmund, O. (2011). On projection methods, convergence and robust formulations in topology optimization. Struct Multidisc Optim 43, 767-784. *https://doi.org/10.1007/s00158-010-0602-y*.

Zeguer, T., & Bates, S. (2012). Robust Design Optimization of an Automotive Knee Bolster. 49th AIAA/ASME/ASCE/AHS/ASC Structures, Structural Dynamics, and Materials Conference. *https://doi.org/10.2514/6.2008-2145*.

Zhou, M., Fleury, R., Shyy, Y., Thomas, H., & Brennan, J. (2002). Progress in topology optimization with manufacturing constraints. 9th AIAA/ISSMO Symposium on Multidisciplinary Analysis and Optimization. *https://doi.org/10.2514/6.2002-5614*.

Zhou, M., Shyy, Y., & H.L., T. (2001). Checkerboard and minimum size control in topology optimization. Struct Multidisc Optim 21, 152-158. *https://doi.org/10.1007/s001580050179*.

Zuo, K., Chen, L., Zhang, Y., & Yang, J. (2006). Manufacturing- and machining-based topology optimization. The International Journal of Advanced Manufacturing Technology 27, 531-536. *https://doi.org/10.1007/s00170-004-2210-8*.

APPENDIX A

Detailed FEA results from the first iteration with a maximum Von Mises stress of 260 MPa, legend colors in Figure 23.

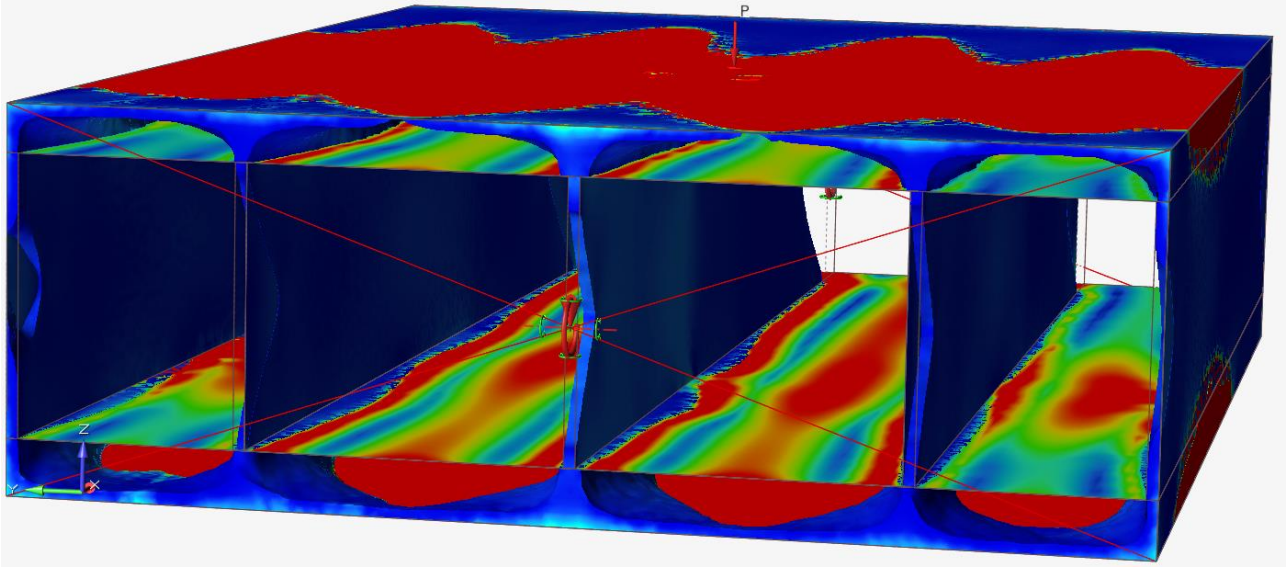

Figure 37 – Total mid-section structure

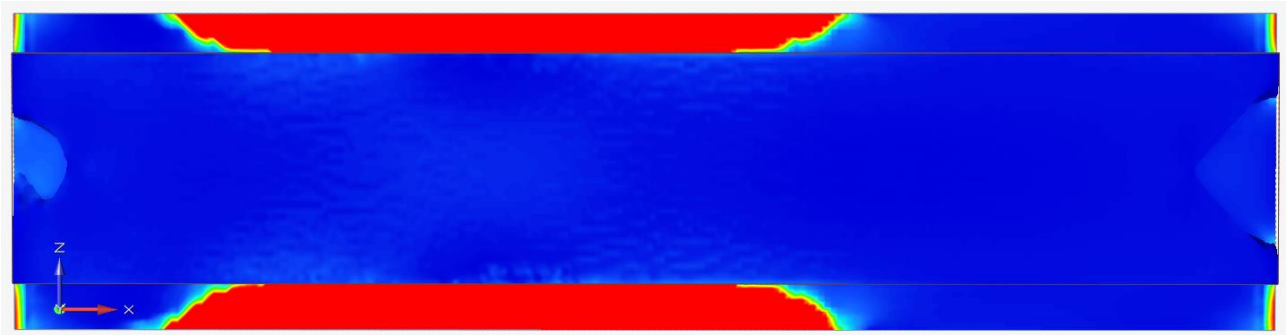

Figure 38 – Structure hull side plate

Figure 39 – Structure longitudinal bulkhead plate

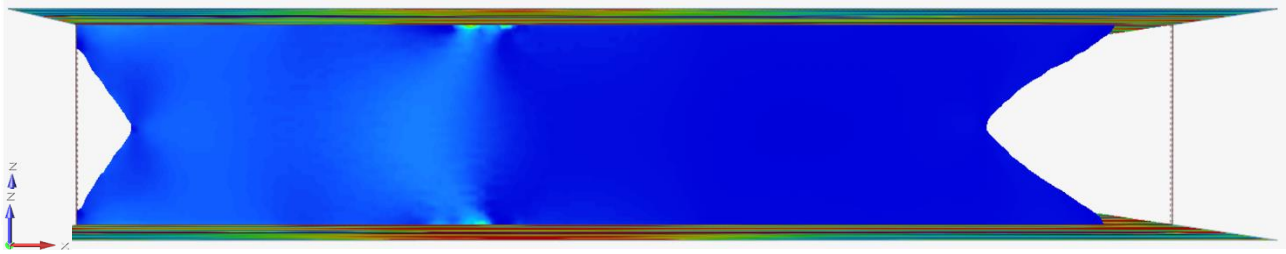

Figure 40 - Structure longitudinal mid support

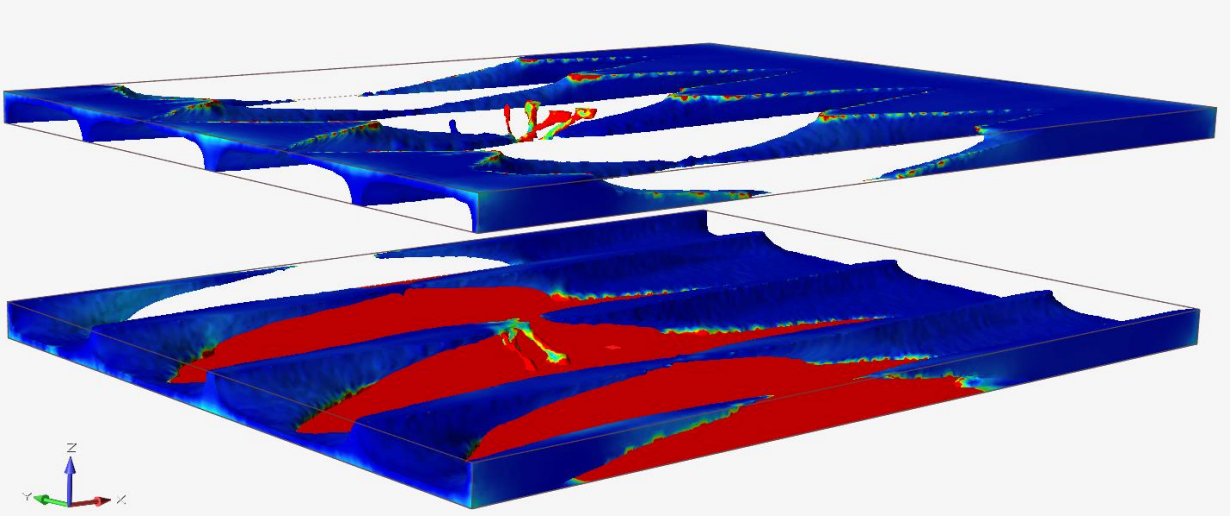

Figure 41 – Structure double bottom and double deck

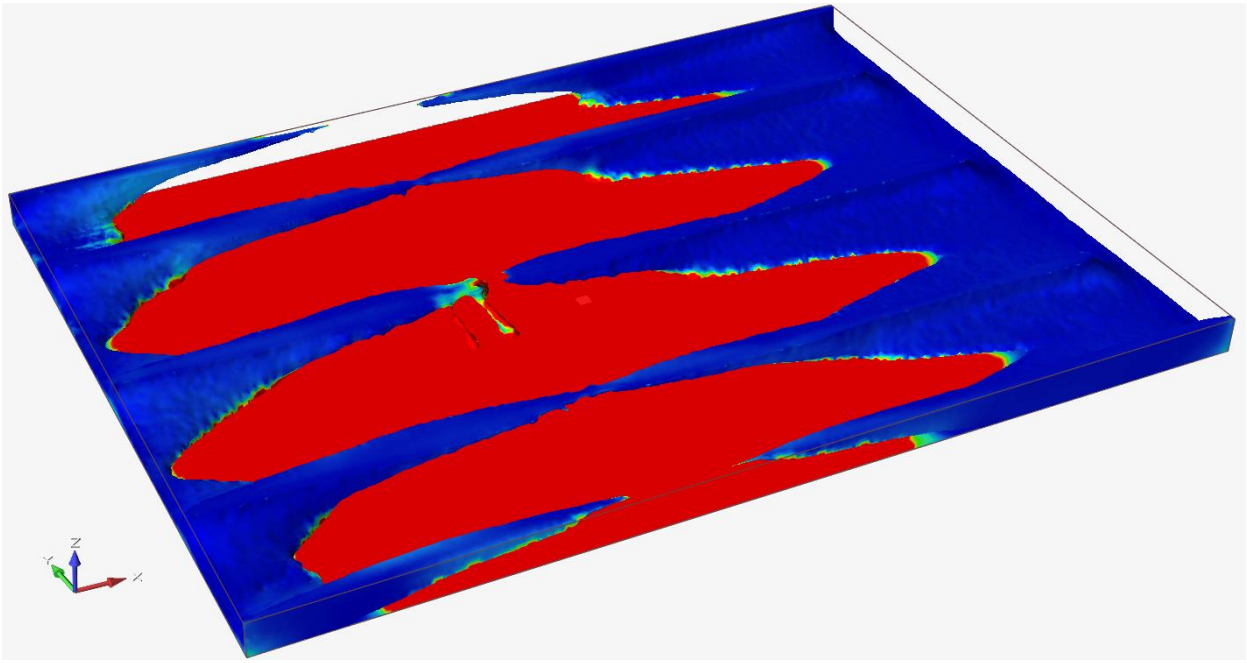

Figure 42 – Structure double bottom

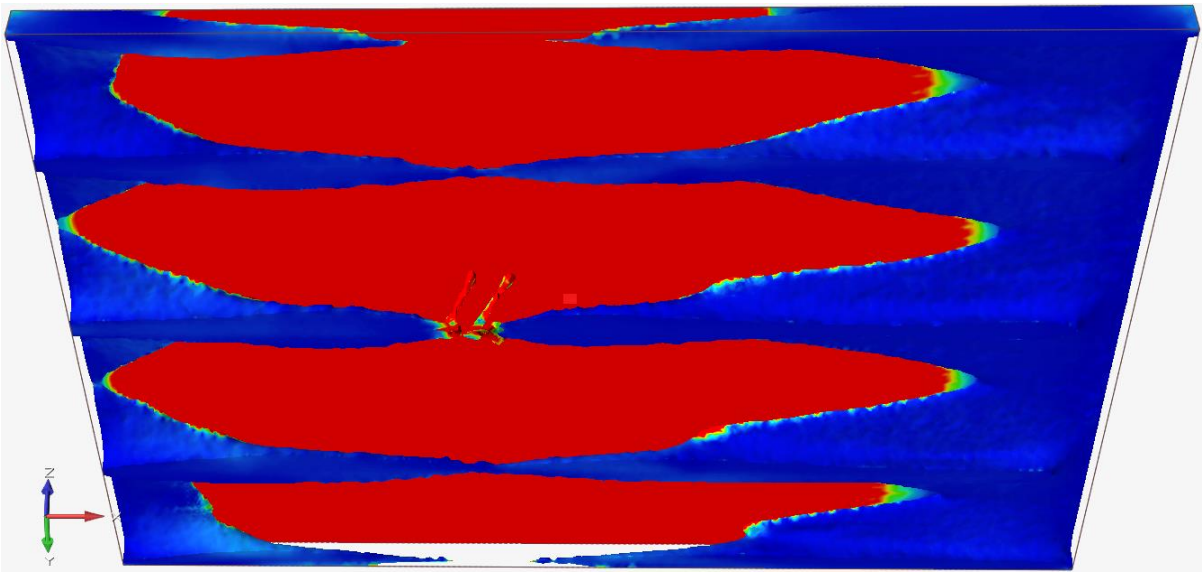

Figure 43 – Structure double deck

APPENDIX B

Detailed FEA results from the second iteration with a maximum Von Mises stress of 260 MPa, legend colors in Figure 23.

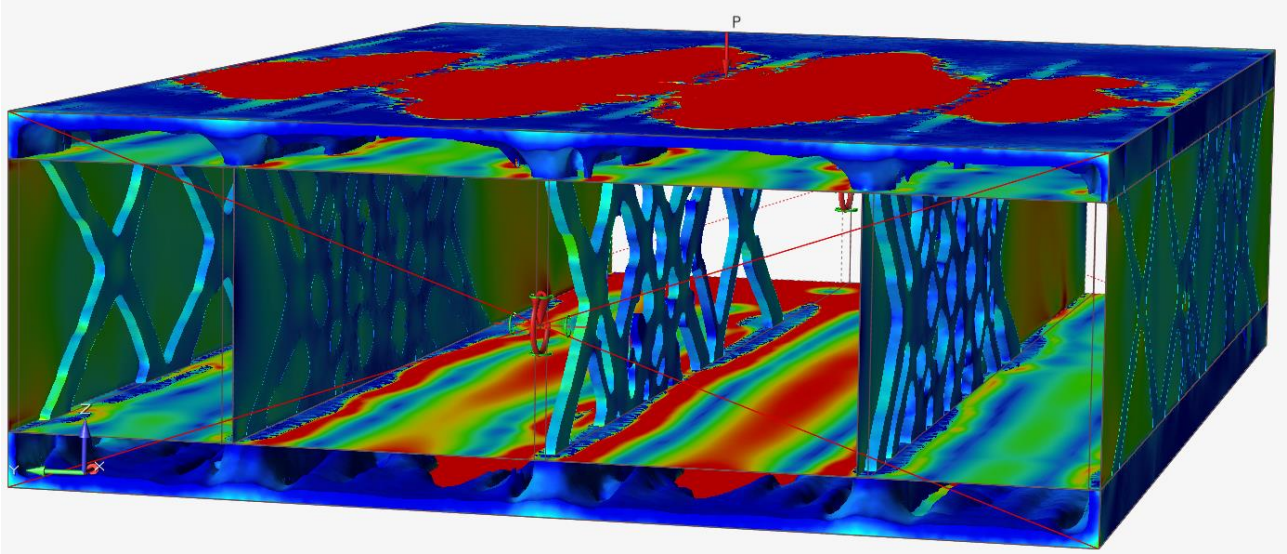

Figure 44 – Total mid-section structure

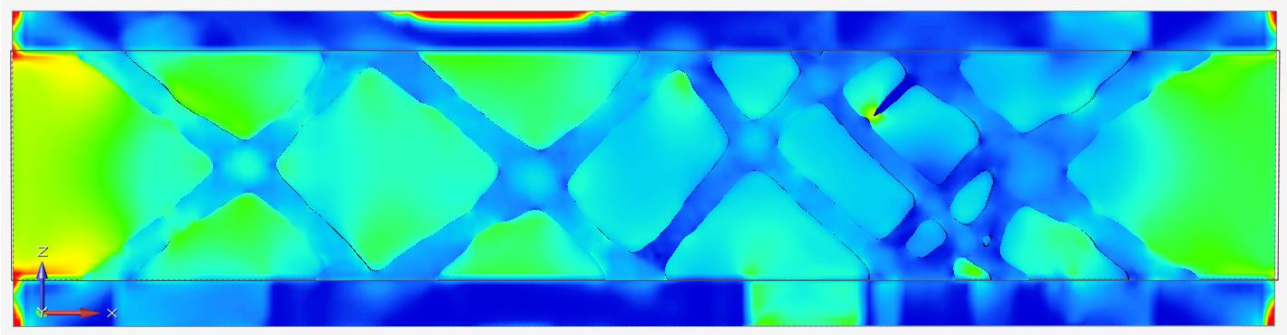

Figure 45 – Structure hull side plate

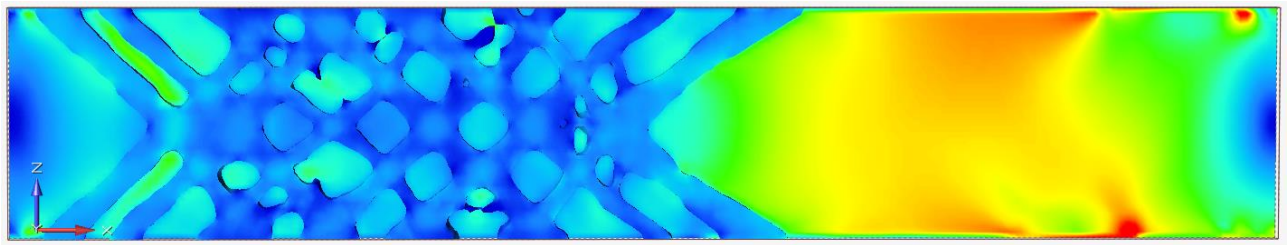

Figure 46 – Structure longitudinal bulkhead

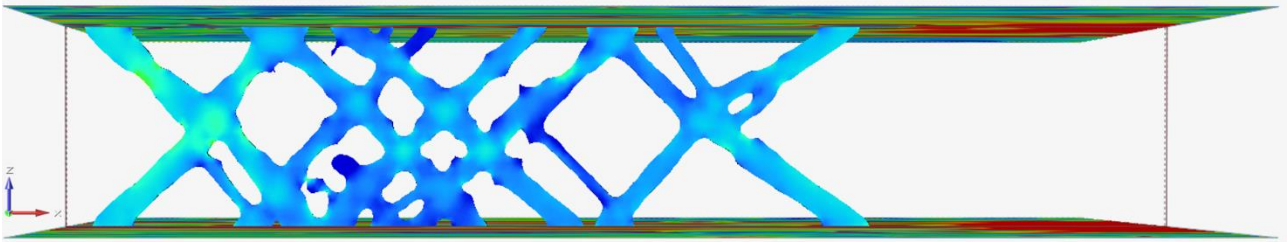

Figure 47 – Structure longitudinal mid support

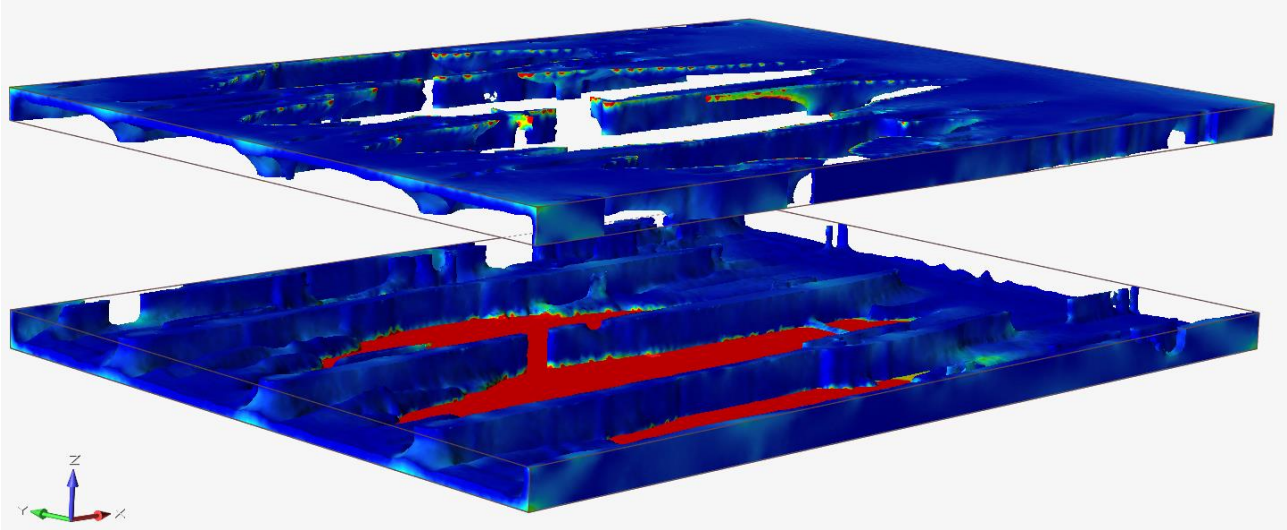

Figure 48 – Structure double bottom and deck

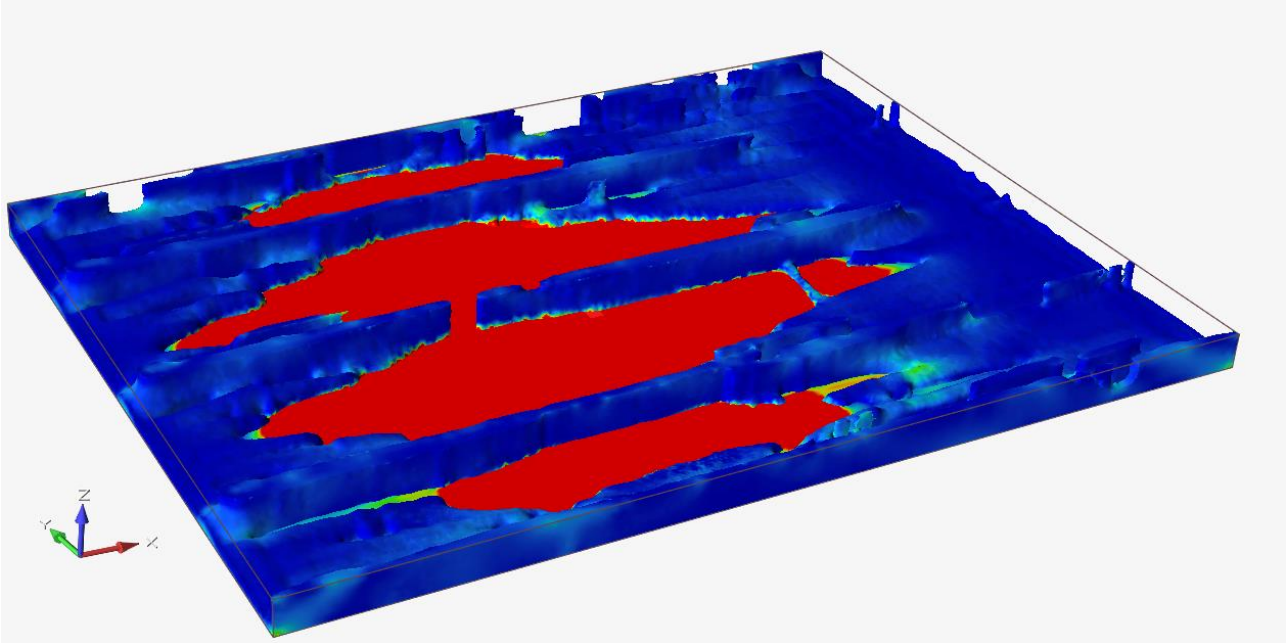

Figure 49 – Structure double bottom

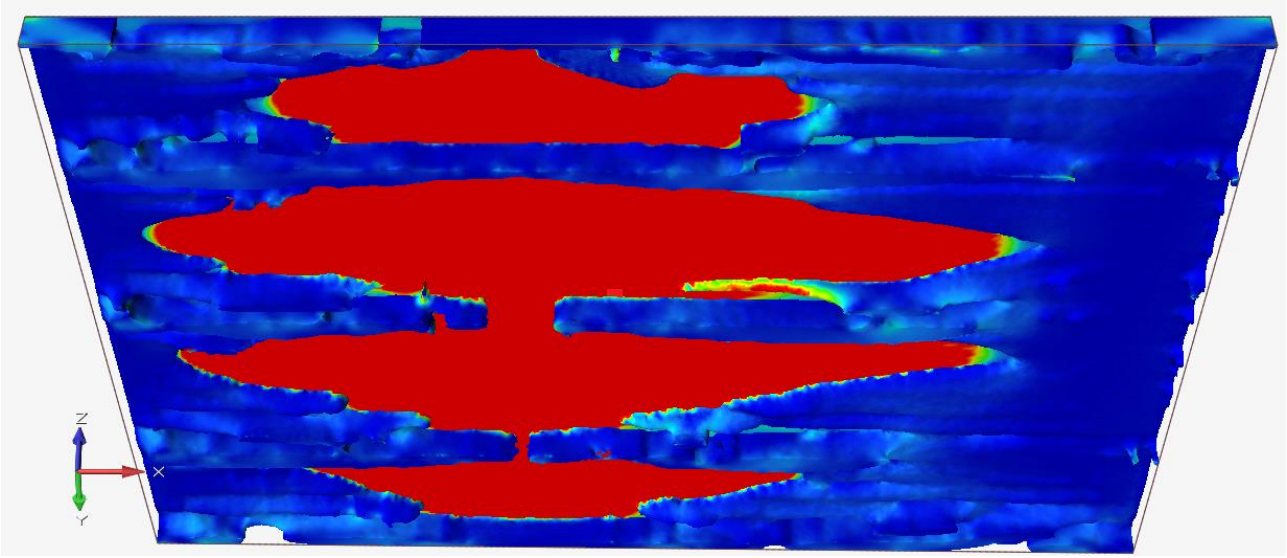

Figure 50 – Structure double deck

APPENDIX C

Detailed FEA results from the third iteration with a maximum Von Mises stress of 260 MPa, legend colors in Figure 23.

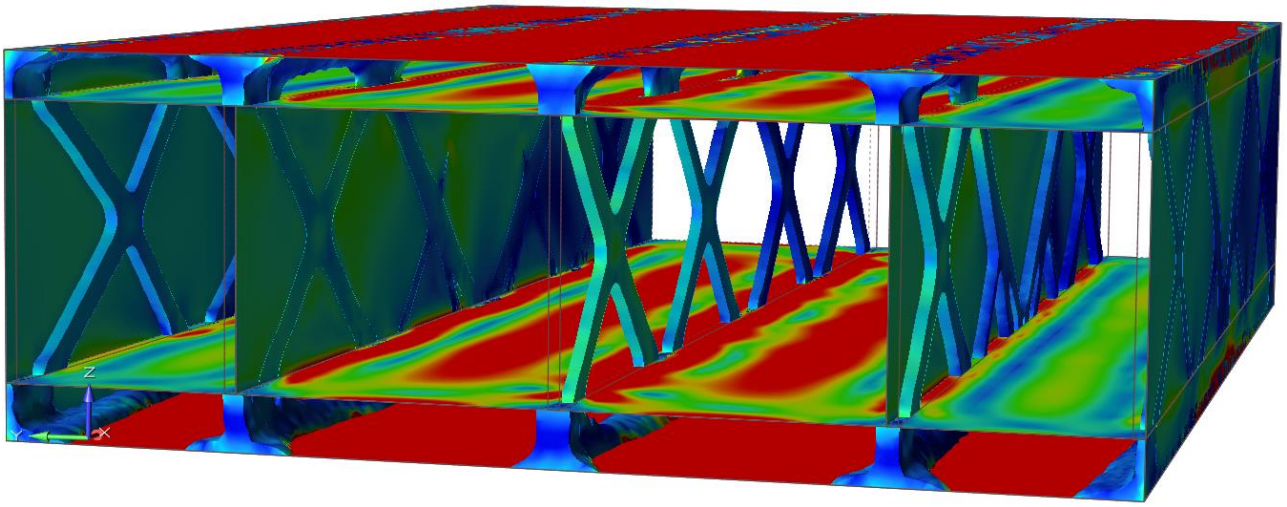

Figure 51 – Total mid-section structure

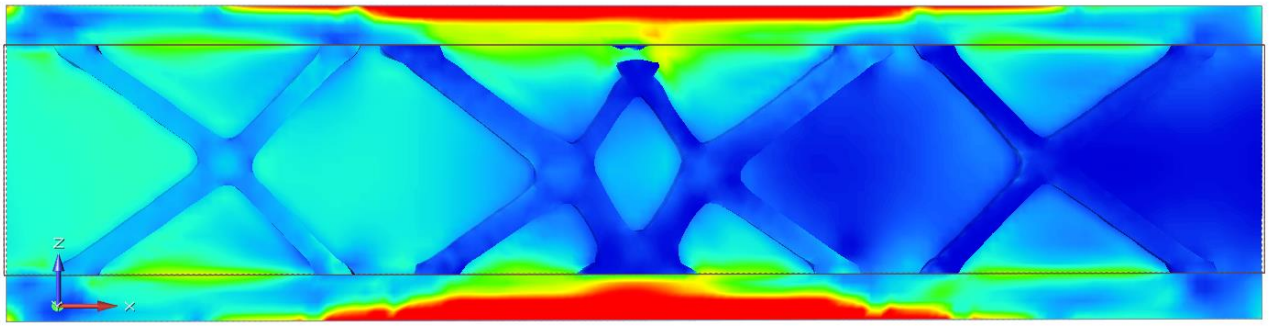

Figure 52 – Structure hull side plate

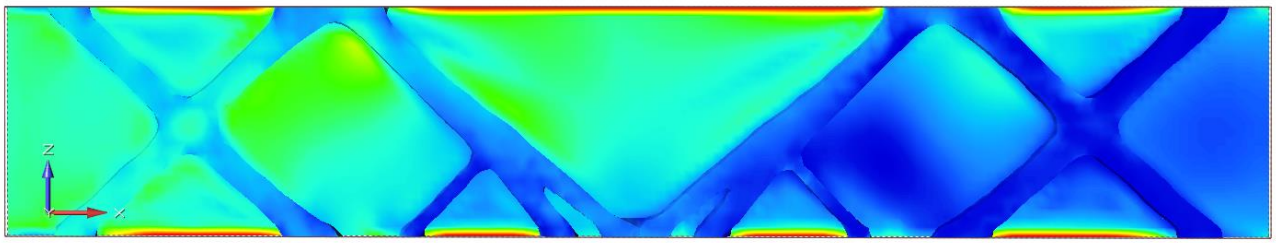

Figure 53 – Structure longitudinal bulkhead

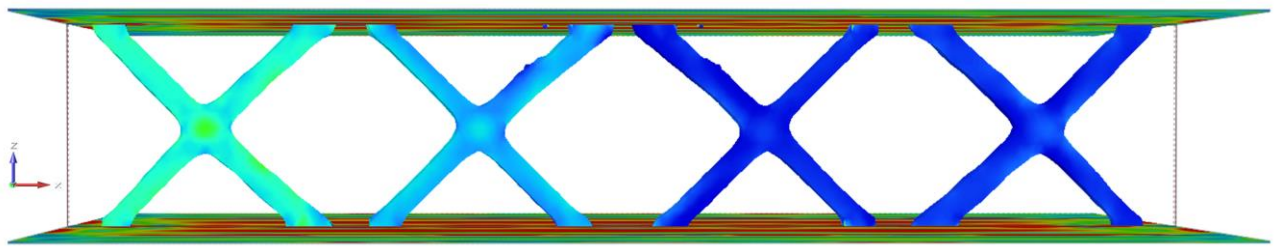

Figure 54 – Structure longitudinal mid support

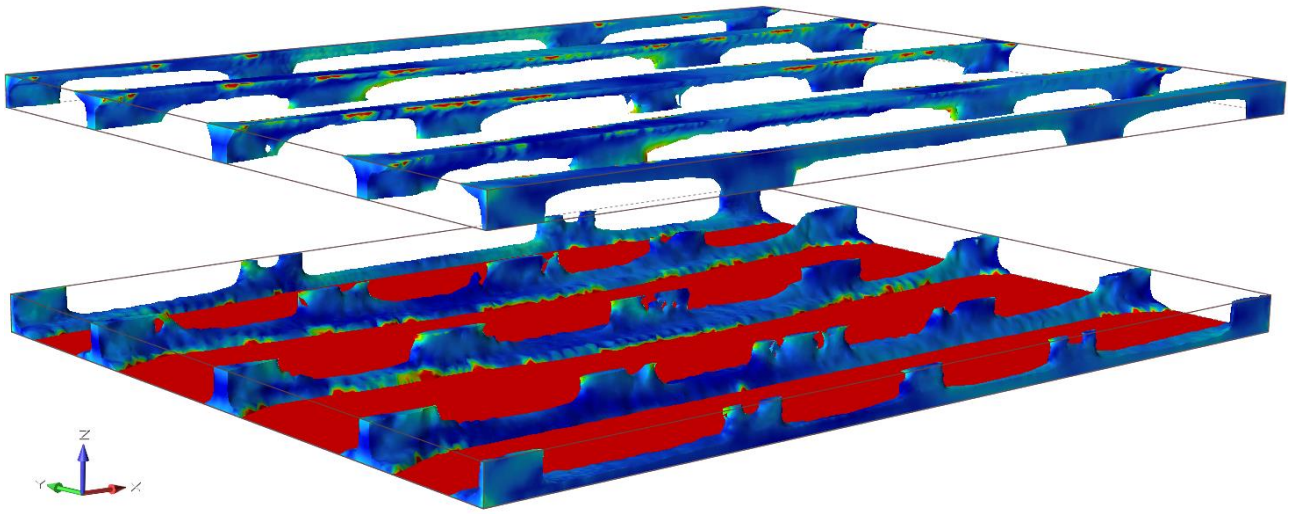

Figure 55 – Structure double bottom and deck

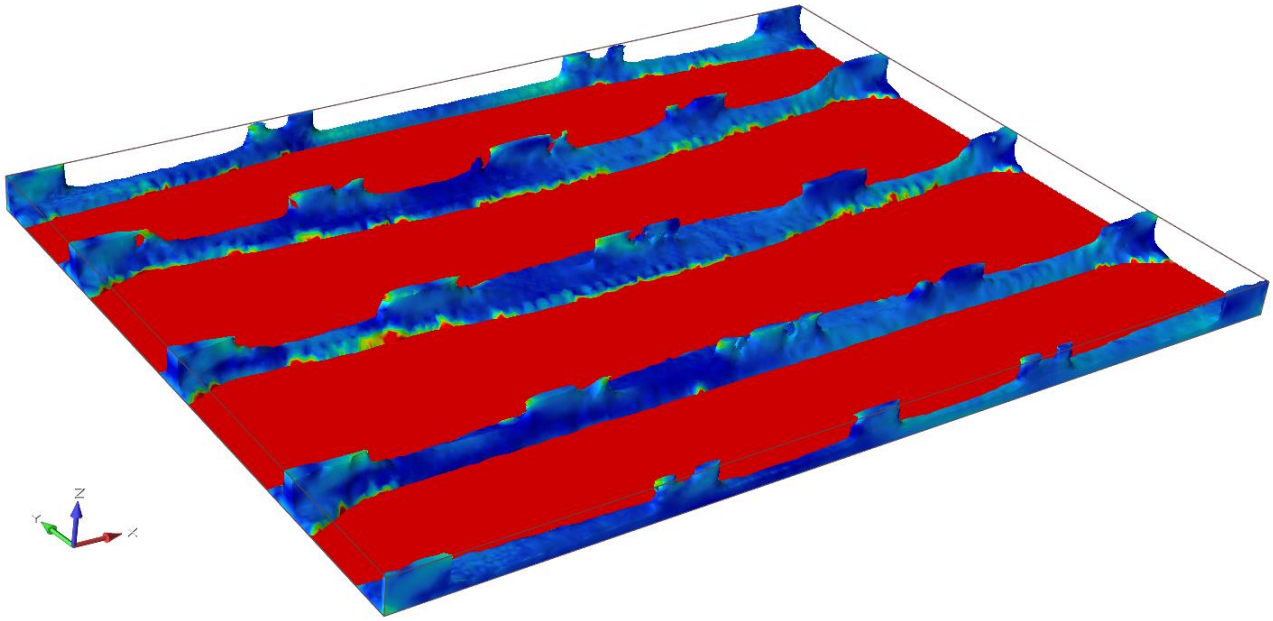

Figure 56 – Structure double bottom

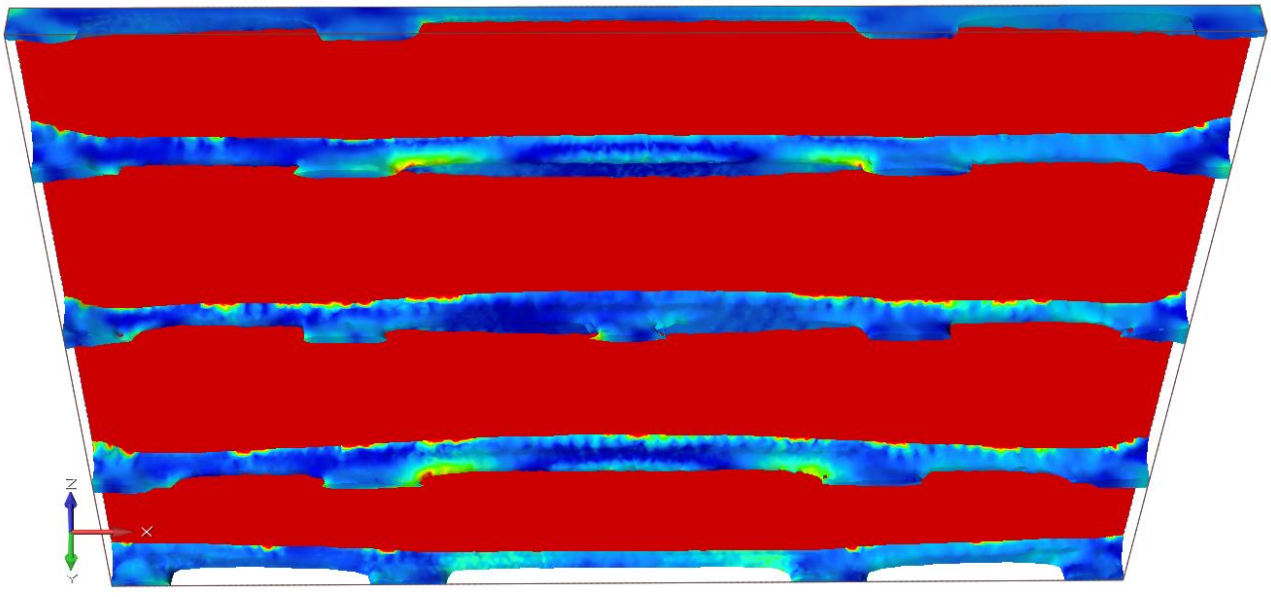

Figure 57 – Structure double deck

APPENDIX D

Detailed FEA results from the fourth iteration with a maximum Von Mises stress of 260 MPa, legend colors in Figure 23.

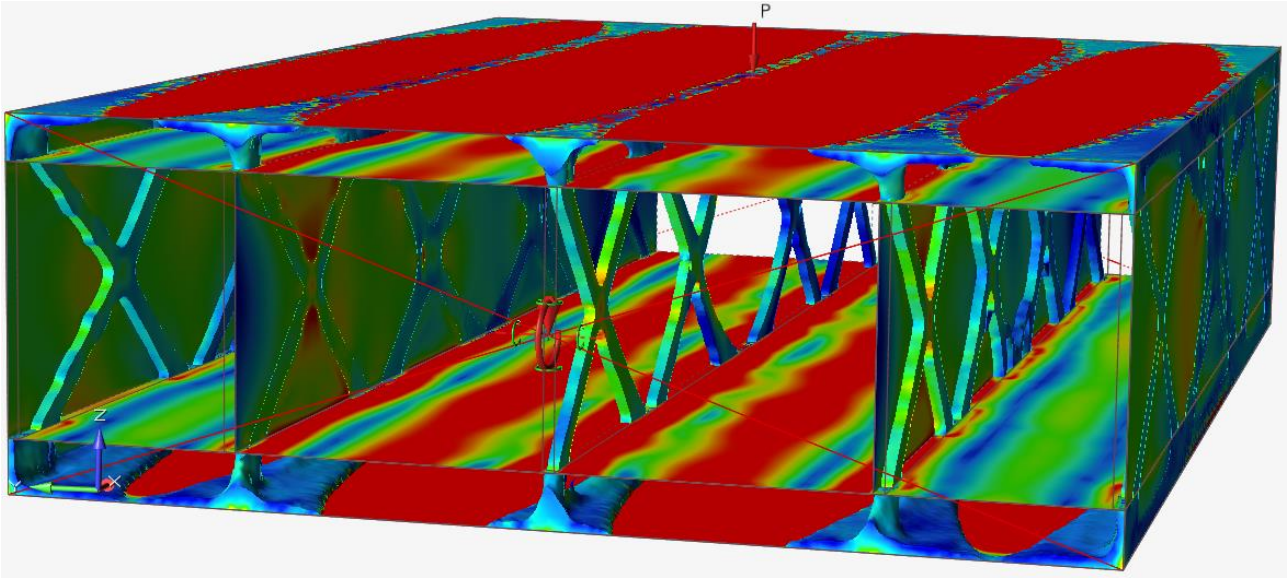

Figure 58 – Total mid-section structure

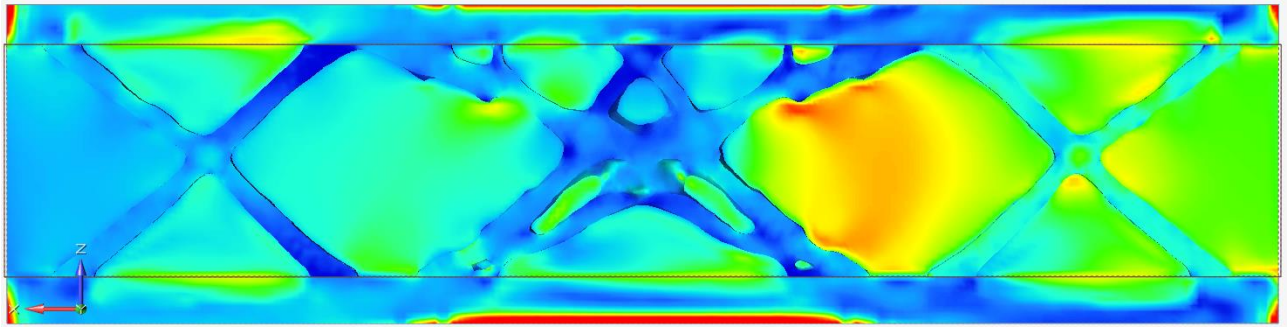

Figure 59 – Structure hull side plate

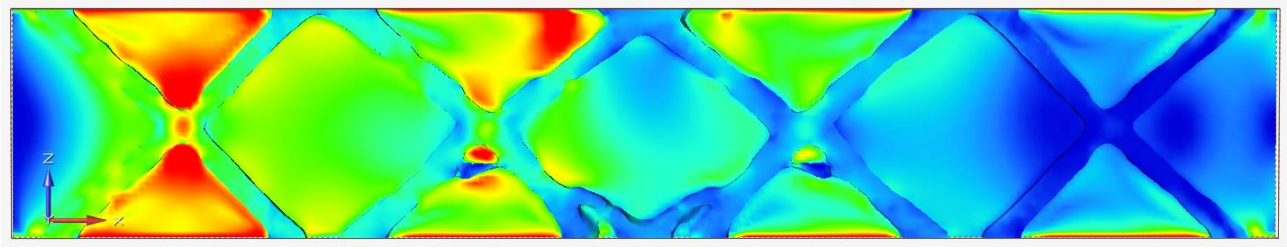

Figure 60 – Structure longitudinal bulkhead

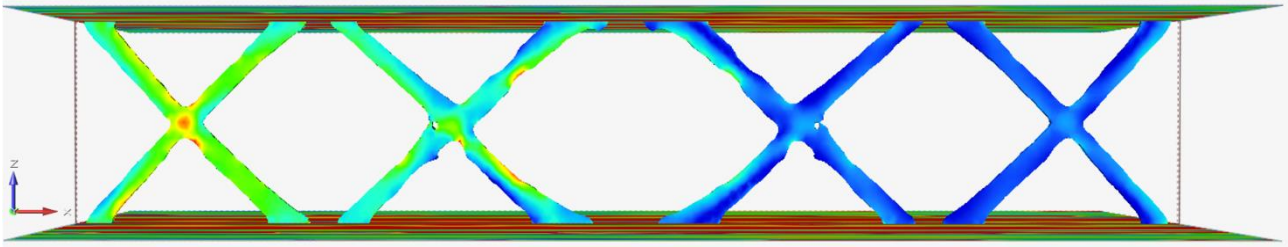

Figure 61 – Structure longitudinal mid support

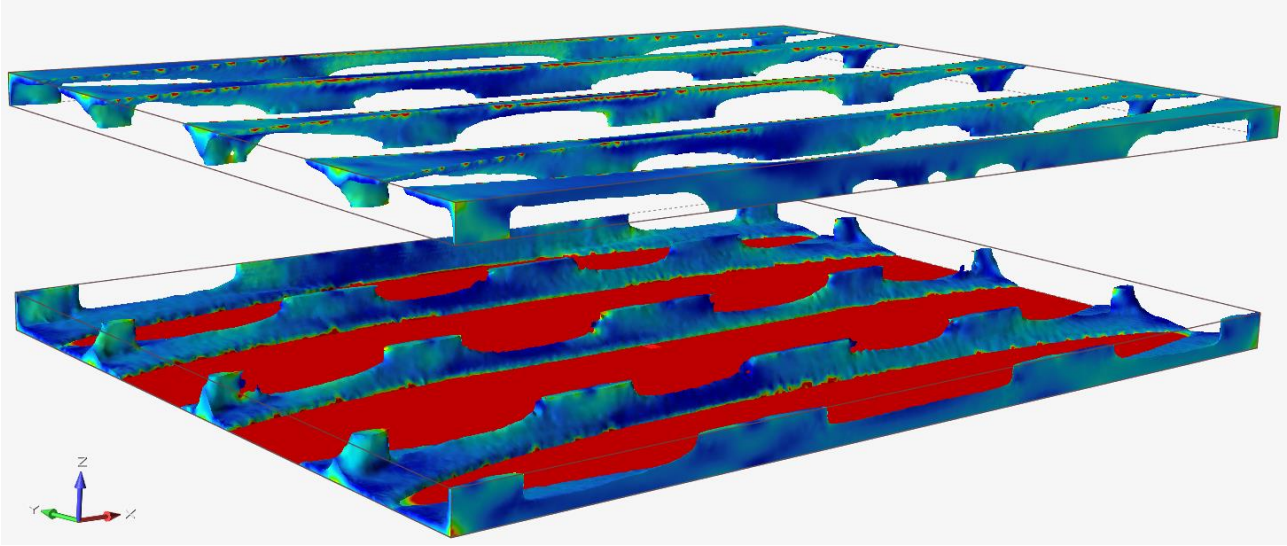

Figure 62 – Structure double bottom and deck

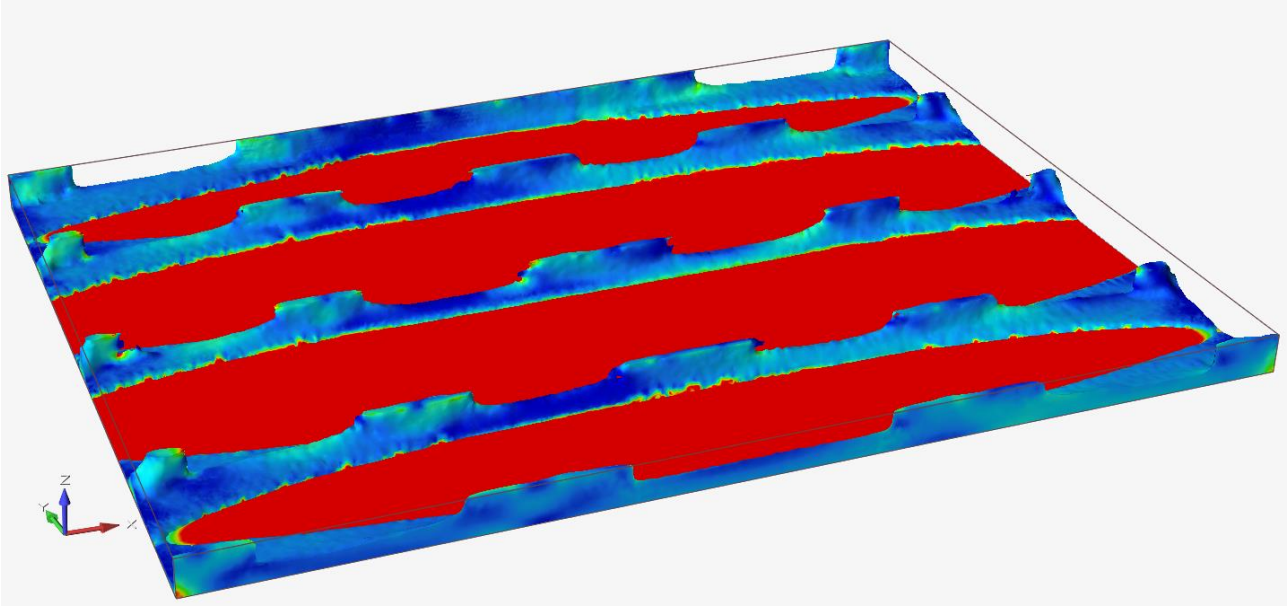

Figure 63 – Structure double bottom

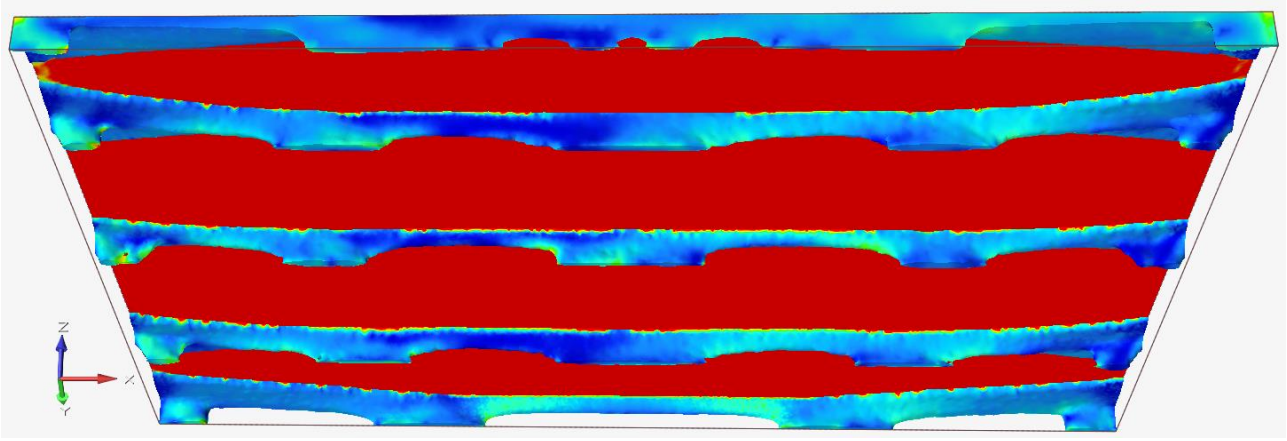

Figure 64 – Structure double deck

APPENDIX E

Detailed FEA results from the fifth iteration with a maximum Von Mises stress of 260 MPa, legend colors in Figure 23.

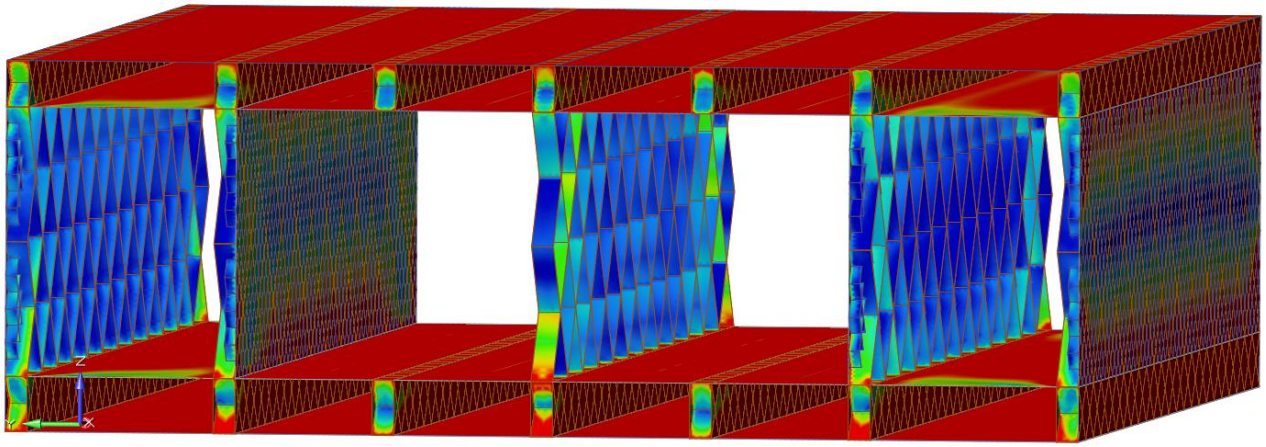

Figure 65 – Total mid-section structure

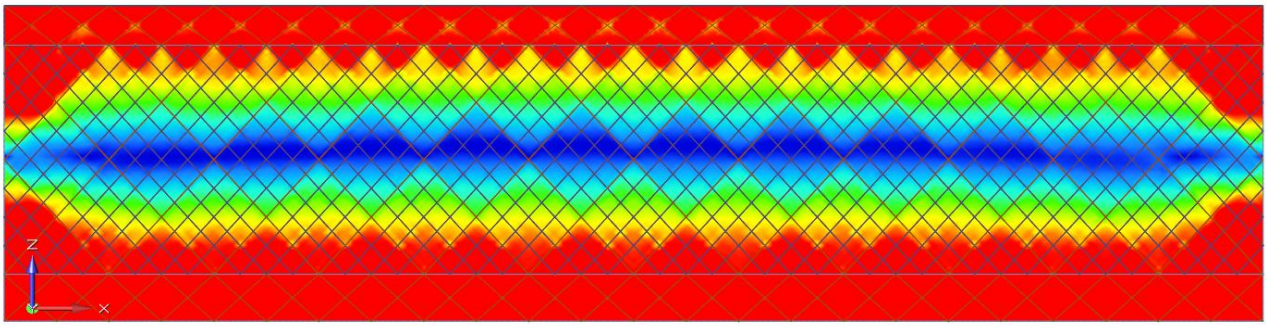

Figure 66 – Structure hull side plate

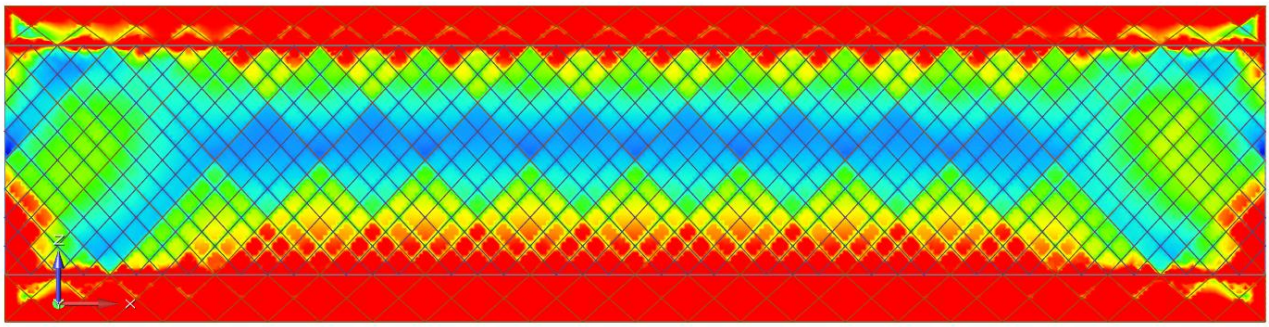

Figure 67 – Structure longitudinal bulkhead

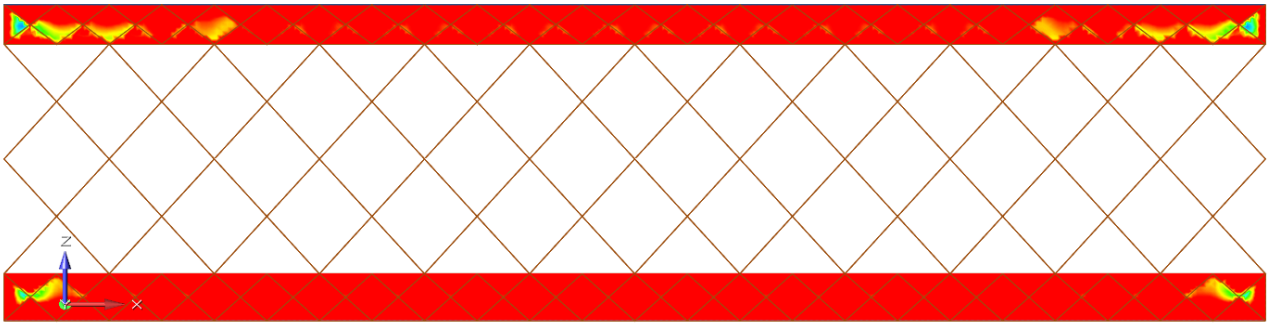

Figure 68 – Structure longitudinal mid support

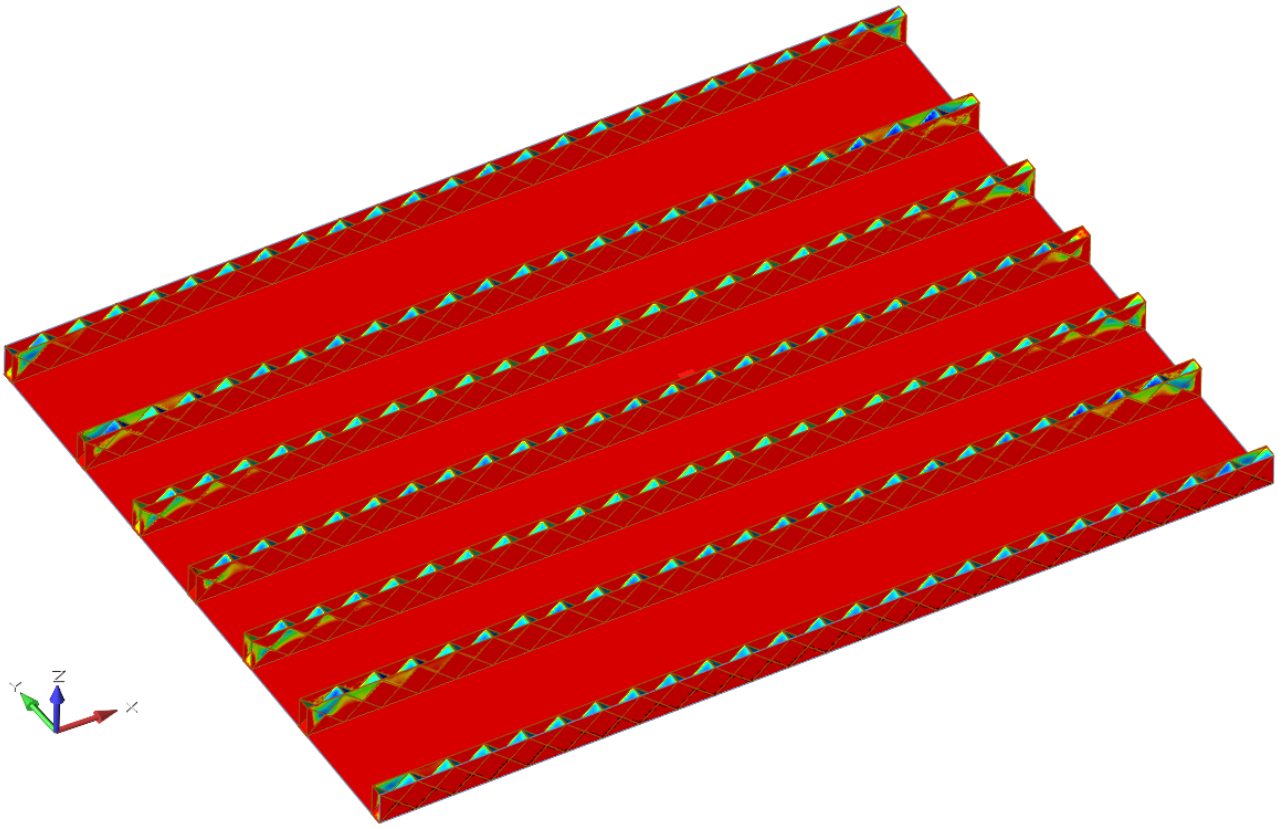

Figure 69 – Structure double bottom

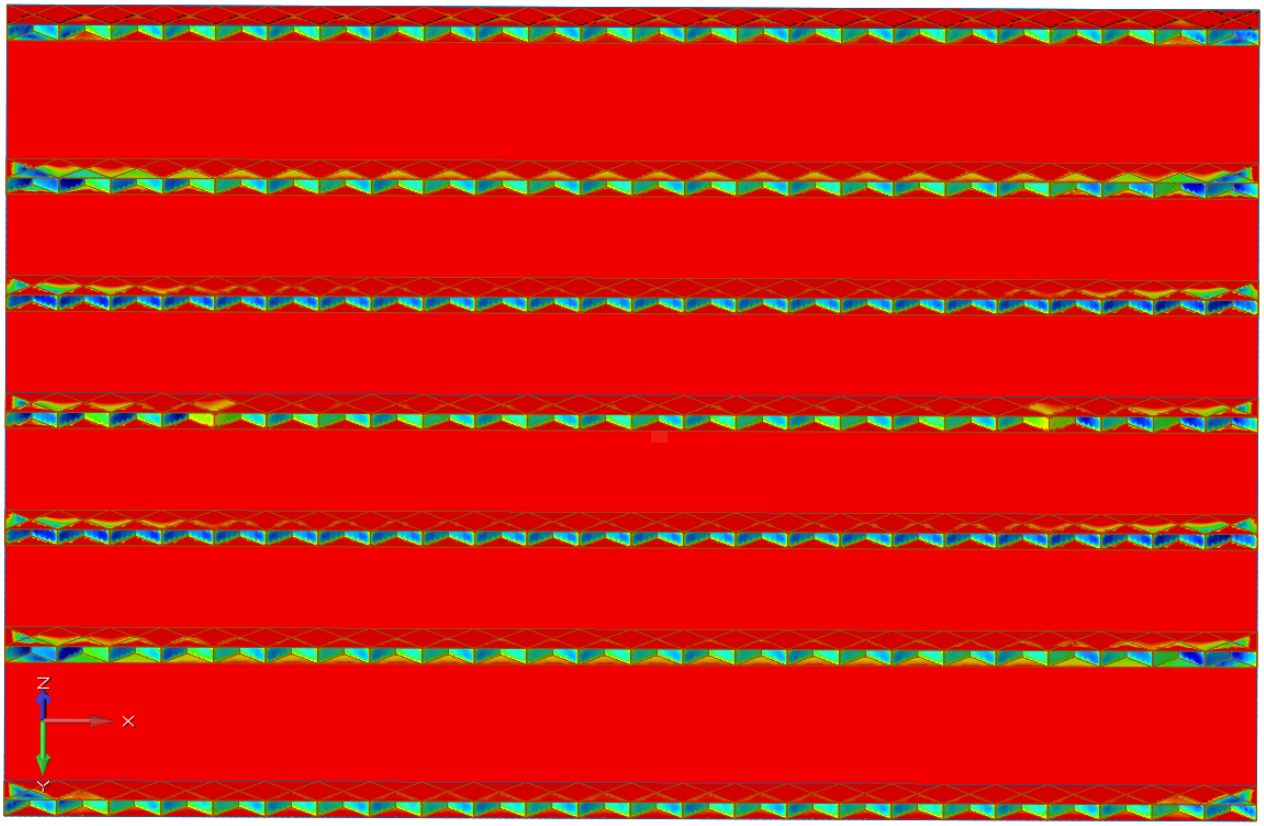

Figure 70 – Structure double deck

APPENDIX F

Detailed FEA results from the fifth iteration with a maximum Von Mises stress of 260 MPa, legend colors in Figure 23.

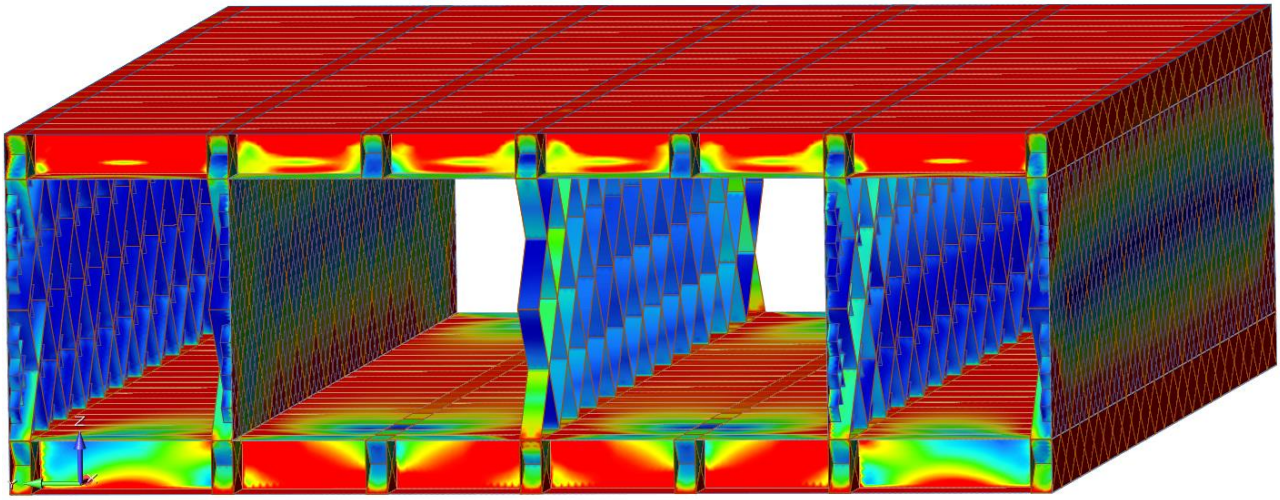

Figure 71 – Total mid-section structure

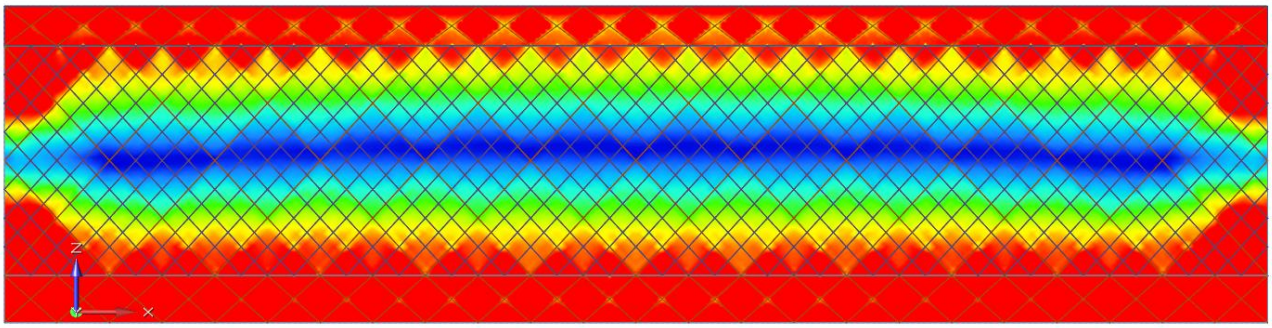

Figure 72 – Structure hull side plate

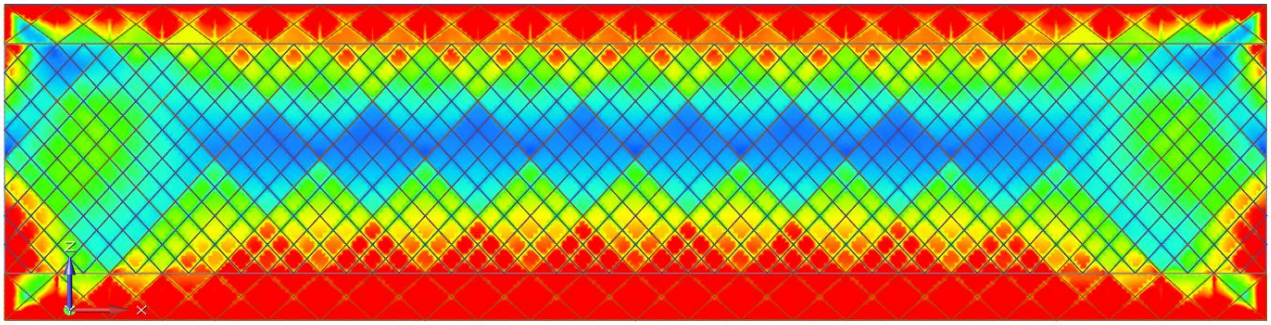

Figure 73 – Structure longitudinal bulkhead

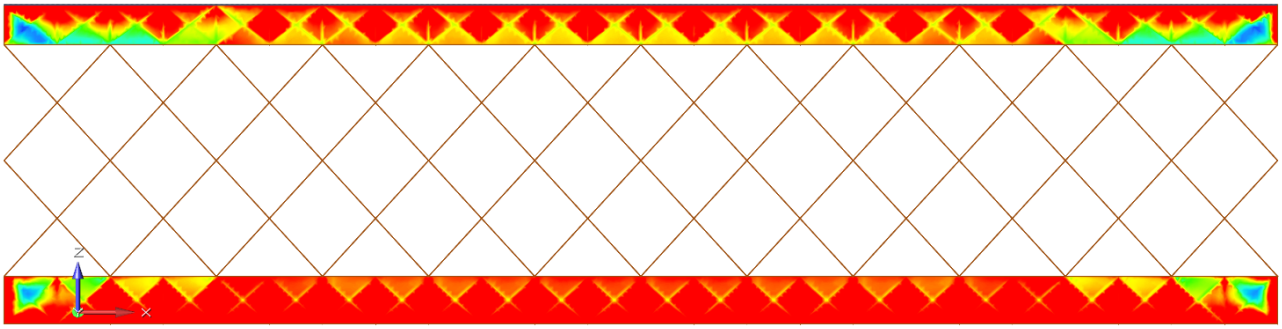

Figure 74 – Structure longitudinal mid support

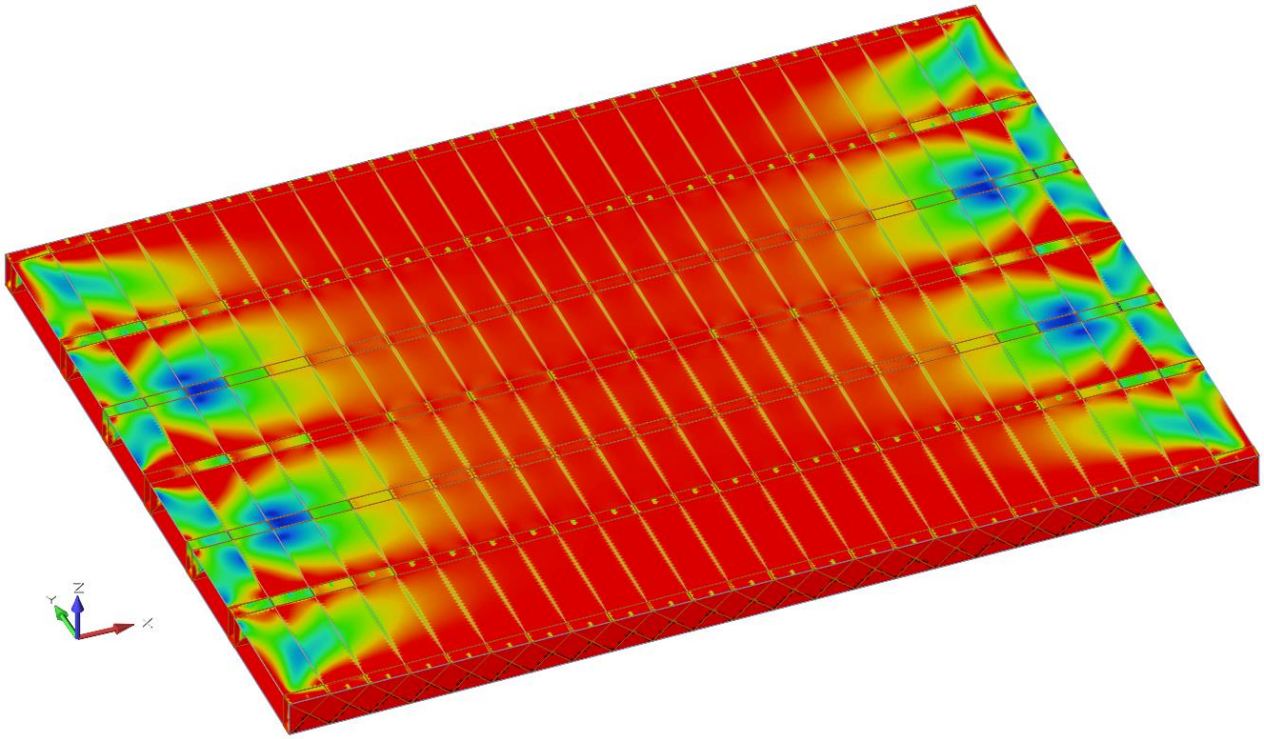

Figure 75 – Structure double bottom

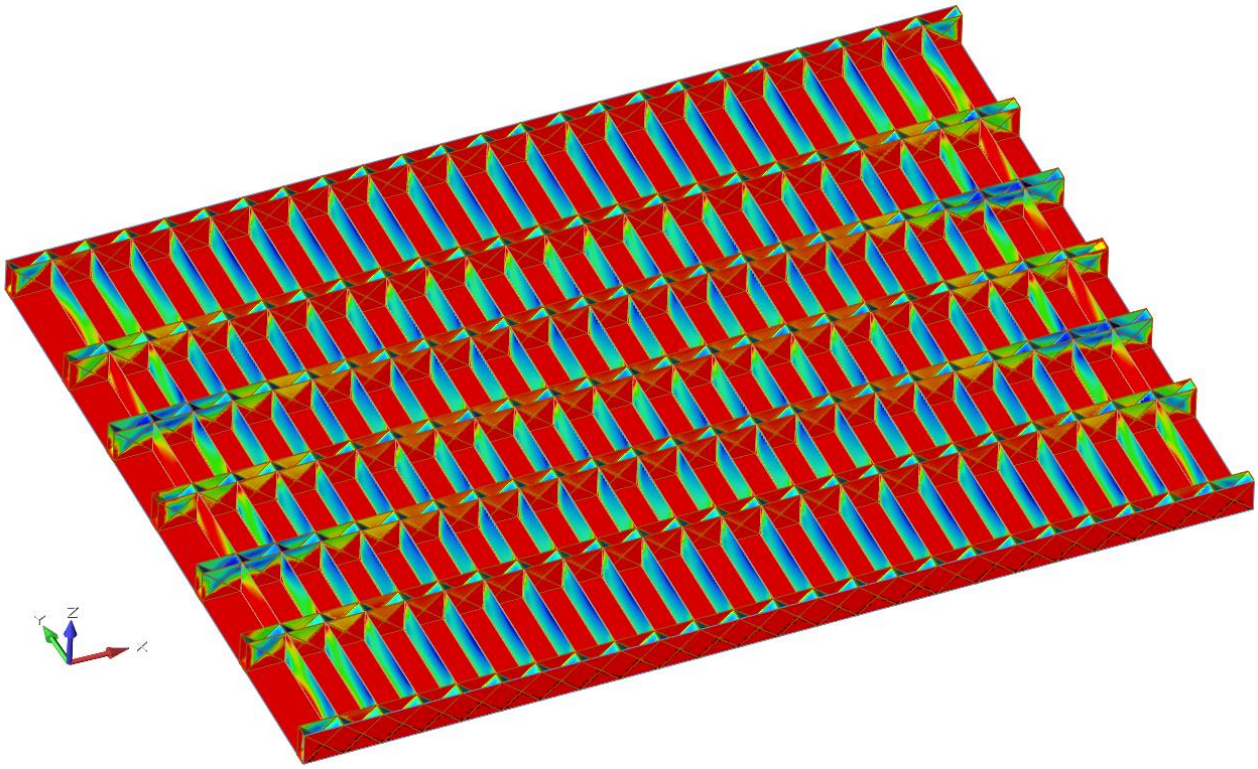

Figure 76 – Structure double deck

APPENDIX G

Detailed FEA results from the fifth iteration with a maximum Von Mises stress of 260 MPa, legend colors in Figure 23.

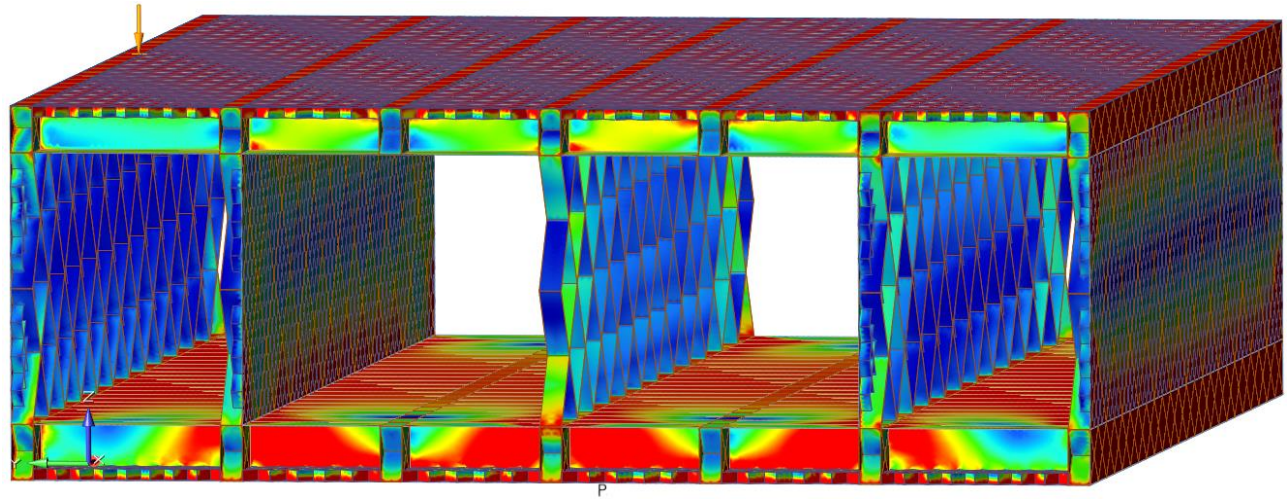

Figure 77 – Total mid-section structure

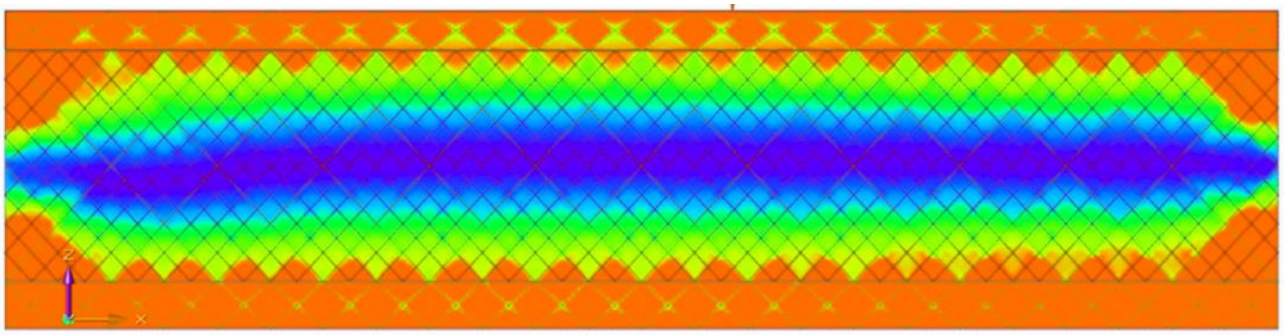

Figure 78 – Structure hull side plate

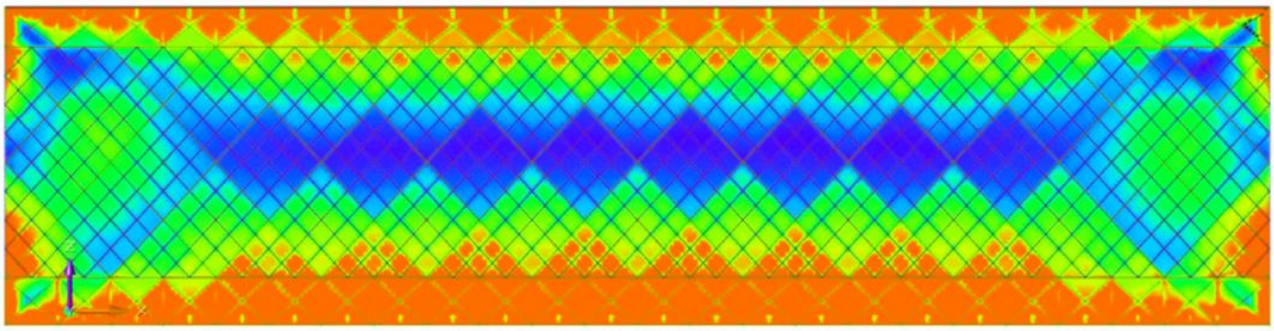

Figure 79 – Structure longitudinal bulkhead

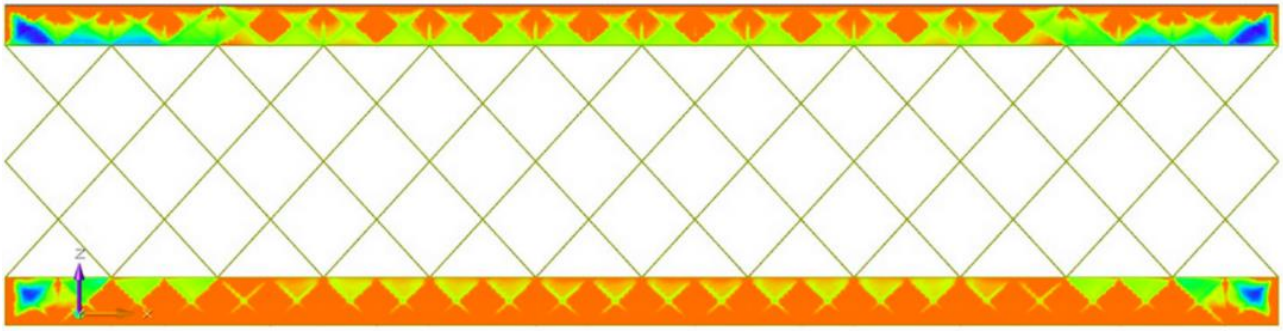

Figure 80 – Structure longitudinal mid support

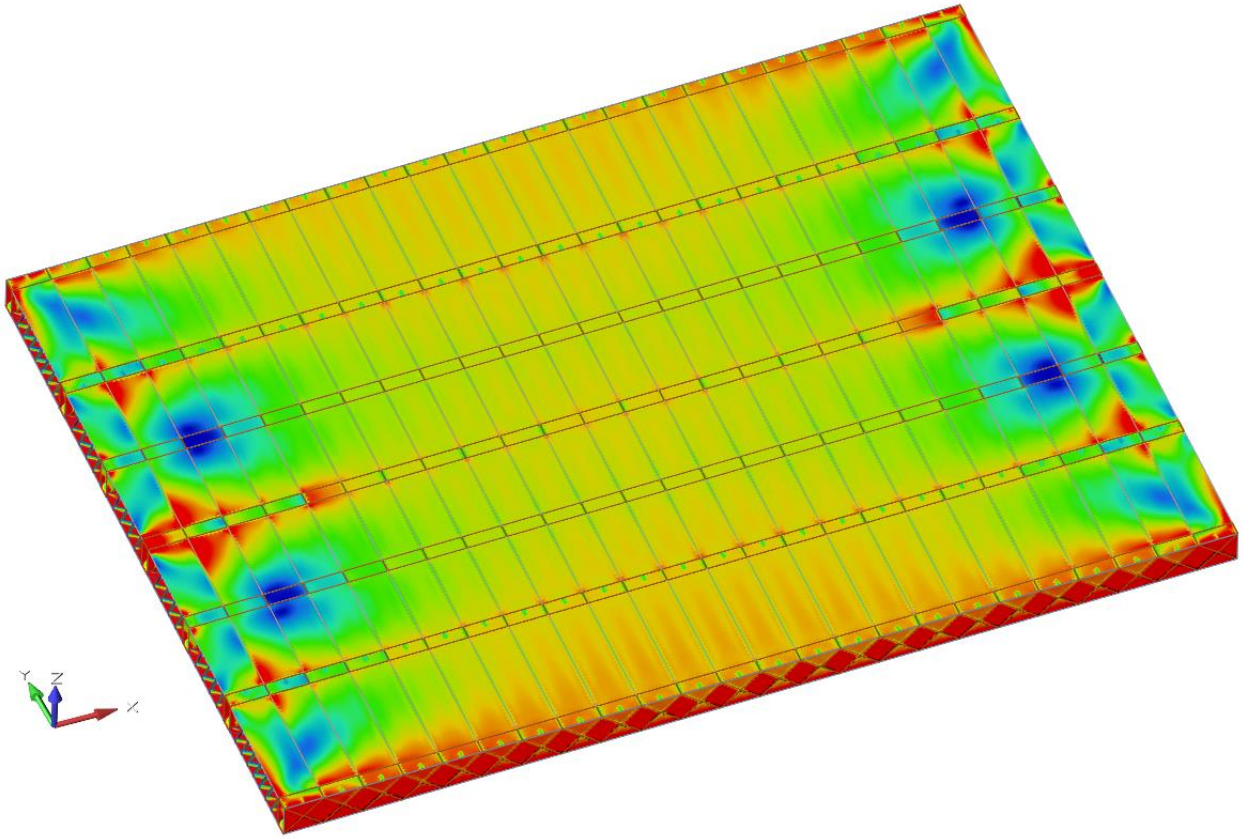

Figure 81 – Structure double bottom

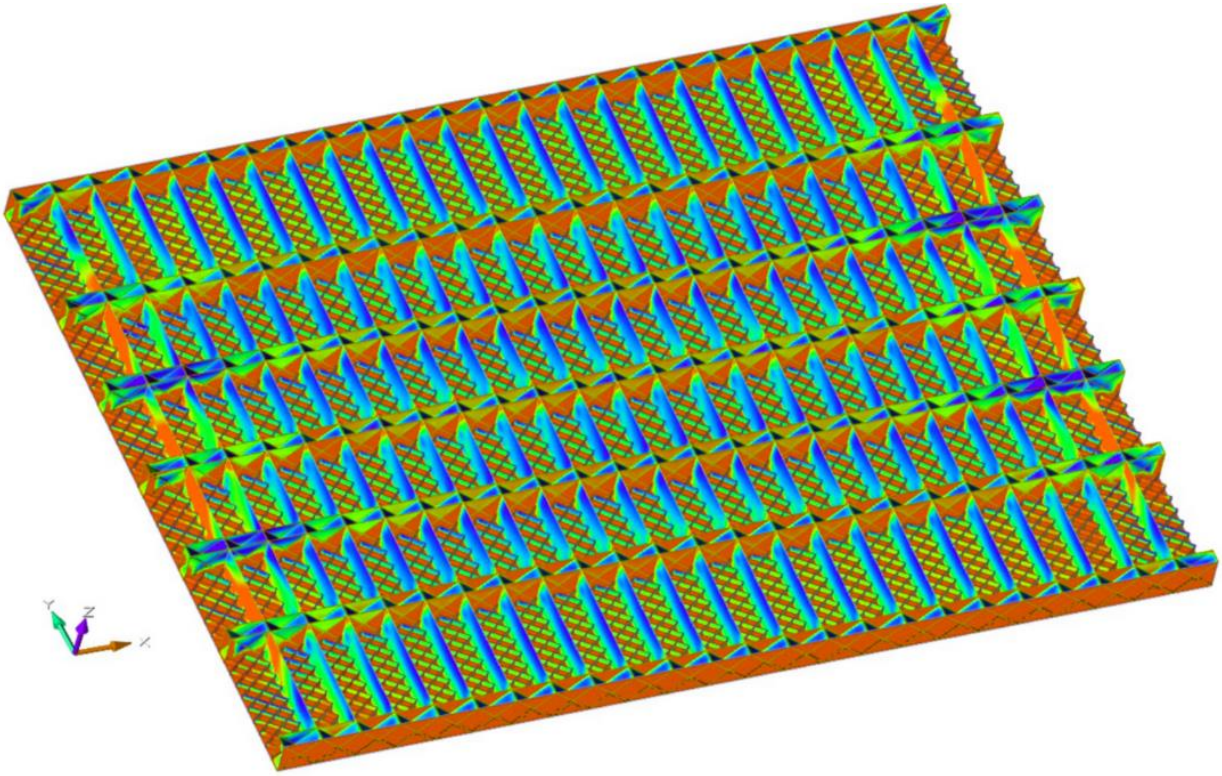

Figure 82 – Structure double deck